APTECH engineering services, inc ENGINEERING CONSULTANTS

795 SAN ANTONIO ROAD • PALO ALTO • CALIFORNIA 94303 (415) 858 - 2863

GUIDELINES AND PROCEDURES FOR THE EVALUATION OF COMPONENT SUPPORTS BASED ON FRACTURE MECHANICS

(RP 1757-2)

Prepared by

Russell C. Cipolla

Aptech Engineering Services
795 San Antonio Road
Palo Alto, California 94303

Prepared for

Electric Power Research Institute
3412 Hillview Avenue
Palo Alto, California 94303

Project Managers
R. E. Nickell
T. U. Marston

February 1981

LEGAL NOTICE

This report was prepared by the organization(s) named below as an account of work sponsored by the Electric Power Research Institute, Inc. (EPRI). Neither EPRI, members of EPRI, the organization(s) named below, nor any person acting on their behalf: (a) makes any warranty or representation, express or implied, with respect to the accuracy, completeness, or usefulness of the information contained in this report, or that the use of any information, apparatus, method, or process disclosed in this report may infringe privately owned rights; or (b) assumes any liabilities with respect to the use of, or for damages resulting from the use of, any information, apparatus, method, or process disclosed in this report.

Prepared by:

Aptech Engineering Services, Inc.
795 San Antonio Road
Palo Alto, California 94303

ABSTRACT

This report provides some guidelines and procedures for the evaluation of component supports using the principles of linear elastic fracture mechanics (LEFM) in order to assure, by an optional analysis procedure, an acceptable level of material toughness. This report documents the work performed on the Unresolved Safety Issue A-12 and it addresses the practical application of LEFM to component support designs, and the stated NRC concerns regarding fracture toughness determination, treatment of residual stress, assumptions on flaw size, and the calculation of applied crack driving force. It is the purpose of the report to cover each of these issues and to demonstrate the feasability and potential benefit of LEFM to certain cases where other evaluation methods may be incapable of providing a means of assessing integrity.

This report should be viewed as a working document; to be modified as new information or data are obtained from this project or other programs. It is anticipated that under this project, the report will be revised at the end of the work scope (July 1984) since many areas discussed herein are still active tasks.

ACKNOWLEDGEMENTS

The author wishes to acknowledge the technical assistance of his colleagues, Dr. D. J. Hayes, Dr. G. R. Egan, Mr. W. C. McNaughton, Mr. J. L. Grover, and Mr. R. Cargill. Also, Dr. W. Oldfield of MRCS provided valuable guidance during the preparation of Appendix A of this report. Many helpful comments and suggestions from Dr. R. E. Nickell and Dr. T. U. Marston of EPRI were very much appreciated.

CONTENTS

CONTENTS
(Cont'd)

ILLUSTRATIONS

ILLUSTRATIONS
(cont'd)

TABLES

Section 1

INTRODUCTION

NRC UNRESOLVED SAFETY ISSUE A-12

Background to A-12

The Unresolved Safety Issue known as A-12 is an NRC safety issue which deals with the potential for low fracture toughness properties of component support materials. During the construction and licensing of the North Anna nuclear power plants Units 1 and 2, the fracture toughness of materials for the steam generator and coolant pump supports was called into question. The specific technical concern was the capability of the supports to maintain their structural integrity under postulated accident conditions. As part of this issue, a concern for lamellar tearing was also expressed and questions regarding the potential of such a condition to exist were raised. The immediate licensing concerns were resolved through fracture toughness testing of two of the support materials -- ASTM A36 and ASTM A572. The A572 toughness was determined to be inadequate at 80°F (27°C), resulting in a requirement to preheat the beams in the steam generator supports to 225°F (107°C) prior to reactor coolant system pressurization above 1000 psi (6.9MPa), with the stipulation that additional heating be available should the heat from the reactor coolant loop be insufficient to maintain desired support temperatures. The Nuclear Regulatory Commission's (NRC) concern in the North Anna licensing process led to a generic investigation known as the A-12 technical activity.

NRC Resolution

The NRC contracted the Sandia National Laboratories to examine the questions of low fracture toughness of component supports and lamellar tearing on a generic basis. Sandia submitted its findings in February 1979 and NUREG-0577 (1-1) was issued in draft form in October 1979 for comment, with the Sandia report as an appendix. With the issue of this document, the NRC considered both issues, and thus the Technical Activity A-12, to be generically resolved. However, subsequent to NUREG-0577, the NRC issued two letters (2) over the signature of the Director, Division of Licensing, which significantly amended the NUREG document. These letters, dated May 19, 1980 to all power reactor licensees,

and May 20, 1980 to all pending licensees, construction permit applicants, and licensees of plants under construction in effect, expanded the scope of the A-12 issue to also include:

1) Reactor vessel and pressurizer supports
2) BWR designs as well as PWR
3) All plants, not just operating units, and
4) Stress corrosion cracking assessment of high strength materials.

Among other items, Attachment 1 to these letters provided review procedures and criteria which differed from NUREG-0577 in that: (1) the fracture mechanics based assessment procedure was excluded (2) an evaluation procedure based on a consequence-of-postulated-failure analysis was added, and (3) if the consequence analysis failed to demonstrate conformance, then the NRC specified course-of-action is to control the operational temperature by ancillary heating. The intent of these changes was to minimize NRC staff involvement in the review of licensee and applicant submittals. By complying with these proposed procedures and criteria, the A-12 issue was considered resolved.

INDUSTRY RESPONSE AND COMMENTS

After issuing the May letters, the NRC staff received comments from utilities and vendors on many aspects of the requirements. The Electric Power Research Institute (EPRI), after examining the letters, and discussing the subject with its utility advisory structure became concerned about the exclusion of a fracture mechanics procedure in the NUREG amendment, and the expansion of scope to include all LWR plants. Questions were also raised about the difficulties in performing and the staff work load in reviewing assumptions and calculational procedures required for a proper failure consequence analysis. EPRI staff and contractors began to demonstrate the feasibility and utility of a generic procedure, based upon well-established principles of linear elastic fracture mechanics (LEFM), for addressing the issue of component support integrity following a briefing of utility representatives in June 1980.

A skeletal outline of this optional procedure was presented to the NRC and interested utility, vendor, and architect/engineering representatives at a meeting in Bethesda, Maryland, on August 27, 1980. Following this

presentation NRC staff responded that:

1. A fracture mechanics approach would be considered by the NRC as an option, provided that EPRI research satisfied concerns about the adequacy of the fracture toughness data base, stress intensity calculations for complex support geometries, methods for incorporating residual stresses, and definition of reference flaws.

2. The NRC would delay the final draft of the revised NUREG-0577 until the EPRI research was available (December 1980), and would delay the implementation date for NUREG-0577 until December 1982.

The December 1980 date was determined to give ample time for EPRI and its contractors to complete the assembly of the methodology and to demonstrate the use of the fracture mechanics approach on representative support geometries.

An interim meeting to brief the NRC and interested parties on the progress of the research was held in November 1980 in Bethesda. At that time NRC requested that the licensees and applicants commit to the EPRI approach as an option prior to the end of December 1980. To this end a meeting was held in Palo Alto, California, on December 10, 1980, to describe the fracture mechanics methodology in detail, with special emphasis on the NRC concerns: specifically the fracture toughness data base, stress intensity calculations for complex geometries, residual stresses, and reference flaw definition.

One week later a similar presentation was given in Bethesda, Maryland, to NRC staff and interested parties. The intent of this presentation was to demonstrate feasibility of the fracture mechanics alternative, and this demonstration was apparently successful, based upon NRC response (December 30, 1980, Memorandum from R. Snaider to K. Kniel). The NRC continues to be concerned, however, about excessive staff review time and has asked that

EPRI submit, by January 31, 1981, a document which contains:

(1) Specific applications in which LEFM can be applied and in which it would appear to be of the greatest benefit;

(2) Geometries in which LEFM usage is proposed, including a proposed solution for each geometry;

(3) Detailed definition of residual stress for each proposed geometry:

(4) Detailed list of fracture toughness data available, especially K_{Ic} listed by materials:

(5) A definition of the "reference flaw" to be used in the LEFM analysis; and

(6) Proposed margins of safety, and the parameter(s) to which they should apply.

This document attempts to address the NRC request while recognizing that, as a research organization with constraints, the request goes beyond the bounds in which EPRI can properly operate. The organization of this report has been structured in such a way, however, that additional information can be incorporated as it is developed or acquired.

SCOPE OF REPORT

The purpose of this report is to provide the bases for the optional evaluation procedures, with appropriate guidelines and recommendations for implementation of a fracture-mechanics-based assessment of structural supports. The report defines the necessary elements for an LEFM analysis; the important parameters included in the evaluation, and standardized analysis assumptions, method of approach and material acceptance criteria. Although work is currently underway to address the stress corrosion

cracking (SCC) aspect high strength structural materials, this subject is not discussed here, and the strategy and evaluation steps contained in this document exclude SCC considerations. It is anticipated that SCC evaluation procedures will be incorporated later.

As mentioned earlier, this report is intended to be a working document so that contributions from this and other organizations can be added as new information and data are obtained, such as stress intensity factor solutions for additional geometries, residual stress states, reference flaw size data, and fracture toughness data for other materials. The bulk of the analytical methodology and analysis input information is contained in the appendices. The main body of the report provides the evaluation strategy and the step-by-step procedures to be followed. It should be stated that the evaluation based on fracture mechanics is an optional method to the consequence analysis approach. Since it is an optional method, it can be employed at the discretion of the analyst, and that satisfying either type of evaluation (i.e. consequence analysis or fracture mechanics analysis) will be an acceptable disposition of nonconforming materials. Guidelines are provided as to the type of applications where a fracture mechanics analysis will be the most beneficial.

REFERENCES

1-1 Snaider, R.P., et.al. "Potential for Low Fracture Toughness and Lamellar Tearing on PWR Steam Generator and Reactor Coolant Pump Supports", U.S. Nuclear Regulatory Commission Report, NUREG-C577, October 1979.

1-2 Letter to all power reactor licensees (May 19, 1980), and to all pending operating licensees, permit applicants and plants under construction (May 20, 1980), from D.G. Eisenhut NRC Division of Licensing.

Section 2

STRATEGY AND METHOD OF APPROACH

GENERAL STRATEGY

An evaluation strategy is required to establish the necessary procedures that will ensure an adequate failure prevention approach to the A-12 issue. In applying fracture mechanics concepts to this issue, a philosophy has been adopted which involves the use of a "reference flaw" to demonstrate an acceptable level of toughness for the design. A reference flaw represents the largest flaw thought to exist in a structure, reflecting the fabrication procedures, quality control and preservice inspection used in the construction. Where appropriate a reference flaw would also account for flaw growth resulting from service loadings. Under this condition, the fracture toughness of the material and the service-induced loads are combined in an LEFM model to determine the critical flaw size for the structure. The acceptability of this critical flaw size is judged by comparing this flaw size with the reference flaw and including an appropriate safety factor.

A flowchart showing the integration of this information and the conditions which lead to an acceptable design is given in Fig. 2-1. The strategy outlined in Fig. 2-1 is based on preventing nonductile failure and combines the basic approach and methodology of the ASME Code Section III, Appendix G (2-1) and Appendix A of Section XI (2-2). The approach is divided into four parts with each part focusing on a specific step or requirement for the evaluation. The logic and flow of the procedure are therefore reflected in the order of the steps as described below:

- Part I - Definition of service loadings under postulated accident conditions and the determination of applied stress.

- Part II - Determination of fracture toughness, K_{Ic}, for the material under postulated service conditions.

- Part III - Determination of the minimum critical flaw size, a_c, given the applied stress and fracture toughness.

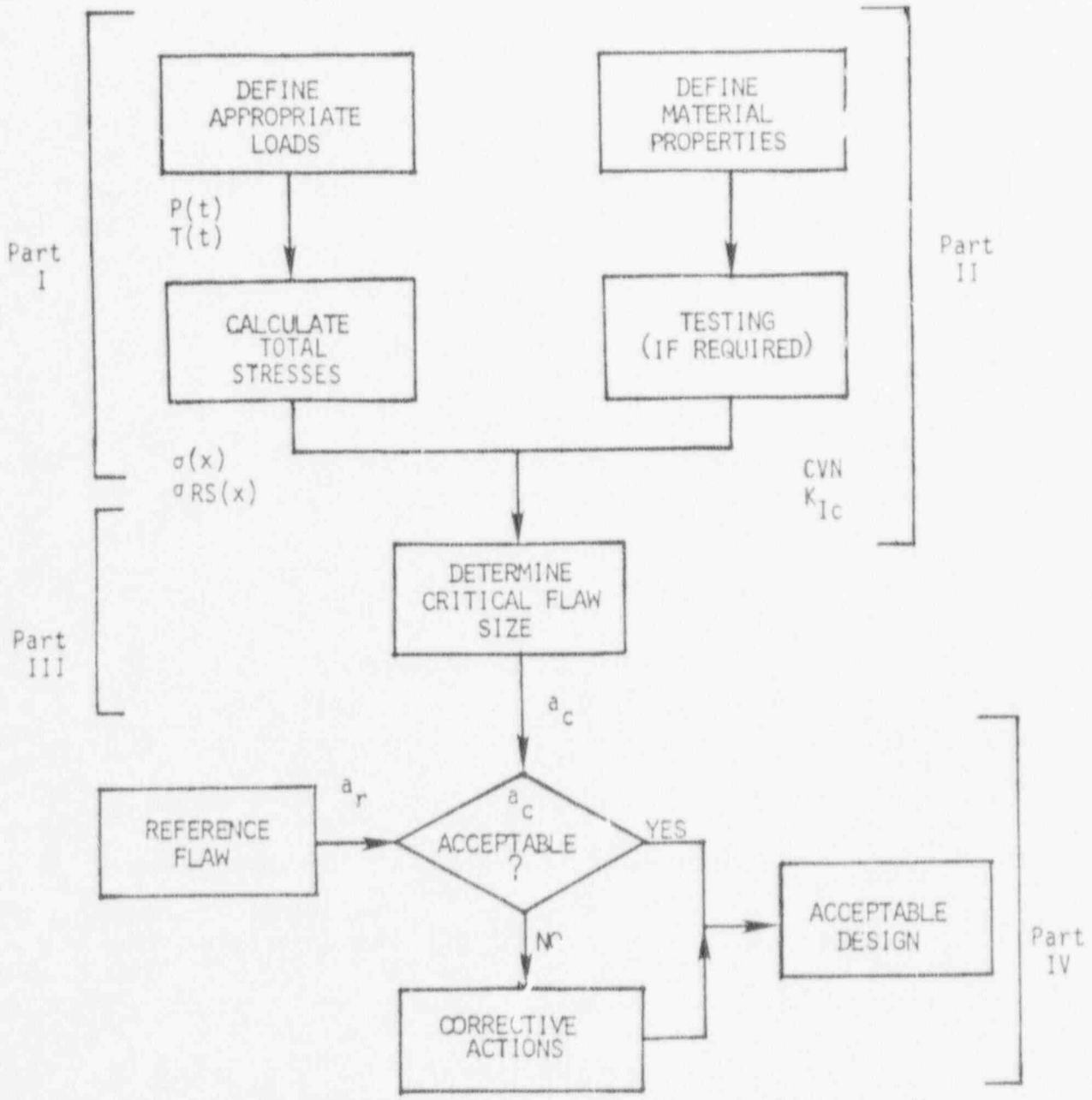

Figure 2-1 Evaluation Strategy Based on Fracture Mechanics

Part IV - Comparison of calculated critical flaw size with a "reference flaw" to establish material toughness acceptability.

The procedural steps for each part of the evaluation are given later in Section 3. With the exception of definition of service loads and stresses (Part I) each of the above analysis requirements is the subject for an appendix given in the back of this document. A review of typical plant designs indicates that although some geometries are generic, loads and operating conditions are plant specific. For this reason the examples described later should not be regarded as reflecting any particular plants. These appendices provide guidelines and recommended procedures for completing the evaluation.

FRACTURE MECHANICS CONCEPTS

Introduction

In applying fracture mechanics analysis to failure prevention studies where protection from nonductile failure under monotonically increasing loading is the criterion, it is important to establish the possible modes by which the structure may fail and the parameters which are important in determining the residual strength of a structure continuing defects. The failure behavior of structural steels can be classified into four regimes and the discipline required to assess these regimes are:

(1) Linear Elastic Fracture Mechanics (LEFM) - The structure fails in a brittle manner and, on a macroscale, the load to failure occurs within nominally elastic loading.

(2) Elastic-Plastic Fracture Mechanics (EPFM) - The structure fails in a ductile manner, and significant stable crack extension by tearing may precede ultimate failure.

(3) Local Plastic Instability - The failure event is characterized by local large deflections and local plastic strains associated with ultimate strength collapse at a cross section.

(4) Limit Load and Plastic Collapse - The structure exhausts its redundancy through the development of multiple local plastic instabilities until, under continued application of load, global collapse occurs.

A schematic diagram showing the relationship between critical or failure stress (i.e. residual structural strength), and flaw size is shown in Fig. 2-2 for the three failure modes described above. The shape and position of the failure locus will depend on the fracture toughness (K_{Ic}) and strength properties (σ_y and σ_{uts}) of the material, as well as the structural geometry (t) and type of loading. LEFM is used most appropriately to describe the behavior of low toughness/high strength materials in which the plastic zone is small relative to the structural geometry and little ductility precedes fracture. With this method, no account is taken of increased material resistance to brittle failure when significant plasticity occurs. Under LEFM conditions, the most useful parameter for characterizing the behavior of cracks is the stress intensity factor, K, which characterizes the singular stresses near the crack tip. In contrast, plastic instability, when it occurs without prior crack extension, is dominated by the flow properties of the material. In these circumstances, the failure condition is independent of fracture toughness and crack tip characteristics, and cross sectional properties are used to define the failure conditions. Elastic-Plastic Fracture Mechanics (EPFM) analysis can be used to predict failure behavior in the transitional regime between LEFM and limit load, and under EPFM conditions, the crack tip singularity, the material toughness, and net section strength are all important parameters for failure assessment. EPFM principles which incorporate a J-integral approach or COD have been applied to predict simple cross-sectional failure states under elastic-plastic conditions and well defined loading conditions.

Returning to Fig. 2-2, it can be seen that, at low values of applied stress or large values of a/t, LEFM is a conservative method for calculating critical flaw size or maximum load. For this reason, LEFM has been adopted by the ASME Code for demonstrating structural integrity, and with the addition of conservative assumption for material properties, initial flaw size, and safety factors, LEFM should always yield a conservative estimate for a_c provided that the computed value of a_c is greater than the flaw depth a_o illustrated in Fig. 2-2. Flaw depths smaller than a_o indicate a non-conservative estimate for a_c when LEFM principles are applied.

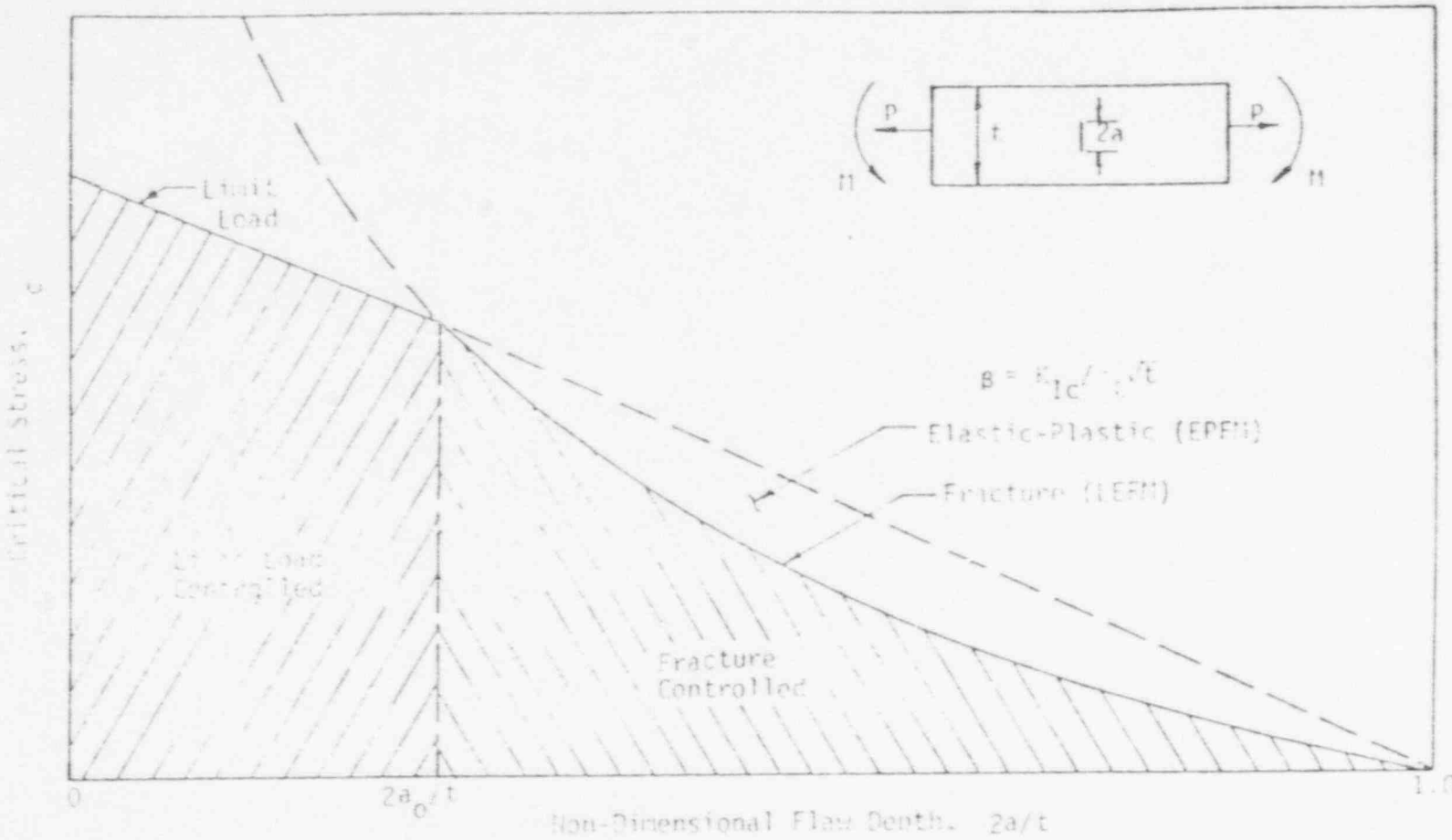

Figure 2-2 - Schematic Showing the Relationship Between Failure Stress and Flaw Size for Two Limiting Failure Modes

As a measure of susceptibility to brittle fracture, the relative positions of the different failure curves can be judged by defining a non-dimensional parameter which is the ratio of K_{Ic} to the material strength times the square root of thickness defined as β in Fig. 2-2. Typically, reactor pressure vessel steels under normal operating conditions (upper shelf behavior) have a β equal to unity. As β decreases, the susceptibility to brittle fracture increases.

LEFM Principles

The principles of linear elastic fracture mechanics effectively link three parameters: the defect size, the fracture toughness, and the applied stress; if any two of these are known, the critical value of third can be quantified. Although the stress distribution of a cracked structure for an arbitrary mode of loading and shape of body and crack can be quite difficult to determine, only three deformation modes can occur near the tip of the crack: the faces can be pulled apart (Mode I) or sheared perpendicular or parallel to the leading edge of the crack (Modes II or III). These three loading modes are shown schematically in Fig. 2-3a, and the character of the near-crack tip stress distribution is illustrated in Fig. 2-3b. The crack opening mode or Mode I, in which the load is applied normal to the crack face, is normally the most damaging of the three modes.

The most useful parameter for describing the character of the near-crack tip stress distribution is the stress intensity factor. The stress intensity factor, K, defines the local crack tip response to global conditions and is calculated in terms of the nominally applied stress, σ, the crack length, a, and a factor that depends on the flaw geometry, stress distribution, and structural displacement constraints, F(a), from the relation

$$K = F\sigma\sqrt{\pi a}. \qquad (2\text{-}1)$$

Assuming Mode I loading, fracture is predicted when the applied K_I value reaches a critical level. For plane strain conditions, this critical level

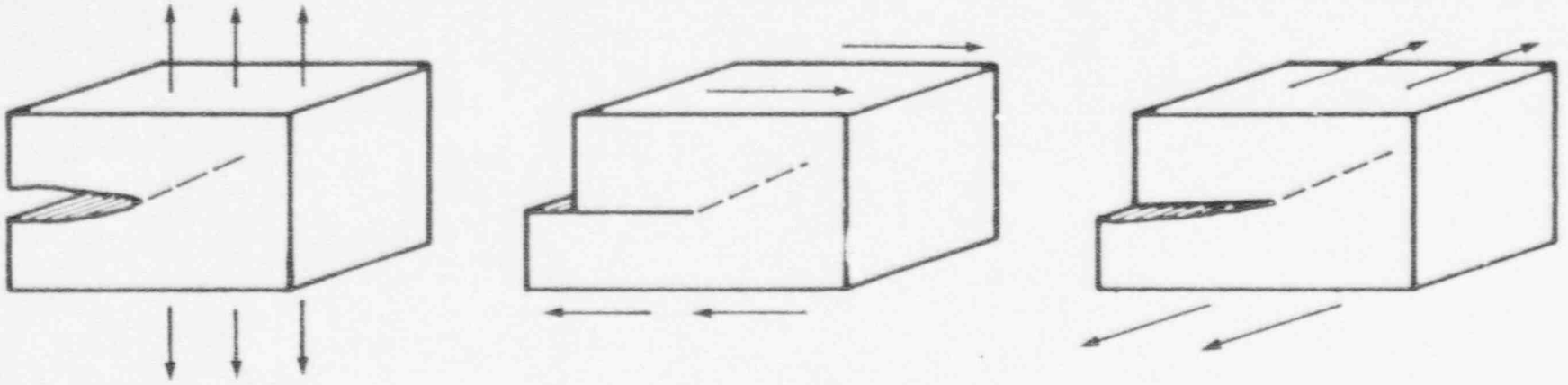

Mode I

Mode II

Mode III

a) Crack Tip Loading Modes

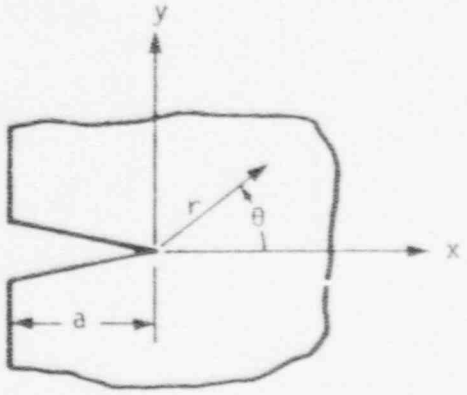

All Stress Components Have the Form:

$$\sigma_{ij} = \frac{K_k}{\sqrt{2\pi r}} f_{ij}^{(k)}(\theta)$$

Where i = x, y, z; j = x, y, z, and k = I,II,III.

No Summation is Implied and Stress Intensity Factor, K is Proportional to

(Nominal Stress) $\sqrt{(\text{Crack Length})}$.

b) Near-Crack Tip Stress Component

Figure 2-3 - Review of Linear Elastic Fracture Mechanics.

is the fracture toughness, K_{Ic}, and a requirement for safe operation is

$$K_I < K_{Ic}. \tag{2-2}$$

The critical value of applied stress can be computed in terms of flaw size and fracture toughness from the expression

$$\sigma_c = \frac{K_{Ic}}{F\sqrt{\pi a}}. \tag{2-3}$$

Likewise, given the applied stress and critical toughness, the critical flaw size can be determined implicitly from

$$a_c = \frac{1}{\pi}\left(\frac{K_{Ic}}{\sigma F}\right)^2. \tag{2-4}$$

A detailed discussion on the computation of K_I is given later in Appendix C.

In order to apply LEFM methods the analyst must have a knowledge of two of three important parameters. The appendices to this report outline methods for determining fracture toughness, stress intensity factor and flaw size to be used in the analysis.

NRC REQUIREMENTS FOR LEFM ANALYSIS

Upon consideration of the comments and proposals presented at the August 27, 1980 meeting, the NRC staff summarized the requirements for a fracture mechanics analysis. Contained in these requirements are criteria which are necessary ingredients that must be addressed in evaluation procedures. These requirements fall into five areas listed below:

1) The NRC will require confirmation of correlations between CVN and K_{Ic} data.

2) In developing correlations and material toughness curves, the NRC staff will require data from several K_{IC} or K_{IC} - like tests at appropriate temperatures for each class of material.

3) Residual stresses must be addressed in the fracture mechanics analyses.

4) K_I solutions must be applicable to the specific geometries being evaluated.

5) The NRC staff will need to examine the criteria used to define the reference flaw size. If NDE is used to define this flaw size, the staff will require a demonstration by mockup or model to confirm the reliability of the inspection system.

DEFINITION OF LOWEST SERVICE TEMPERATURE

A definition for the lowest service temperature (LST) for a structural support is required to determine the appropriate fracture toughness for the support members. The use of LST in the design of components is established in the ASME Code (2-3, 2-4) and a suitable definition of LST has been adapted here from the Code for component supports as:

> The lowest service temperature for a defined region in a component support shall be the minimum temperature which the material may experience when the pressure within the component being supported exceeds 20% of the preoperational system hydrostatic test pressure. The temperature shall be established by appropriate calculations or experiments and be based on atmospheric ambient conditions, insulation or enclosure provided, temperature of the foundation and consideration of heat transfer to or from the component through the support.

It is the intent of the evaluation procedures to determine the LST for the nonconforming members by this definition or similar definition as part of the fracture toughness assessment under Part II.

REFERENCES

2-1 ASME Boiler and Pressure Vessel Code, Section III, Division 1 Appendices - Appendix G, "Protection Against Nonductile Failure," 1980 Edition.

2-2 ASME Boiler and Pressure Vessel Code, Section XI, Appendix A, "Analysis of Flaw Indications", 1980 Edition.

2-3 ASME Boiler and Pressure Vessel Code, Section III, Subsection NB - Class 1 Components, Article NB-2300, 1980 Edition.

2-4 ASME Boiler and Pressure Vessel Code, Section IV, Subsection NE - Class MC Components, Article NE-2300, 1980 Edition.

Section 3

EVALUATION PROCEDURES

SCOPE

This section provides the step-by-step procedures for applying the fracture-mechanics-based method to the assessment of component supports fabricated from non-conforming materials. The procedure is based upon LEFM principles and is subdivided into four parts: 1) definition of service loads; 2) determination of fracture toughness; 3) critical flaw size calculation, and 4) material acceptance criteria. Appendices in the back of this document provide the details to perform the key aspects of the above analysis Steps 2, 3 and 4. Although these procedures apply to the structural materials and support geometries described in the appendices, the basic intent of the evaluation can be expanded to other situations by collecting more information and data. Wherever possible, guidelines and recommendations are provided in the appendices to expand or adapt the information and procedures to plant-specific applications. In applying these procedures, it is assumed that the location(s) of the nonconforming members have been identified and that the material specification is known.

PART I - DEFINITION OF SERVICE LOADS

The following subsection outlines the steps required to define the structural loads for input into the analysis. The support must be analyzed for the maximum postulated accident loading condition. It should be noted that loads for LOCA and SSE are not to be combined but the worst individual load case is to be used in the analysis. The following is an outline of the steps under Part I:

1) Identify the loading conditions for the structural support to be evaluated,

2) Determine the maximum loading condition for the structure and identify the most highly loaded nonconforming member or members in the support design,

3) Determine by measurement or analysis the lowest service temperature (LST) for each location identified in Step 2 above. If the LST for regions are not known, then a value of 75°F (24°C) may be assumed,

4) For the service load and temperature conditions defined above, calculate the stress for the regions or members which are nonconforming within the support. All forms of loading should be considered including mechanical loads, thermal stresses, and residual stresses. Guidelines for the treatment of residual stresses from welding are provided in Appendix B. The stress definition should be sufficient to include discontinuity and local stress concentration effects.

PART II - DETERMINATION OF FRACTURE TOUGHNESS

The fracture toughness, K_{Ic}, is required in the computation of critical flaw size and is based on a statistically determined bound of static initiation critical values of K_I measured as a function of temperature. The procedures given below and in Appendix A are intended to determine the appropriate K_{Ic} value for two situations: 1) when data from the actual product form are not available, and 2) when data from impact tests (Charpy V-notch) are available.

Data Not Available

For the case when fracture toughness properties are not available for the actual material, the following steps are to be followed:

1) From the material specification, establish the material composition, heat treatment, melt practice, strength level and grade, and other parameters which are important to the determination of material condition.

2) Determine the value of K_{Ic} at LST from the statistically-based bound curves compiled in Appendix A. The curve selected should be for the same material specification as the actual material, and match as closely as possible the actual material condition as identified in Step 1.

3) If a fracture toughness curve for the particular material specification is not available in Appendix A, then use the material classification provided in the appendix to determine the material class or group. The fracture toughness to be used will be the lowest value of K_{Ic} at LST determined from the materials in the group.

Charpy Impact Data Only

For the case when only Charpy data are available for the actual material, the following steps may be followed in lieu of using the statistically-based bound curves:

1) Develop a CVN versus temperature curve from the available CVN data which satisfy the requirements given in Appendix A.

2) With this curve, use the CVN-K_{Ic} referencing procedure provided in Appendix A to determine the bounding K_{Ic} curve as a function of temperature.

3) From this curve, select the value of K_{Ic} at LST for the support member.

4) If only a few CVN data points are available use the guidelines in Appendix A to establish the full CVN curve.

Material Testing

In the event that the procedures for the above situations give overly conservative estimates for K_{Ic}, results from actual tests conducted on similar heats of the material in question may be used to define K_{Ic}. The

values so determined should represent the product form and take into account material variability, testing techniques, and any other variables which may lower K_{Ic}.

PART III - CRITICAL FLAW SIZE CALCULATION

The results from Parts I and II are now combined in the LEFM model to calculate the critical flaw size, a_c. The procedure for determining the minimum critical flaw size is as follows:

1) From the results of Part I, determine the highest stress location or locations for the nonconforming member.

2) Using the guidelines given in Appendix D, establish the flaw shape and orientation to be postulated for each location to be evaluated.

3) Again from Part I, determine the stress profile through the thickness of the member at the postulated flaw location.

4) Calculate the stress intensity factor, K_I, as a function of crack depth by the procedures given in Appendix C.

5) The crack depth at which the calculated K_I exceeds the K_{Ic} value corresponds to the critical flaw size, a_c.

6) Repeat steps 2 through 5 to calculate a_c for each location identified in Step 1.

7) The smallest value of a_c determined by the above procedure after all postulated accident load cases have been considered is the minimum critical flaw size for the structure or member.

PART IV - ACCEPTANCE CRITERIA

The procedures and criteria to be used to demonstrate acceptance for nonconforming materials are proposed below and are consistent with ASME Code Section XI (see Appendix D):

1) Determine the reference flaw size, a_r, from the guidelines provided in Appendix D.

2) The structure is acceptable for continued service if either of the following conditions are satisfied.

$$a_r < 0.5a_c,$$

$$K_I < K_{Ic}/\sqrt{2},$$

where K_I is the maximum applied stress intensity factor for the flaw size a_r, and K_{Ic} is the available fracture toughness.

3) When NDE techniques are used to establish the postulated flaw size for the support, smaller defect sizes will be allowed provided that it can be assured that the inspection system employed can reliably detect the smaller flaw.

Section 4

APPLICATIONS

SCOPE

The purpose of this section is to discuss specific applications to demonstrate the implementation of the evaluation procedures presented in Section 3. Some sample evaluations for typical support geometries are presented herein with the analysis details to follow in Appendix E. These analyses will serve as examples as to the effort required to complete an evaluation. Before these examples are introduced, the situations requiring evaluation are considered, and the advantages and disadvantages among the various evaluation options are presented.

SITUATIONS REQUIRING EVALUATION

Evaluation of structural supports will be required in lieu of replacement or heating when a material has been identified as nonconforming by the toughness acceptance standards similar to those proposed in the attachment to the May 1980 letters. These acceptance standards provide the requirements for NDT or CVN data and give guidelines for the situation when no plant material data are available. If a material initially fails the acceptance test and is therefore deemed nonconforming there are several options available without the need for evaluation or corrective actions as given below:

1) If no data are available, impact tests may be performed to generate plant-specific data to be applied in the toughness acceptance comparisons.

2) Engineering judgement may be applied in order to rationalize the material properties for the situation when the data do not clearly satisfy or violate the acceptance standards.

3) Demonstrate that the LST for the support is sufficient to satisfy the requirements.

These options should be reviewed prior to initiating an evaluation subject to the cost-benefit tradeoff associated with performing testing versus analysis. If after these considerations it is concluded that evaluation is required (accepting that material replacement or operational temperature control of support temperature is only to be considered as a last resort) then any one or all of the following situations regarding nonconforming materials may need to be addressed:

1) All instances where a material with the specified minimum yield is greater than 180 ksi (1241 MPa).

2) Structural steel with available toughness data

3) Structural steel with no data.

4) Bolting material with available toughness data, and

5) Bolting material with no data.

The areas where there potential benefits for fracture mechanics evaluation are discussed next.

CONSEQUENCE ANALYSIS VERSUS FRACTURE MECHANICS

The best method to be applied to the five nonconforming cases identified above depends on many factors, the most important being:

1) redundancy of design

2) location of nonconforming member in the support

3) effective utilization of strength in the design (σ / σ_y)

From a structural point of view, a consequence analysis will have the best chance of success if the structure is comprised of many members, hence forming a highly redundant structure. The requirements for this type of analysis are summarized in Table 4-1, and the removal of one member will not appreciably degrade such a system. Likewise, it may be concluded by inspection that certain less redundant support designs will fail a consequences analysis and these situations are candidates for evaluation by fracture mechanics.

Table 4-2 provides a summary of typical support designs and the suggested analysis method to be applied. Those supports with a high degree of redundancy and load shedding capacity are the truss/frame design, especially the one type with moment-resistant members, and bolted connections where large numbers of bolts or studs are employed. The applications for a flaw evaluation are the pin-column design where three or four leg-columns are used to support steam generators or coolant pumps.

It is recommended that some bounding calculations be performed before embarking on one approach, using strength-of-materials stress estimates and simplified fracture mechanics equations, to decide which approach will give the highest probability of success.

SUMMARY OF EXAMPLE PROBLEMS

Three typical support geometries were evaluated with the procedures specified in this document. These evaluations were for

1) a beam-to-beam welded connection typical of a space-frame structure,

2) a pin-column support for a steam generator, and

3) a reactor coolant pump anchor stud.

TABLE 4-1

EVALUATION BY CONSEQUENCE ANALYSIS

The following are the assumptions and requirements for a consequence analysis (4-1):

1) Assume the highest stressed nonconforming member has failed;

2) The support provided by piping and adjacent structures, if connected, may be included;

3) Apply maximum accident loads (i.e., LOCA or SSE);

4) Under the above conditions, the calculated displacements of the support must not:

   (a) Impair the function of the component required to shutdown and cooldown safely, and

   (b) Rupture the pressure boundary severely enough to prevent safe shutdown and cooldown.

TABLE 4-2

SUMMARY OF SUPPORT DESIGNS

SUPPORT SYSTEM	MOST BENEFICIAL APPLICATIONAL METHOD
1. Truss/Frame Design	
• Moment Resistant Members (Space-Frame)	Consequence Analysis
• Pinned-End Type (Pinned-Frame)	Consequence Analysis and Possible Fracture Mechanics
2. Pin-Column Design	
• Structural Shape Columns	Fracture Mechanics
• Forged Columns (Eyebar)	Fracture Mechanics
• Pipe Columns	Fracture Mechanics
3. Skirt Supported	Fracture Mechanics
4. Sliding Pedestal	Most Beneficial Method Not Yet Defined
5. Bolting	Consequence Analysis or Fracture Mechanics

Although Example 1 is a situation where a consequence analysis may be a better choice for evaluation, this analysis illustrates the application of the LEFM procedures to a welded structure including added complexity of residual stress.

Each example is aimed at demonstrating some important aspect of an LEFM analysis rather than cataloging support structure evaluations. This effort demonstrates the feasibility and utility of fracture mechanics based evaluations of non-complying support structures.

REFERENCES

4-1 Letter to all power reactor licensees (May 19, 1980), and to all pending operating licensees, permit applicants and plants under construction (May 20, 1980), from D.G. Eisenhut NRC Division of Licensing.

Section 5

SUMMARY AND CONCLUSIONS

After investigating the applicability of linear elastic fracture mechanics (LEFM) to component support designs, it is concluded that LEFM analysis would be beneficial in many situations and possibly the only viable way to demonstrate adequate integrity for cases that can not be evaluated under the assumptions of a consequence analysis. It has been shown that for each concern raised by the NRC staff, there are available methods and data to perform a proper LEFM analysis.

Having demonstrated the feasibility of the application of LEFM to supports, it should be noted that LEFM analysis is not a cure-all procedure and that there may be situations where the LEFM option is not the optimal procedure. However, there are situations where application of this method will be simple and direct. Proper review of plant-specific geometries and materials will identify those nonconforming situations where the evaluation procedures presented herein will be the most useful. The intent of this report is to be a working document, to be expanded as additional data are acquired.

Three examples are presented which illustrate some important aspect of LEFM analysis and the evaluation procedures as applied to some typical component support designs.

APPENDIX A

DETERMINATION OF FRACTURE TOUGHNESS

INTRODUCTION

The purpose of this appendix is to outline the procedures for determining the static fracture toughness, K_{Ic}, for support materials. In applying these procedures it is assumed that the information for the nonconforming material is known to include the ASME, ASTM or AISI specification, the chemical composition, heat treatment, and grade or strength level. This information is essential in selecting the correct fracture toughness curves.

This appendix provides guidance for two situations: 1) the case when the toughness of the material is not known, i.e., no plant-specific data are available, and 2) some toughness data are available in the form of Charpy impact tests. It is anticipated that the no-data system will be the most prevalent. This case is handled by providing statistically-based bounding curves for support materials that are frequently encountered. A compendium of these toughness curves is provided at the end of this appendix, and this listing will expand as new data are obtained.

The second case entails the use of a referencing procedure to correlate CVN data to K_{Ic} based on a procedure under development by a MPC/PVRC Task Group on Reference Toughness. Since this methodology is the basis of the fracture toughness curves given at the end of this appendix, the subject of referencing fracture toughness properties, given Charpy V-Notch (CVN) data, will be presented next.

CONCEPT OF REFERENCE FRACTURE TOUGHNESS

The fracture mechanics procedures recommended for the evaluation of supports are those of linear elastic fracture mechanics (LEFM) and are consistent with the rules established by the ASME Boiler and Pressure Vessel Code, Section III (A-1) and Section XI (A-2). The ASME procedure was first

developed for the fracture-safe design of nuclear pressure vessels and was incorporated into the ASME Code, Section III, Appendix G in 1972. The design-by-analysis method allows some flexibility in deriving solutions to design requirements, as long as the solutions meet certain guidelines and performance specifications. The basic concept of the reference fracture toughness curve was recommended in WRC Bulletin 175 (A-3) and the approach entails the use of a lower bound fracture toughness called K_{IR} which is defined over a range of temperatures for a given population of steels. Through the use of a nil ductility reference temperence (RT_{NDT}), a given heat of steel can be indexed to the K_{IR} curve through the use of simple tests, that is drop weight-NDT or Charpy V-notch for the material. By plotting fracture toughness data (K_{Ic}, K_{Id} and K_{Ia}) as a function of T-RT_{NDT}, the variability among heats of materials was believed to be reduced. A large research effort has been sponsored by EPRI in the last seven years to validate the K_{IR} concept and to incorporate a statistical basis (A-4 through A-7). The most important findings are summarized in Fig. A-1. Although none of the low temperature data seriously violated the K_{IR} curve, a number of important results were obtained. This figure shows a large collection of fracture toughness measurements for over 50 heats of reactor pressure vessel materials plotted against a temperature ordinate (T - RT_{NDT}). The test results included static compact, dynamic compact, and impact bend fracture toughness test methods, together with J-R curve data and all data were valid by the current methodology.

This brief description of the K_{IR} concept is provided to give some background to problem of providing a reference curve to toughness. However, some important concerns regarding the K_{IR} curve should be noted (A-9):

1) The current K_{IR} curve is based on the graphical lower bound of static (K_{Ic}), dynamic (K_{Id}) and crack arrest (K_{Ia}) fracture toughness.

2) By defining the K_{IR} curve as the lower bound to all available fracture toughness data, any new data added to the data base will

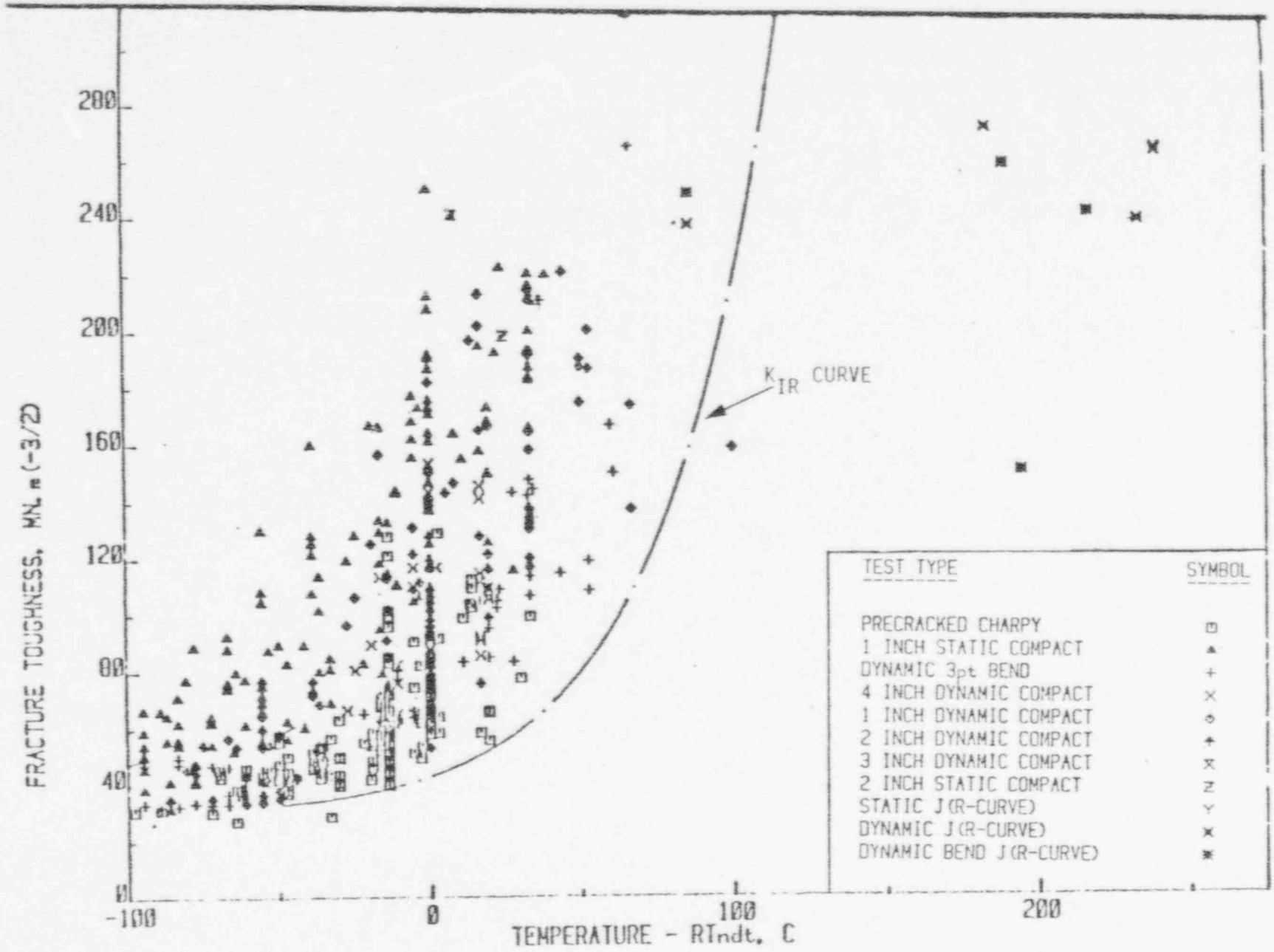

Figure A-1 Fracture Toughness versus Temperature

cause K_{IR} curve to be revised lower, or remain unchanged at best, leaving no chance for improving the technique unless the definition of K_{IR} is changed.

3) The K_{IR} approach avoids the requirement of measuring fracture toughness on current production heats by relying on the drop weight-NDT and Charpy V-notch tests to indicate heat-to-heat variability. However, the referencing procedure (the use of $T - RT_{NDT}$), was untested when the Code was introduced and the major part of the data was obtained from a single heat of material so that the empirical basis for the assumption that a reference temperature ($T - RT_{NDT}$), could be used to relate all heats of material to the same fracture toughness bound was untested.

4) The current K_{IR} curve approach is not statistically-based and thus the uncertainties associated with establishing the lower bound or the indexing parameters are not defined.

Upon examining the K_{IR} with relation to the data, as shown in Fig. A-1, the bound is extremely conservative in the transition temperature region when applied to static test data. Another observation which is not obvious from Fig. A-1, is that the unreferenced data show slightly less spread than the referenced data of Fig. A-1. In other words, referencing by RT_{NDT} increased the variance of the data instead of reducing it. It was many of these concerns which has led to the current effort to revise the K_{IR} philosophy.

REVISED REFERENCE CURVES

Background

A PVRC/MPC Task Group has been developing methodology to address many of the questions regarding reference toughness. The ultimate goal of the group will be to recommend a statistically-based bound to all toughness with an appropriate technique to reference this new fracture toughness curve. The

methodology development is being funded by EPRI with the following objectives:

1. Develop a more precise referencing procedure
2. Incorporate a treatment of upper shelf fracture toughness
3. Show a statistical bound to fracture toughness

A summary of the progress to-date is given by Oldfield (A-9).

Representation of the Fracture Toughness Curve

The fracture toughness dependence on temperature is well represented by a hyperbolic tangent fit to the data (A-4). This curve-fit expression for toughness is given below:

$$K_{Ix} = A + B \tanh \left[\frac{T - T_o}{C}\right] , \qquad (A\text{-}1)$$

where K_{Ix} is the fracture toughness (K_{Ic}, K_{Id}, etc.), and A, B, C and T_o are four curve-fit constants. In the context of this work, Eq. A-1 will be used to express the static fracture toughness, K_{Ic}. The constants in Eq. A-1 have a physical interpretation with respect to the toughness-temperature curve as shown in Fig. A-2. The quantity A-B represents the lower shelf toughness and A+B the upper shelf, and the ratio of B to C is the slope of the transition region between shelfs. The value of T_o is the mid-point temperature of the transition region. This representation of fracture toughness will prove to be useful when correlating CVN test results to fracture toughness.

Indexing Fracture Toughness via CVN Test

After study of a number of alternative procedures by the Task Group, the Charpy V-Notch (CVN) test was selected as the reference test, aided by statistical regression procedures. The same tanh-fit model which has been used to express fracture toughness as a function of temperature also works well for CVN. When the CVN energy is transformed by taking the square root

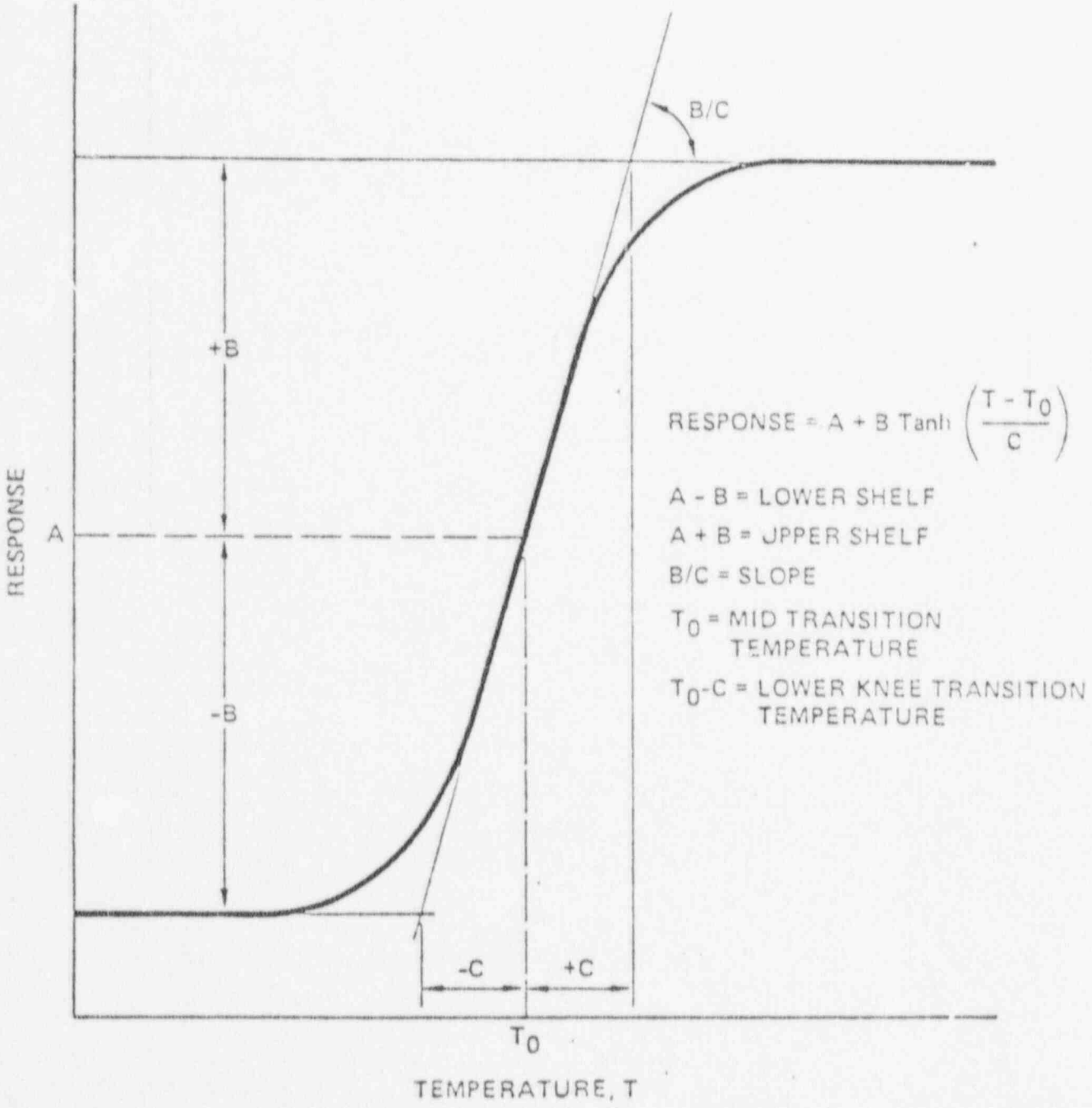

Figure A-2 Features of the Hyperbolic Tangent Model.

of the product of the temperature-dependent modulus (E) and the CVN energy (Y), the resulting variable (y) is (for CVN samples with a constant cross-section area) dimensionally the same as fracture toughness:

$$y = (E \quad Y)^{1/2}, \tag{A-2}$$

where E is modulus of elasticity. A suitable formula for incorporating the temperature dependence of modulus into Eq. A-2 is to use the following expression:

$$E = 207200 - (57.1)T, \tag{A-3}$$

where T is in °C and E has the units of MPa.

An expression for the transformed Charpy curve:

$$y = A_k + B_k \tanh \left[\frac{T - T_{o_k}}{C_k} \right] \tag{A-4}$$

Since most sets of CVN measurements do not include lower shelf data, and study of the data base showed that the position of the lower shelf is fairly constant from one material to another, it was found to be advantageous to use only three variable parameters by fixing the lower shelf for the transformed CVN curve to a low value, $y = 0.730 \text{ksi}\sqrt{\text{in}}$ (0.801 MPa $m^{1/2}$). This value was determined from a weighted average of lower shelf values of y for the steels investigated (A-9). The coefficients B_k, T_{ok}, and C_k were found to have most of the required properties for referencing parameters, i.e., (1) using all the data in a regression treatment, their standard errors are minimized, and (2) their accuracy is known from the regression treatment.

The referencing scheme developed in this way was more general than the K_{IR} procedure, which was really an adaptation of the older DWTT concept. The quantities A and B define the position and range of the toughness transition; the quantities T_o and C correspondingly show the position and range in the temperature scale. Reference toughness and reference temperatures can be defined,

$$k = \frac{K_{Ic} - A_k^{\alpha}}{B_k}, \qquad (A\text{-}5)$$

$$t = \frac{T - (T_{o_k} - \gamma)}{C_k^{\delta}}, \qquad (A\text{-}6)$$

where k and t are the reference toughness and temperature values; K_{Ic} and T are valid fracture toughness and temperature measurements, A_k, B_k, T_{ok} and C_k are developed from y, T data generated by CVN tests on the same material from which the K data were obtained. The quantities α, β, γ and δ are scaling parameters which allow the magnitude of y to be comparable with that of fracture toughness. By this procedure, it was possible to compile large collections of fracture toughness data on a single plot.

To illustrate this point, the static fracture toughness data from the EPRI data base (A-8) were plotted in Fig. A-3. In plotting the actual toughness data the reference toughness and temperature were determined from

$$k = \frac{K_{Ic} - A}{B}, \qquad (A\text{-}7)$$

$$t = \frac{T - T_o}{C}, \qquad (A\text{-}8)$$

where the constants in the above equations result from the curve-fit of Eq. A-1 to the data. To provide a means of indexing the data (or curve) present in Fig. A-3, one possible procedure would be to determine the reference temperature from CVN test with Eq. A-6 before entering Fig. A-3. However, an alternate way which will result in the complete toughness curve for a given heat of material is to provide factors which correlate the parameters between the CVN expression (Eq. A-4) and fracture toughness (Eq. A-1). This indeed has been done (A-9) and the following correlations result:

$$A = K_1 + K_2 B_k$$

$$B = K_3 B_k$$

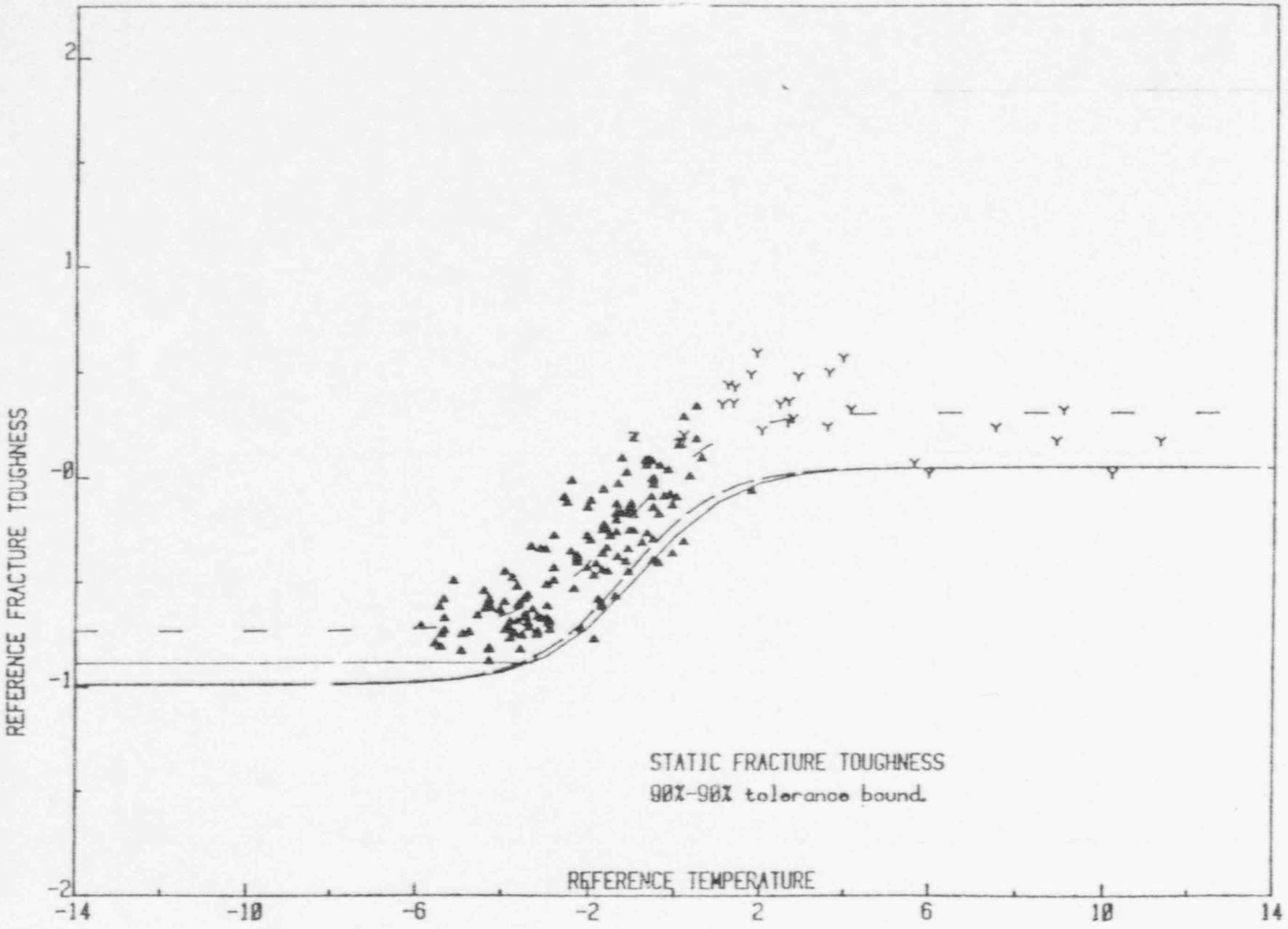

Figure A-3 Static Toughness Data Referenced by CVN Test. Separate Bound For Lower Shelf Has Been Defined.

$$T_o = T_{o_k} + K_4 + K_5 C_k \qquad (A\text{-}9)$$

$$C = K_b C_k$$

A bound on the lower shelf toughness is also provided by an additional constant in the expression

$$\text{lower shelf} = K_1 + K_7 B_k \qquad (A\text{-}10)$$

The values for all the constants are given in Table A-1 for predicting the mean curve, and the 90%-90%, 95%-95% and 99%-99% bounds to the static fracture toughness. The inherent units in these constants are temperature in °C and toughness in MPa $m^{1/2}$.

Verification of Procedure

The procedure has been tested on many heats of similar materials from which the correlation was developed including base plate as well as weld metal and weld heat effected zones. For static properties, the mean and 90%-90% curves shown in Fig. A-3 were constructed from the CVN tests data and show good agreement with the actual K_{Ic} data. Similarly from the same data base, equally good representation is observed with fracture toughness data generated from dynamic and dynamic bend tests shown in Figs. A-4 and A-5.

In addition to reactor pressure vessels, the procedure has been tried on structural steels where the yield strengths ranged from 36 ksi (248 MPa m^{-2}) to 140 ksi (965 MPa m^{-2}) and remarkedly good agreement has been observed. Work to demonstrate the validity of the method is ongoing business with the Task Group. A list of materials where the referencing procedure has been successfully applied is given in Table A-2.

Table A-1

CONSTANTS FOR FRACTURE TOUGHNESS PREDICTION FROM CVN TEST

Constant	Static Fracture Toughness*			
	Mean Curve	90% - 90% Bound	95% - 95% Bound	99% - 99% Bound
K_1	48.3924	48.3924	48.3924	48.3924
K_2	41.3439	22.3145	17.8278	9.8196
K_3	38.0082	37.8396	37.8240	37.7927
K_4	30.2050	30.2050	30.2050	30.2050
K_5	-0.8108	-0.7194	-0.7239	-0.7324
K_6	1.0753	1.1170	1.1191	1.1232
K_7	-	-8.5551	-11.1637	-15.9112**

* Bounds given represent the probability of occurance with a stated confidence level.

**This coefficient gives an excessively conservative prediction since the lower tail of the probability distribution is curtailed.

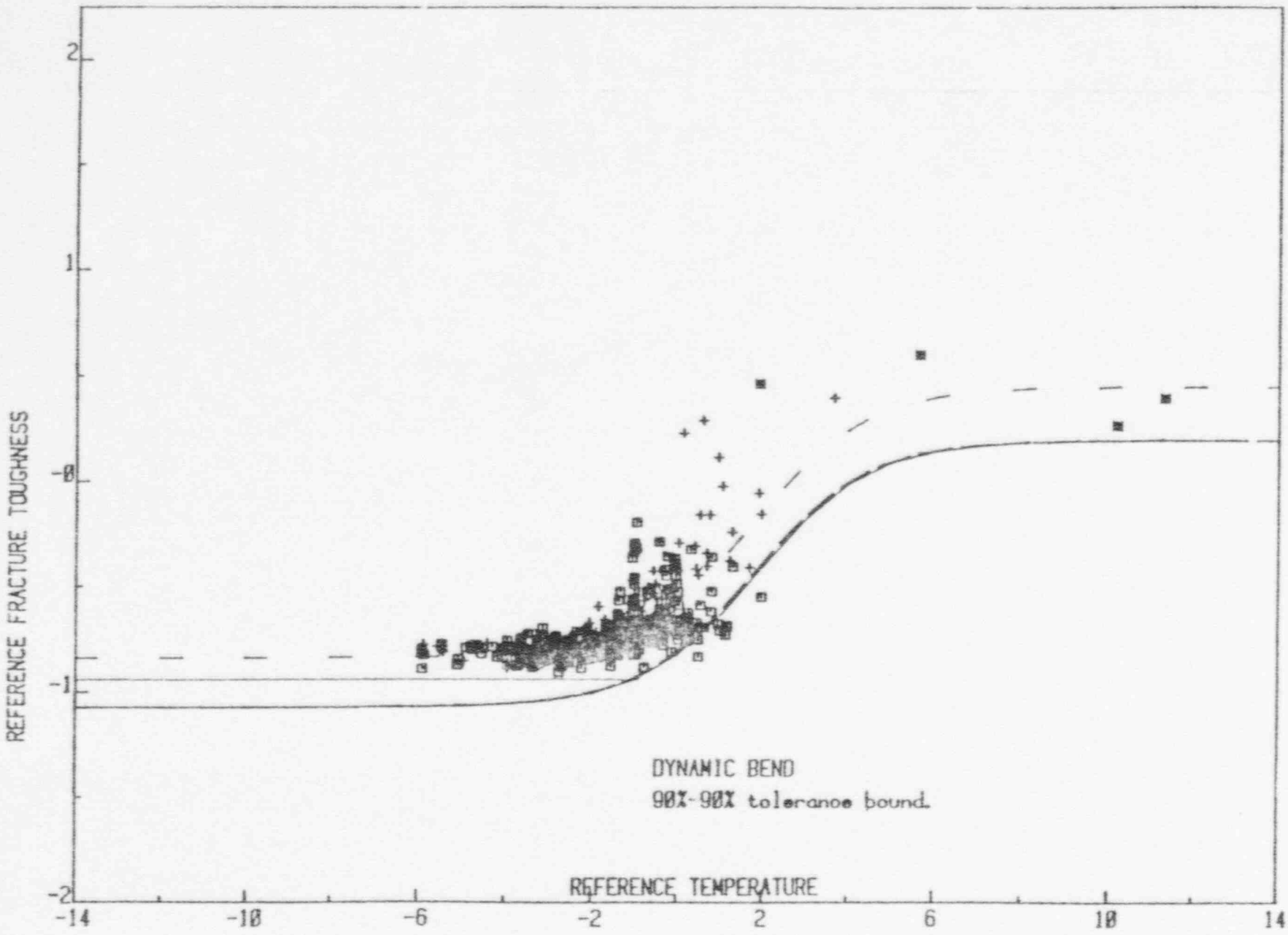

Figure A-4 Dynamic Bend Data Referenced by CVN Test. A Separate Bound For Lower Shelf Has Been Defined.

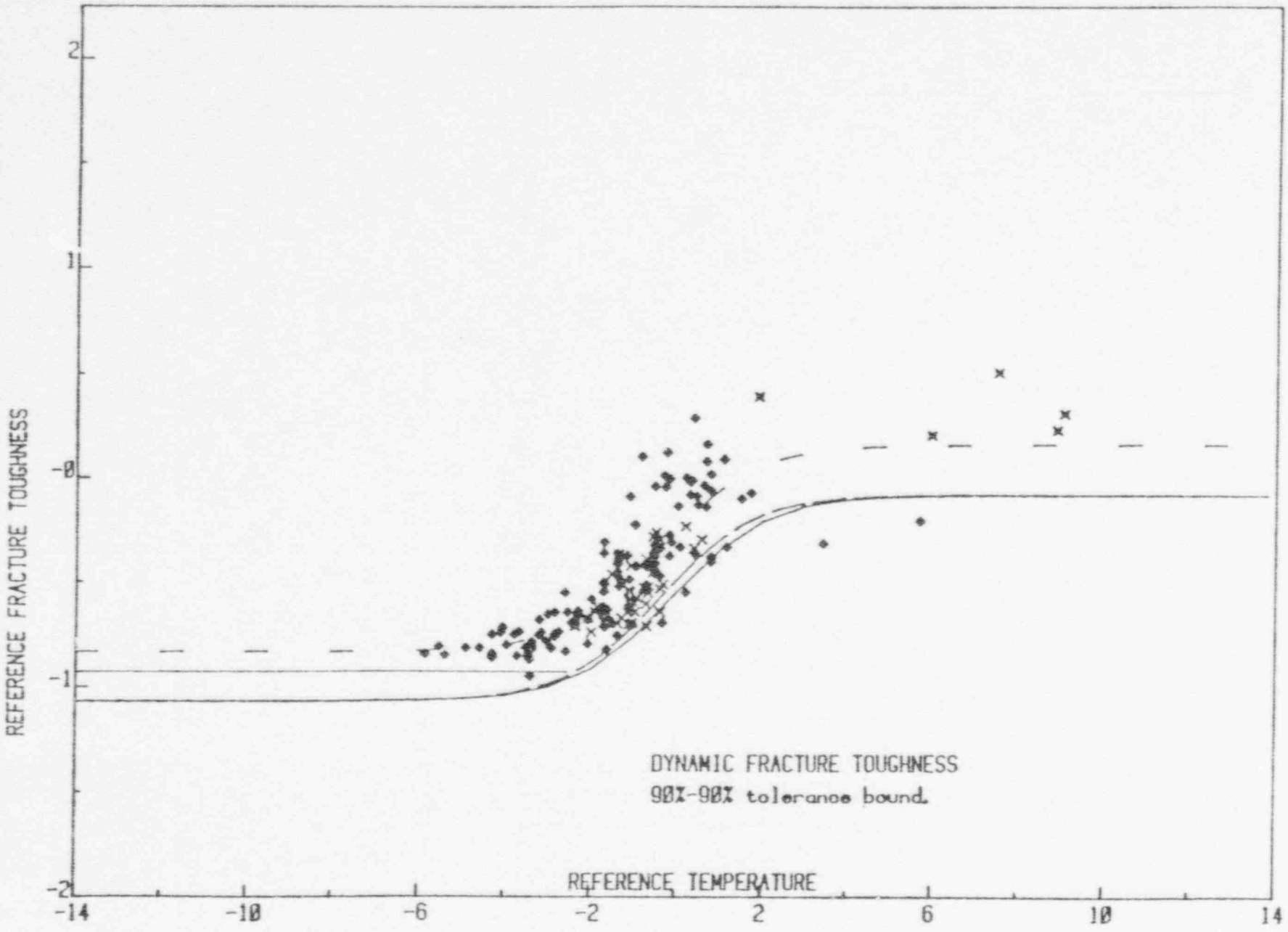

Figure A-5 Dynamic Toughness Data Referenced by CVN Test. Separate Bound For Lower Shelf Has Been Defined.

TABLE A-2

MATERIALS FOR WHICH THE REFERENCING PROCEDURE HAVE BEEN TESTED

MATERIAL	NUMBER OF HEATS
SA533A-2	3
SA533B-1	33
SA508-1	1
SA508-2	21
SA508-3	8
SA302B	1
SA515-70	1
SA516-70	19
SA537-1	1
SA537-2	2
SA105GR.II	1
SA299	2
A543-1	5
SPV-50	1
A36	4
A540	5
	108

APPLICATION OF REFERENCING PROCEDURE

Requirements on the Charpy Curve

Since the referencing procedure requires the CVN energy as a function of temperature, criteria for an acceptable number of test point over a suitable range of temperature needs to be established. The necessary criteria to ensure that the CVN curve is well suited for application is currently being developed by the PVRC/MPC Task Group. Although no specific criteria have been written, the following are some guidelines and recommendations:

1) A minimum number of 8 to 12 CVN test points have been observed to yield good correlations

2) The data should be distributed over several temperatures to include a minimum of 2 to 3 tests conducted on the upper shelf 2 on the lower shelf and the remaining within the transition region.

3) If data on upper shelf are lacking but racture appearance (% shear) data for the specimens tested within the transition region are available, the upper shelf energy may be inferred by extrapolation to 100% with the guidelines given in (A-6).

4) In all cases where data are inadequate to construct a complete Charpy curve, engineering judgement must be exercised to include reviewing data from the data base to make estimates of actual behavior as well as information in the literature.

The set of 8 to 12 CVN energy measurements seems practical, however if only a few points or no data are available, then guidance is provided later on the use of bounding curves.

Summary of Procedure

Once the CVN results have been established, the following are the steps required to generate the fracture toughness curve:

1) Convert the CVN impact energy to the units of fracture toughness with Eq. A-3 and Eq. A-4.

2) Determine the constants A_k, B_k, T_{o_k} and C_k by fitting the hyperbolic tangent model (Eq. A-4) to the now transformed CVN curve, y(T).

3) Given the constants A_k, B_k, T_{o_k} and C_k, calculate the coefficients for the fracture toughness curve, A, B, T_o and C with Eq. A-9 and Table A-2. For consistancy with the toughness requirements specified in NUREG-0577, the constants for the 90%-90% curve (or lower) from Table A-2 should be used, when computing these coefficients.

4) From the expression for static fracture toughness, calculate the available K_{Ic} level at T equal to LST.

USE OF LOWER BOUND CURVES (NO-DATA CASE)

Scope

More often than not, the situation will be that a set impact data for the actual material is either too small or not available at all, and a rational way to implement the referencing procedures cannot be achieved. For this situation, a compilation of static fracture toughness curves for support materials where data have been reported in the literature. These curves are given at the end of this appendix, and have been generated primarily by apply the referencing procedure to sets of CVN data. The curves given herein reflect the worst material for the sample of material collected.

Inherent in the use of these curves is the assumption that the sample size and the statistical treatment of the data is sufficient to allow the use of the curve to represent an estimate of K_{Ic} for a material where limited data is available.

The curves give the mean prediction and the 90%-90%, 95%-95% and 99%-99% bounds. These curves should be considered as being preliminary in that some may only represent the worst heat of a few heats and more data have been collected but not yet incorporated in the analysis. In most cases, the curves presented are only those heats where both CVN and K_{Ic} data both exist so that the referencing procedure could be tested. It is anticipated that existing curves will be improved and new ones added as more of the information collected is analyzed.

Classification of Structural Steels

A division of wrought products used in supports is given in NUREG-0577. This classification of wrought grades into groups is given in Table A-3. Many of the structural steels are included in Table A-3 however some materials used in components supports are not classified in the table. Indicated in the table are those materials where data have been collected, and also the materials where the CVN-K_{Ic} referencing procedure has been tested.

Although the NRC staff has indicated that not all materials within a given group had to be pedigreed and that the fracture toughness established for a group classification would suffice, there exist some problems with the categories. One concern is that a simple ASTM product specification may be inadequate to specific the toughness for an alloy when several alloys or strength levels can satisfy a single ASTM specification. Other concerns with the classification exist and the table is under review in order to determine a revised grouping scheme. For this reason, when using Table A-3, engineering judgement should be used when attempting to classify your actual material to other materials for which data are availabl..

Table A-3

Classification of Wrought Grades into Groups

Plain carbon: A-7, A-53, A-106, A-201, A-212, A-283, A-284, A-285, A-306, A-307, A-501, A-515*

Carbon-manganese: A-36*, A-105*, A-516*, A 537*,

High-strength low-alloy: A-441, A-572, A-588, A-618

Low alloy (not quenched & tempered): A-302; A-322, A-353, A-387

Quenched & tempered: A-193, A-194, A-325, A-354, A-461, A-490, A-508*, A-514, A-517, A-533*, A-537, A-540*, A-543*, A-563, A-574.

Note: Data have been collected for the underlined materials.

*Data available and CVN-K_{IC} referencing procedure has been successfully tested.

Summary of Fracture Toughness Curves

The following graphs given the fracture toughness, curves to be used when no data are available. When using these curves, it is recommended that the 90%-90% bound or lower be used which is consistant with current NUREG proposed requirements for toughness acceptance.

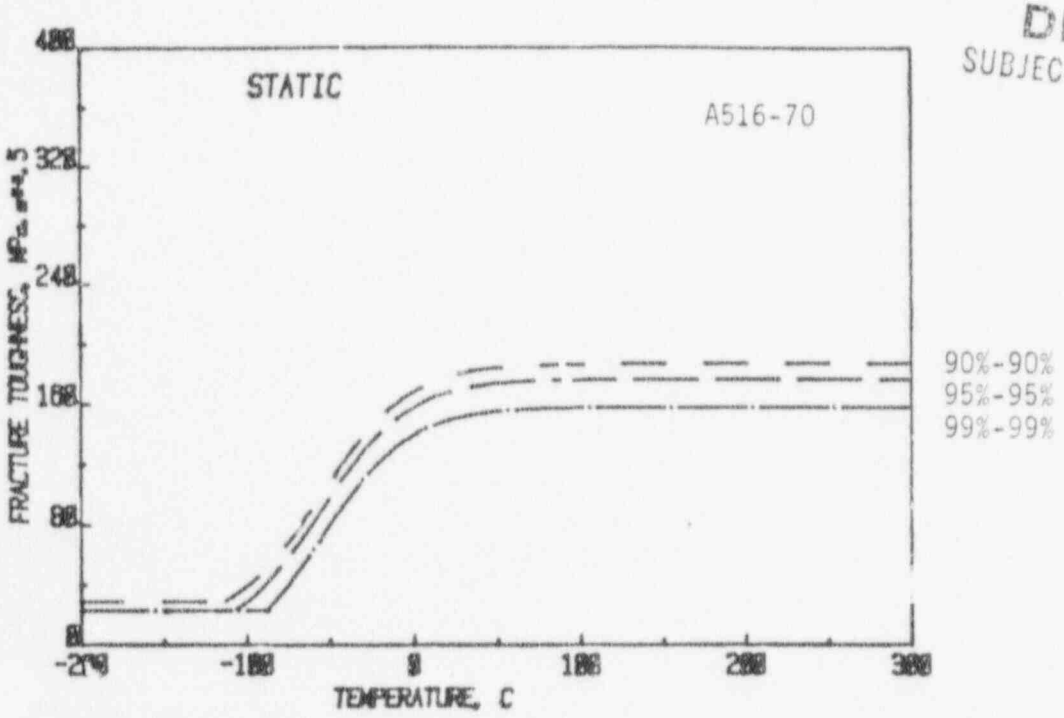

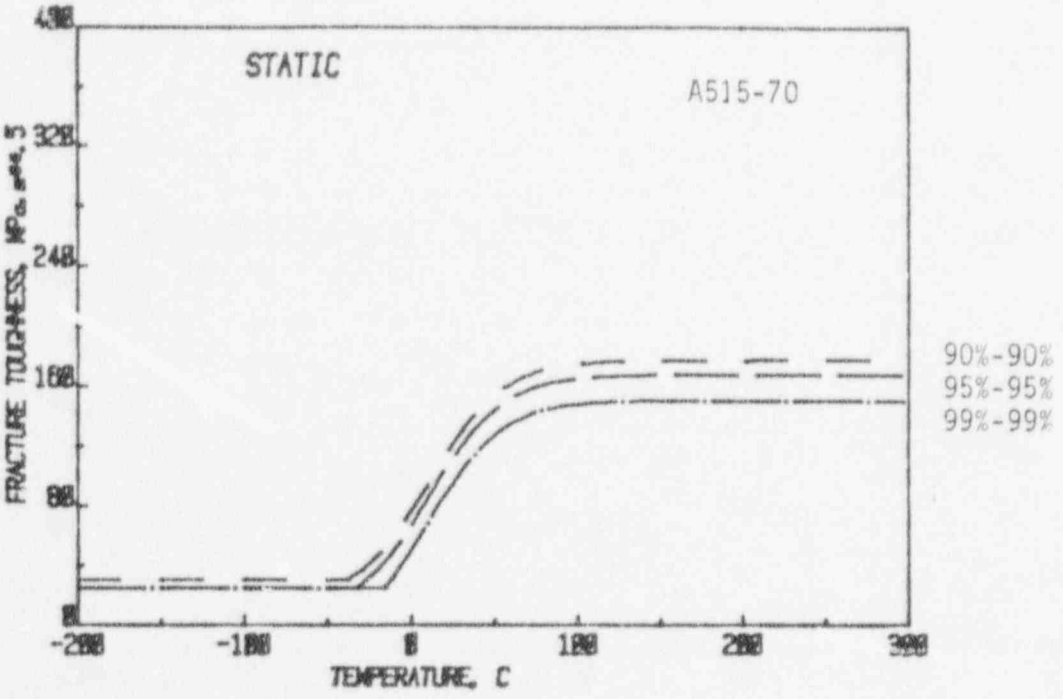

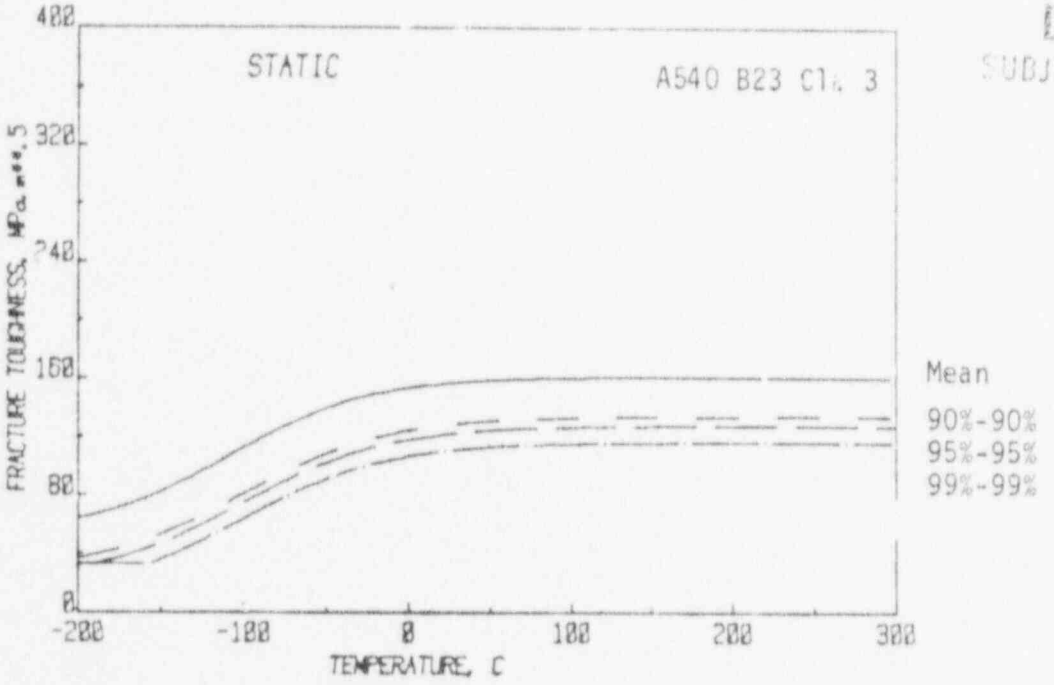

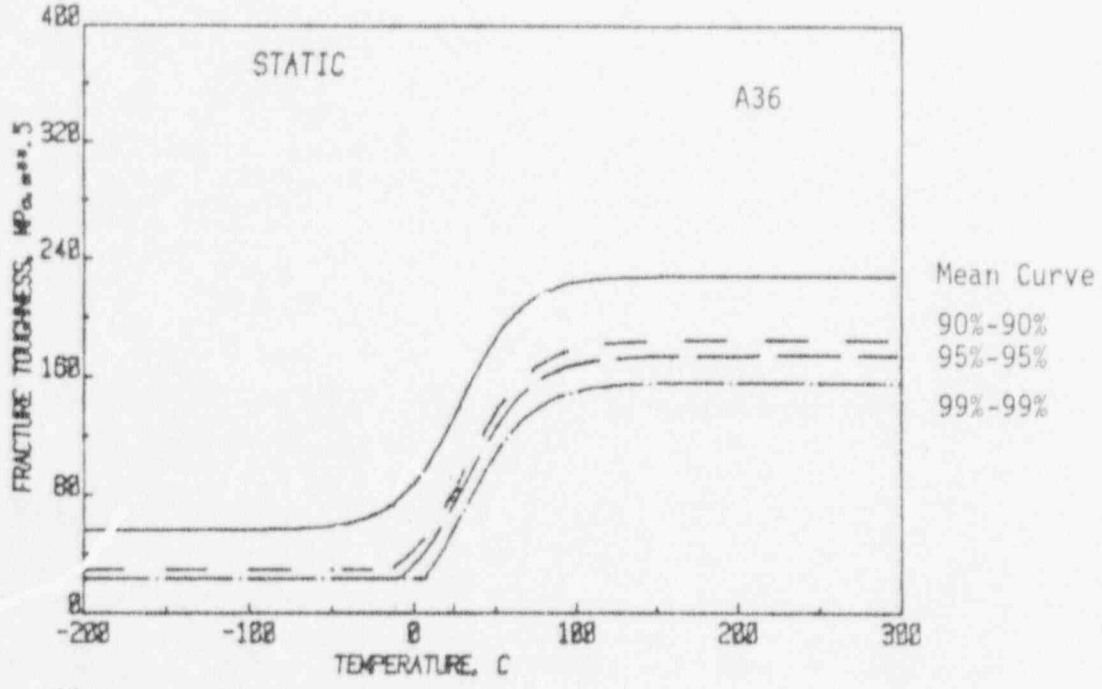

REFERENCES

A-1 ASME Boiler and Pressure Vessel Code, Section III, Appendix G, "Protecting Against Nonductile Failure", 1980 Edition.

A-2 ASME Boiler and Pressure Vessel Code, Section XI, Appendix A, "Analysis of Flaw Indications", 1980 Edition.

A-3 "PVRC Recommendations on Toughness Requirements for Ferritic Materials", Welding Research Council Bulletin 175, August 1972.

A-4 R. A. Wullaert, W. Oldfield, and W. L. Server, "Fracture Toughness Data for Ferritic Nuclear Pressure Vessel Materials: Task A-- Program Office, Final Report, EPRI NP-721, April 1976.

A-5 W. L. Server, W. Oldfield, and R. A. Wullaert, "Experimental and Statistical Requirements for Developing a Well-Defined K_{IR} Curve, EPRI NP-372, May 1977.

A-6 W. Oldfield, W. L. Server, R. A. Wullaert, and K. E. Stahlkopf, "Development of a Statistical Lower Bound Fracture Toughness Curve", International Journal of Pressure Vessels and Piping, Vol.6, 1978, pp. 203-223.

A-7 W. Oldfield and T. U. Marston, "Revised Fracture Toughness Reference Curves", Presented at the 5th International Conference on Structural Mechanics in Reactor Technology, Berlin, Germany, August 13-17, 1979 (paper G 2/7).

A-8 W. L. Server and W. Oldfield, "Nuclear Pressure Vessel Steel Data Base", Topical Report by Fracture Control Corporation to Electric Power Research Institute, EPRI Report NP-933, December 1978.

A-9 W. Oldfield and W. L. Server, "Fracture Toughness of Nuclear Reactor Containment Boundary Ferritic Steel", Contract No. 528217-S, October 1980.

A-10 W. Oldfield, "Fracture Toughness Correlations and Reference Curves", First Annual Report, EPRI Contract RP 1021-4, April 1980.

APPENDIX B

TREATMENT OF RESIDUAL STRESSES

INTRODUCTION

In any evaluation of components based on fracture mechanics principles, it is necessary to properly account for the presence of residual stresses where no effective method to reduce residual stresses (i.e. post-weld heat treatment) is used. Section 2 of the main report discussed the background to failure behavior and LEFM concepts. At the extremes of fracture behavior, that is at low stress where failure would occur by brittle fracture under normally elastic conditions, and at high stress where the failure mode is one of plastic collapse with a material that is behaving in a fully plastic manner, the influence of residual stresses on the initiation of fracture is clear. In the first case, the LEFM regime, which is assumed applicable herein, the effects of residual stresses can properly be accounted for by using the methods of elastic superposition. The total applied stress intensity factor is the sum of that obtained for service loading and that obtained from similar calculation methods using the appropriate distribution of residual stress. Since elastic superposition is used for this process account of negative or compressive stresses is made by generating negative K values which may be subtracted from the positive K values from service loading. In this manner, proper account of tensile and compressive portions of the residual stress field can be made.

Methods of determining the stress intensity factors due to residual stress as a function of crack dimension are provided in Appendix C and applications are given in (B-1, B-2). For stresses below global yield, elastic superposition properly accounts for the effect of residual stresses. In some cases, the sole driving force for fracture is from the residual stress distribution (such as in the case of fractures initiated in beam-to-column connections during shop fabrication).

The magnitude and the distribution of residual stresses must be determined to assess the effect of these stresses in a linear elastic fracture mechanics methodology. Further it is necessary to determine typical residual stress

distributions for specific weld geometry configurations. In this appendix we propose generic distributions for three specific geometries from a review of published literature on measured and calculated residual stress distributions.

These are:

1. Butt weld in a plate geometry
2. Butt weld in a pipe geometry
3. Fillet weld.

For each of these typical details we have determined an upper bound magnitude and distribution which can be used to determine stress intensity factors for a crack growing through the residual stress distribution.

GENERAL METHOD OF APPROACH

The evaluation of welded structures involves an integrity assessment where flaws are postulated in the weld metal and/or heat affected zone material. Thus, it is necessary to propose, for the above weld geometries, bounding residual stress distributions which encompass the complete weldment. From the information we have collected on defect distributions in welded structures, it is clear that the appropriate reference flaws can be either surface defects lying in weld metal or heat affected zone or buried defects contained in these regions. It is necessary to develop a generic residual stress distribution that will allow any orientation and defect type to be analyzed. The peak value and the rate of change of residual stress as it decreases from the peak have been characterized. This has been done for both the longitudinal (parallel to the weld) and transverse stress directions (perpendicular to the weld) to account for all potential defect orientations. Finally, as the flaw grows through the material, the through thickness residual stress distribution will be required to characterize fully the potential for failure.

These determinations have been made and conservative bounding cases are outlined in the sections to follow. Although the majority weld details

of interest can be addressed by these cases, it may be necessary to evaluate particular weld details in depth, using measured or calculated residual stress distributions.

DETERMINATION OF PEAK RESIDUAL STRESS VALUE AND ITS LOCATION

As a general rule, for weld residual stress distributions, the region which is hot last ends up in tension, while those regions which were deposited first end up in compression. A typical distribution for a double V-preparation butt weld in a flat plate is shown in Fig. B-1 (B-3). In this case the pieces that are hot last are the outside weld passes and these generally are in tension balanced by compression through the center of the weld deposit (for electroslag deposits which are made with cooling shoes on the outside of the weld this distribution is reversed with compression at the edge of the weld and balancing tension at the center).

A large number of experimental investigations have yielded information relating to peak residual stresses in weld metal. In most cases the peak value of elastic residual stress approximates the yield strength of the as-deposited weld metal. (B-4 through B-7) In high strength weld deposits there is insufficient volume shrinkage in typical weld sections to provide peak residual stresses up to the yield strength. In most of these cases the peak residual stress level approximates half the yield stress. Specific data on these materials are included in (B-7). These data relate to steels of 80,000 psi (552 MPa m^{-2}) yield strength and above. Generally, the structural steels and corresponding weldments of interest here have relatively low yield strength values, generally less than 60 ksi (414 MPa m^{-2}), although some may have yield strengths above this value.

The question remains then, how to set an upper bound to the peak residual stress level which may exist in weld metal and to define its extent. It is proposed from reviewing the literature that the peak residual stress level be conservatively taken as the yield strength of the weld metal (or base plate) in the as-deposited condition for yield strength up to 60 ksi (414 MPa m^{-2}). For materials of greater yield strength a constant peak value of 60 ksi (414 MPa m^{-2}) will be used as shown in Fig. B-2. This peak value which is material dependent will be termed σ_R for the remainder of this analysis.

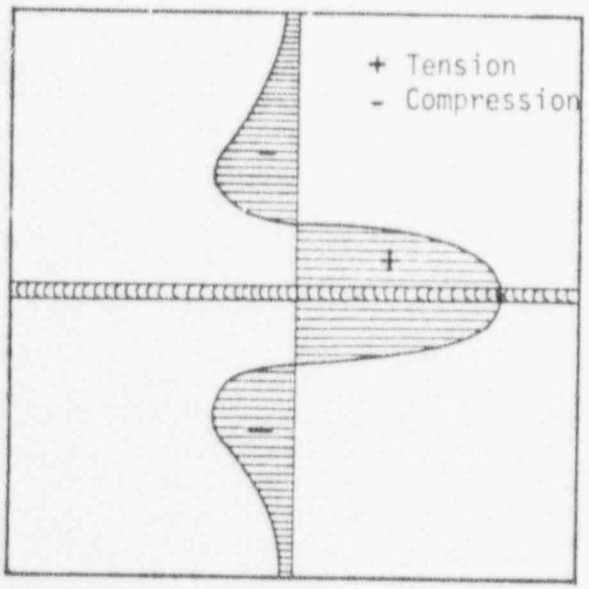

a) Surface Residual Stress (Longitudinal Direction)

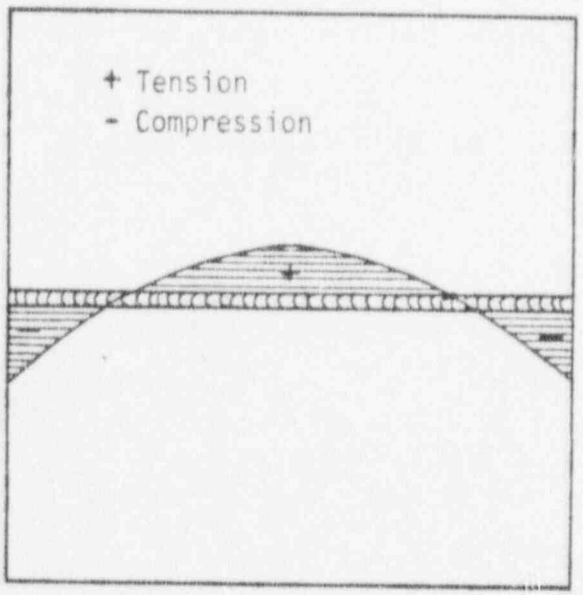

b) Surface Residual Stress (Transverse Direction)

Figure B-1 Schematic Representation of Residual Stress in a Butt-welded Plate

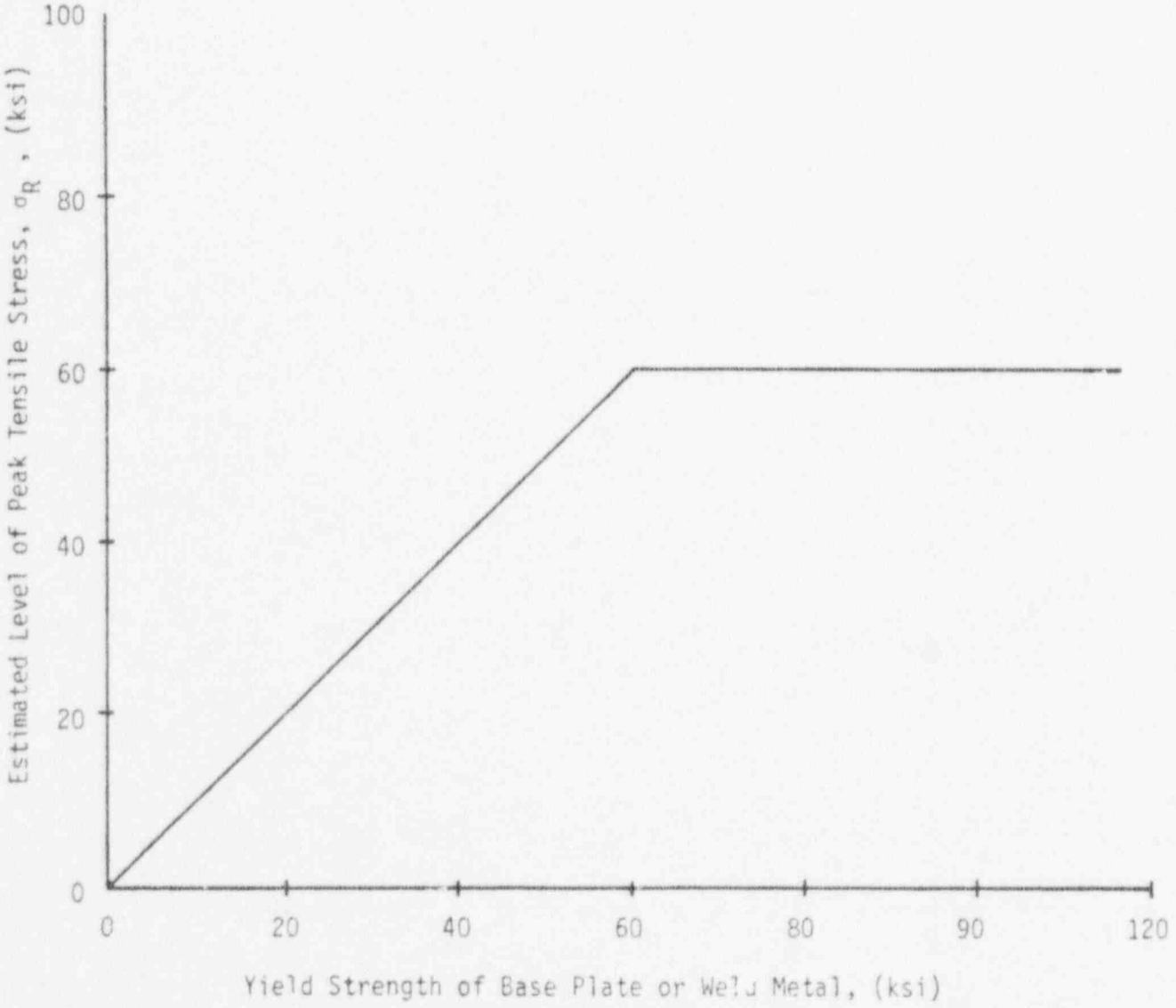

Figure B-2 Estimated Value of Peak Tensile Residual Stress as a Function of Material Strength

It is also proposed that the stress level remain constant for the width of the as-deposited weld metal.

Although it is clear that the peak residual stress in the axial direction (i.e., parallel to the weld) can be equal to the weld metal yield strength, much lower values are measured for transverse residual stresses. In that direction (i.e., transverse to the weld) the shrinkage is less and peak residual stress levels in structural steels (up to about an inch and a half in thickness) have been measured as half the yield strength. Obviously, in very thick sections, where the width of the weld may be 3 or 4 inches (7.6 to 10.2 cm), residual stress measurements will show values approaching the yield strength of the weld metal in the transverse direction as well. We have outlined in the sections that follow our proposals for typical residual stress distributions (which are conservative approximations to the actual residual stress distribution) for specific weld detail geometries. In each case we have used the peak residual stress level equivalent to 1) the yield strength for longitudinal stresses and 2) half the yield strength for transverse stresses. The main difference between the three specific examples is the rate at which the residual stress changes with distance from the fusion line.

RESIDUAL STRESS DISTRIBUTIONS

The generic residual stress distributions for the typical weld geometries are developed by determining the change (decrease) in magnitude of the peak stress along the surface in two directions, and through the thickness. To account for the change along the surface, literature sources were reviewed (B-3 through B-25) and conservative rates of change have been estimated which impose tensile stresses extending over conservatively long distances from the weld. These distributions will result in conservative estimates of fracture potential when incorporated into the LEFM methodology.

Similarly, the through-wall changes in residual stress were researched and conservative stress profiles will be assumed. Hence, stresses in the longitudinal and transverse directions as well as through-thickness distributions are proposed herein with bounding peak values and rates of change.

Residual Stress Model For Plate Butt Weld

A typical schematic representation for the surface residual stresses produced in a butt weld are illustrated in Fig. B-1a and B-1b. A similar distribution will occur for the double (two-sided) butt weld in a plate as illustrated in Fig. B-3a. These distributions are also appropriate for flange-to-flange welds and web-to-web welds in beam connections. A general method for determining residual stresses requires the location of a flaw in the plate (e.g. middle, end, etc.), location of flaw (crack) tip through the thickness and the orientation of the flaw (axial or transverse to the plate and weld axis). The method outlined below will also be used for other geometries although the figures named in this section are specific to the double-V butt geometry.

1) The residual stress of interest (as for service stresses) will be that normal to the flaw. For flaws parallel to the weld the transverse stress distributions (Fig. B-3c for surface and Fig. B-3e for subsurface stresses) are proposed. For flaws perpendicular to the weld the longitudinal stress distributions shown in Fig. B-3b for surface and B-3d for subsurface flaws should be used. In Fig. B-3b we have

2) For shallow surface flaws the location relative to weld centerline is established. The stress as a function of σ_R for the appropriate flaw orientation (parallel or perpendicular to weld) is obtained. As outlined in Fig. B-1b the peak value for transverse stress will be a function of location relative to the plate end. The distribution shown in Fig. B-3c is the maximum value at mid-plate. Other locations, particularly near the plate end will have substantially lower stresses (possibly compressive). Also, the peak values, rate of decay and compressive regions are located after data from references (B-4, B-5) and have been chosen as conservative. To maintain conservative estimates of residual stress we have in some cases ignored equilibrium considerations, (e.g. Fig. B-3d.).

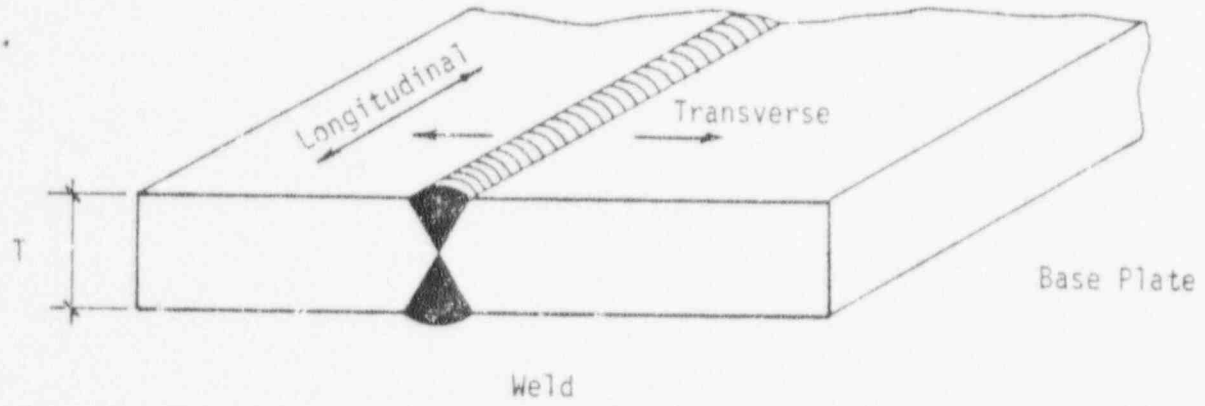

a) Double-V Butt Weld Geometry

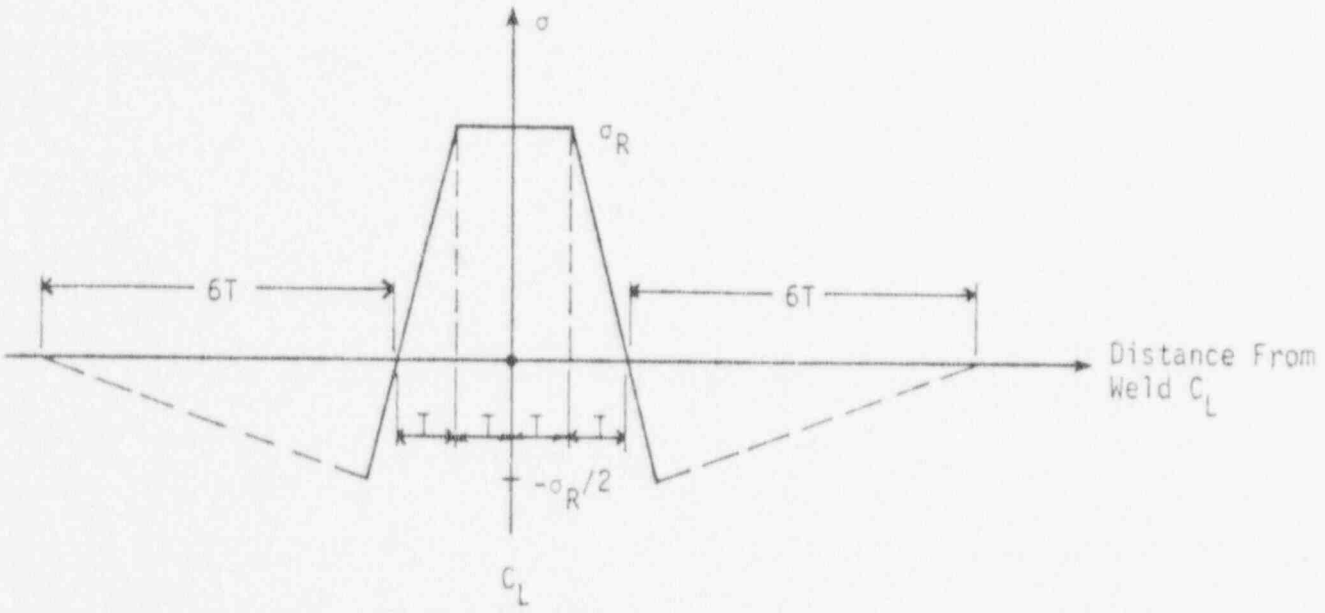

b) Surface Longitudinal Distribution

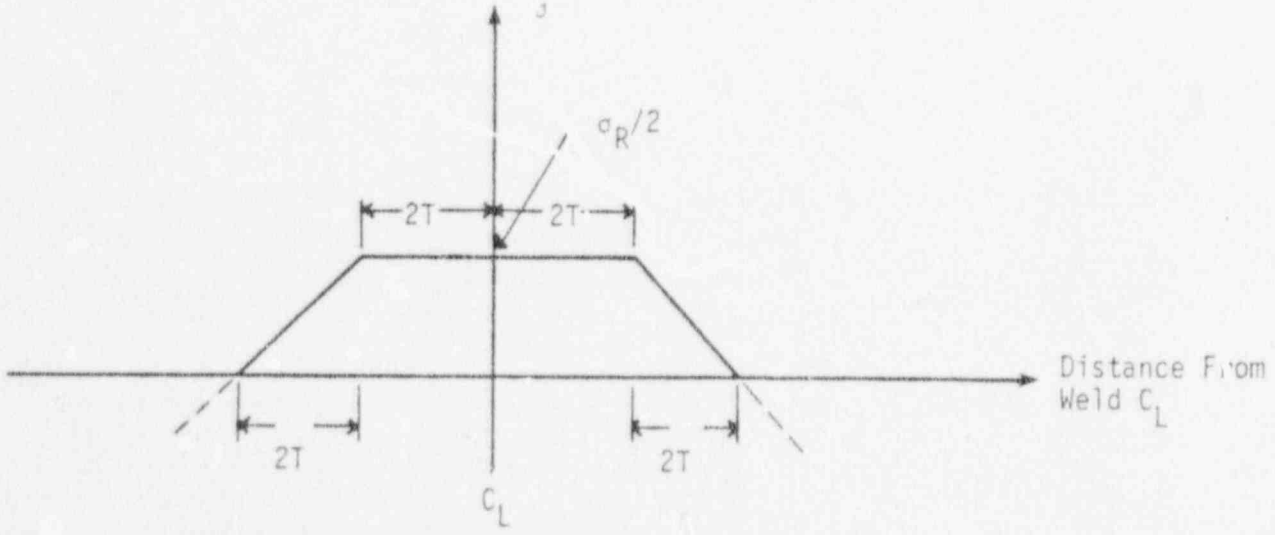

c) Surface Transverse Distribution

Figure B-3 Estimated Residual Stress Distribution for a Double-V Butt Weld

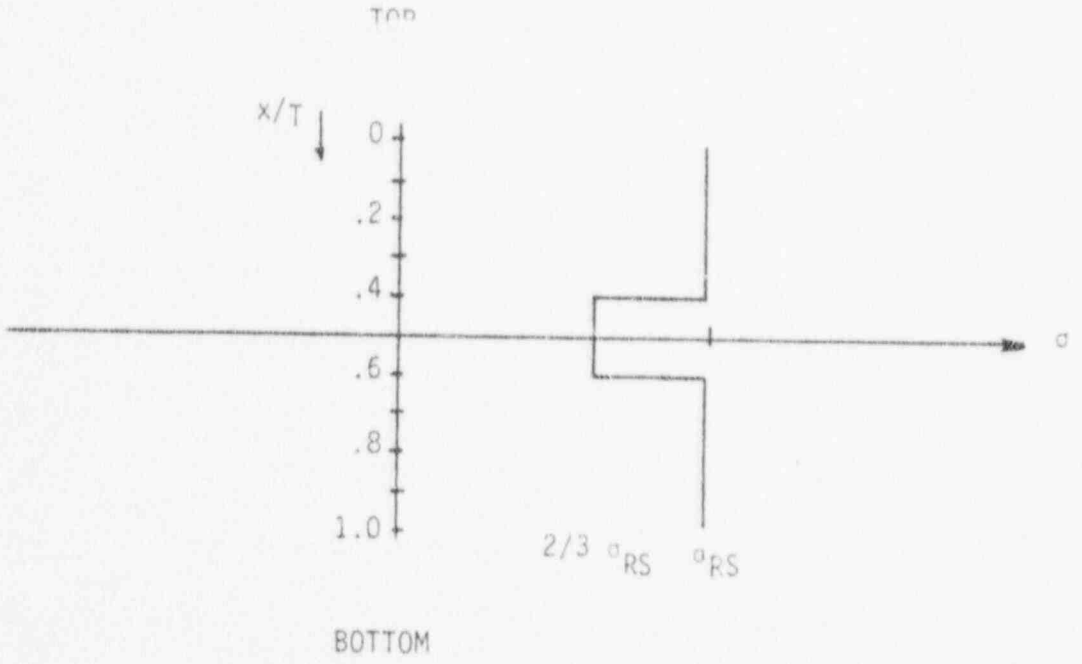

d) Through-Plate Distribution (Longitudinal)

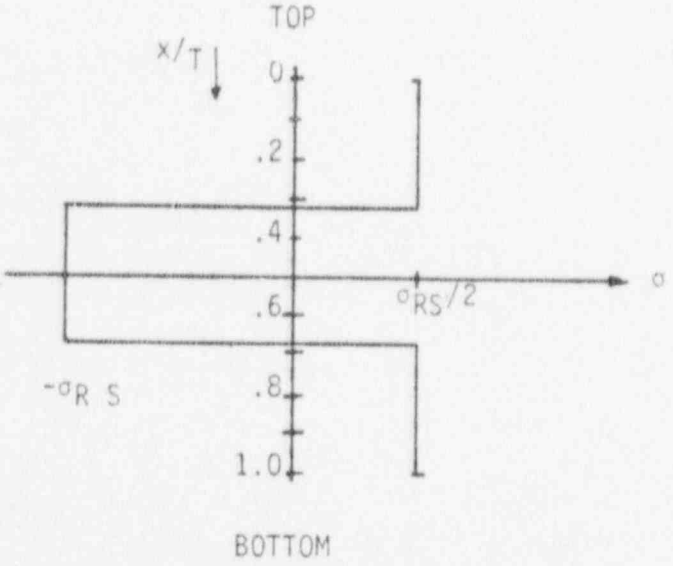

e) Through-Plate Distribution (Transverse)

Figure B-3 Estimated Residual Stress Distribution For Double-V Butt Weld (cont'd)

3) For buried flaws (at depth < 30% wall) and part through-wall flaws with depth greater than 30% of the wall, account must be taken of beneficial effects of through thickness distributions. These are shown in Figs. B-3d and B-3e. These stresses are given in terms of the peak which was in effect at that surface location (σ_{RS}). For example for a flaw perpendicular to the weld located at 3/2 T from the weld centerline the maximum surface stress (Fig. B-3b) is taken as $(\sigma_R + 0)/2 = \sigma_R/2$. If that flaw tip is located at the midsurface the applied stress is 2/3 of the surface value or $2/3(\sigma_R/2) = \sigma_R/3$. In a similar manner the stress at any subsurface location can be determined, by finding the surface stress and appropriate through thickness effect.

Residual Stress Model For Pipe Butt Weld

A schematic of the joint geometry of interest is shown in Fig. B-4a. The procedure is the same as described for the double butt weld in a plate. For a surface flaw the proper residual stress distribution is chosen relative to the defect orientation. Note that the stresses are given as a function of (a material property taken from Fig. B-2) for this geometry in a manner similar to that outlined for the plate butt weld. As well, subsurface flaws must be carefully considered by determining the maximum surface stress relative to the location and factoring in the through thickness decay, if any. Note that the residual stress distribution is modeled conservatively as axisymmetric. Stresses are identified as hoop (equivalent to plate longitudinal) and axial (equivalent to plate transverse) stresses to be compatible with traditional descriptions.

Residual Stress Model for Fillet Weld

The fillet weld geometry shown in Fig. B-5a is a slightly more complicated geometry. An additional step is required from those geometries outlined above, that is the distinction between base plate, weld metal or gusset plate is made. The procedure is outlined below.

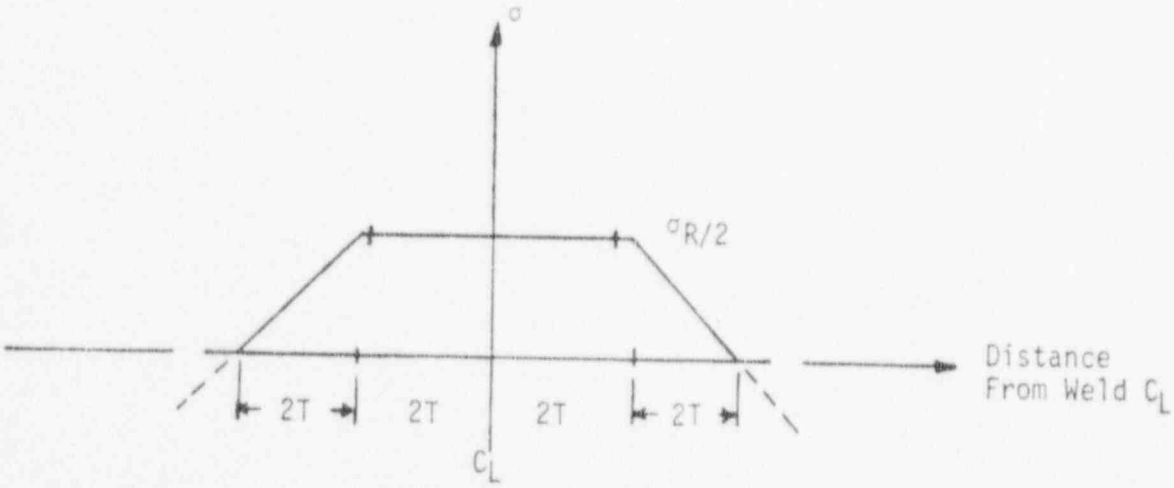

c) Axial Surface Stress Distribution

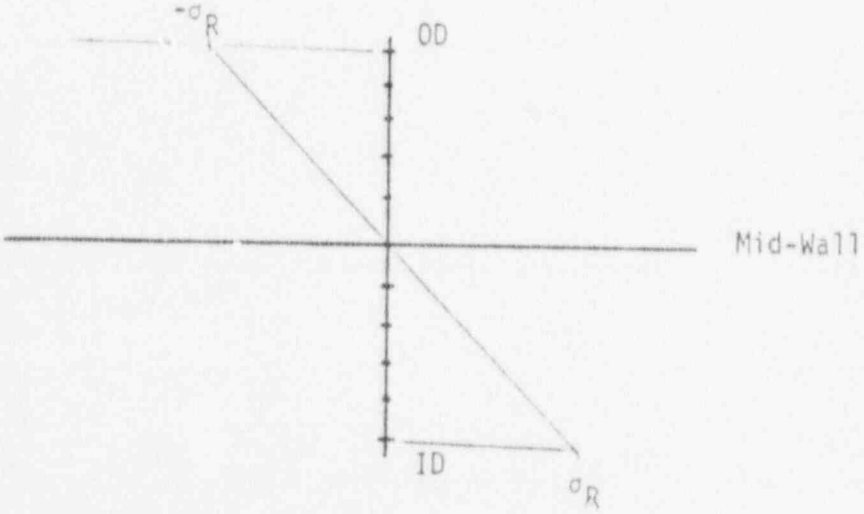

d) Through-Wall Distribution (Hoop)

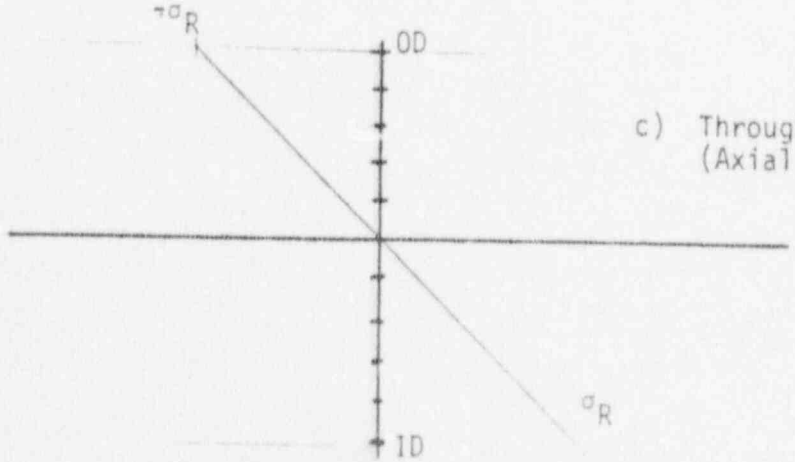

c) Through-Wall Distribution (Axial)

Figure B-4 Estimated Residual Stress For Pipe Butt Weld (cont'd)

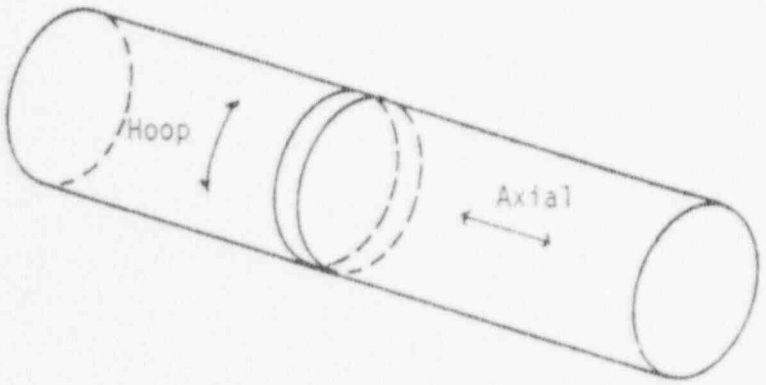

a) Pipe-To-Pipe Butt Weld

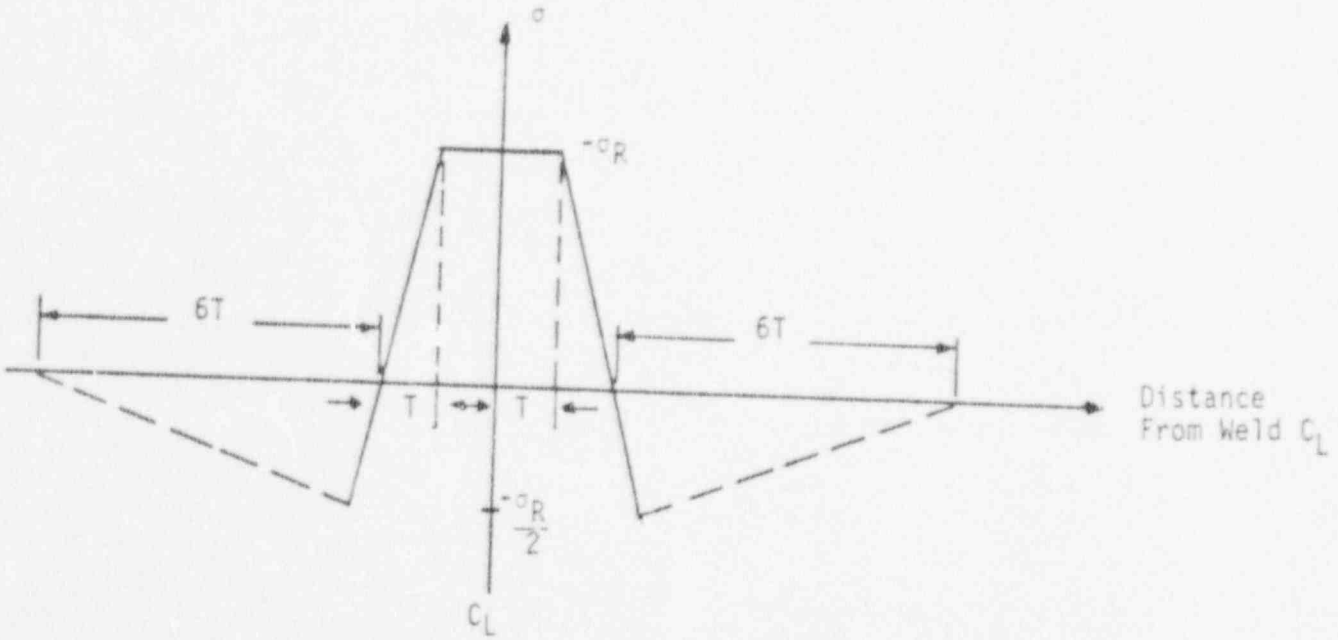

b) Surface Hoop Stress Distribution

Figure B-4 Estimated Residual Stress For Pipe Butt Weld

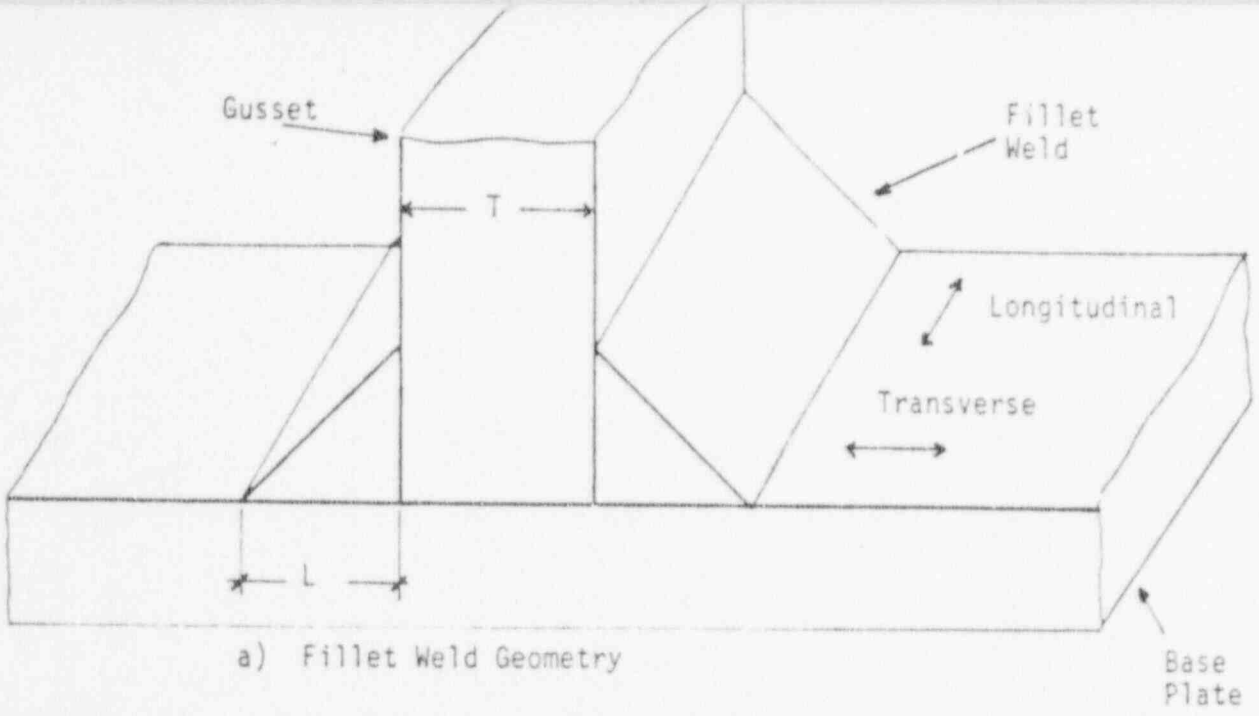

a) Fillet Weld Geometry

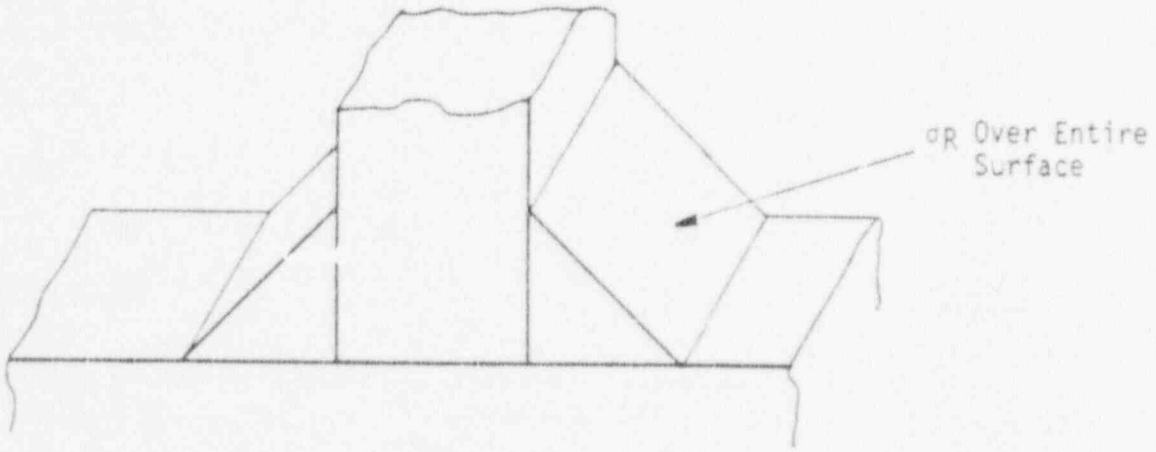

b) Weld Metal Residual Stress

c) Base Plate Residual Stress (Surface)

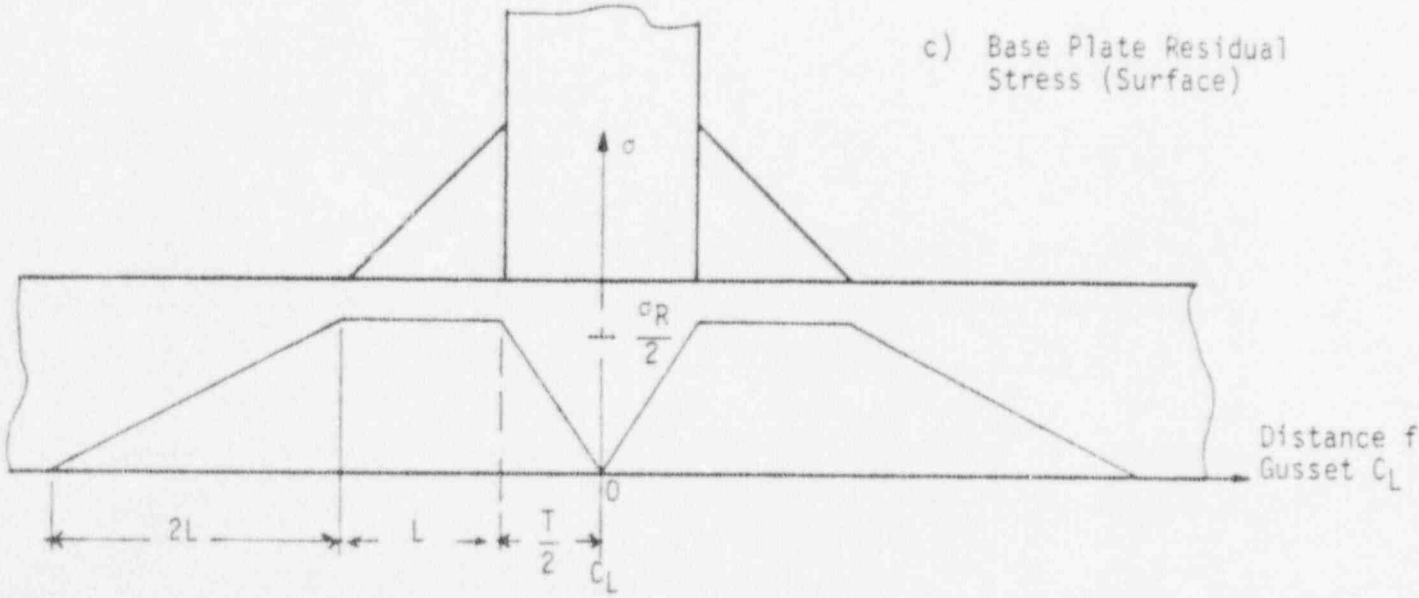

Figure B-5 Estimated Residual Stress For Fillet Weld

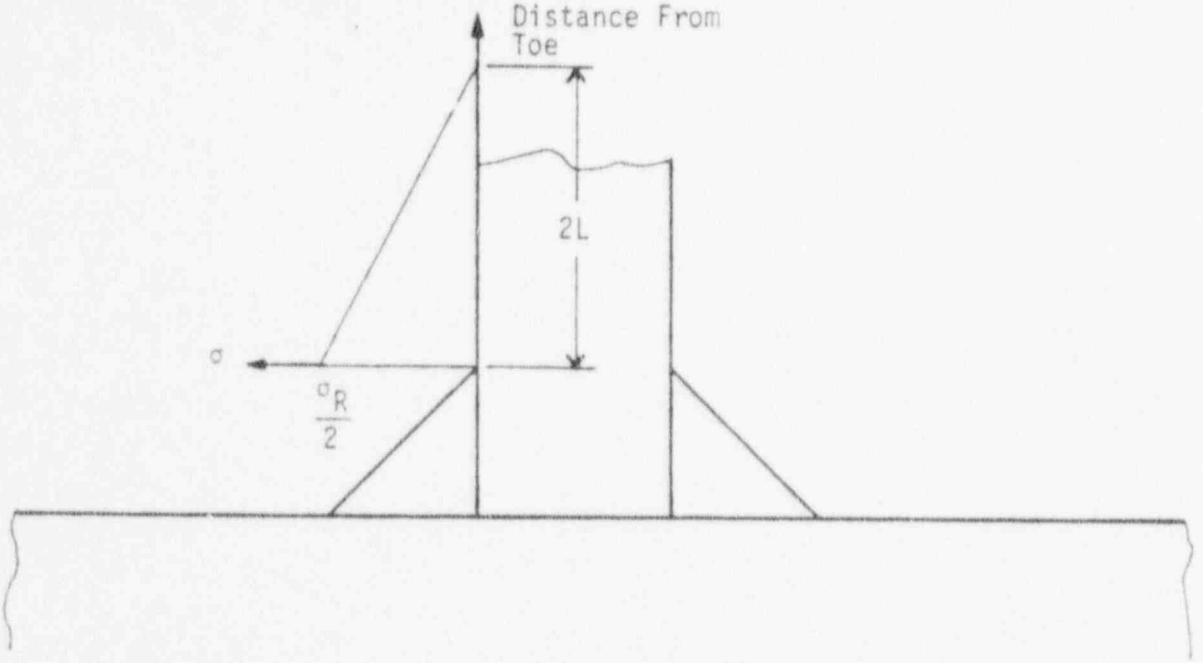

d) Surface Residual Stress Distribution-Gusset Plate

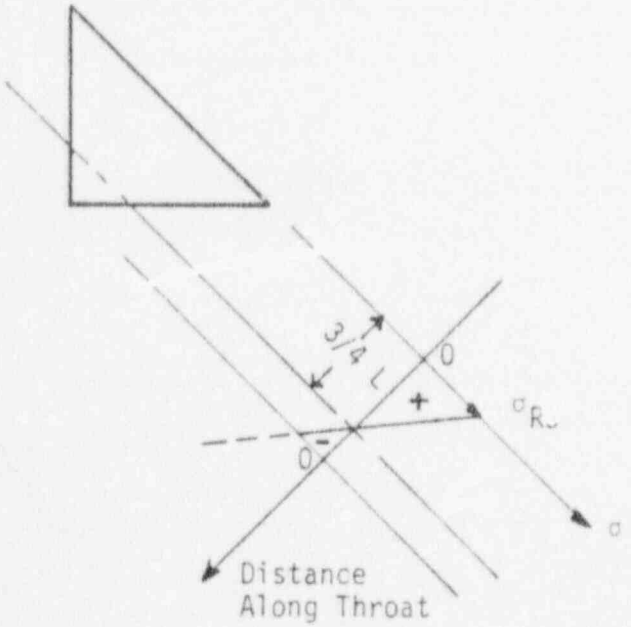

e) Through-Weld Residual Stress

Figure B-5 Estimated Residual Stress For Fillet Weld (cont'd)

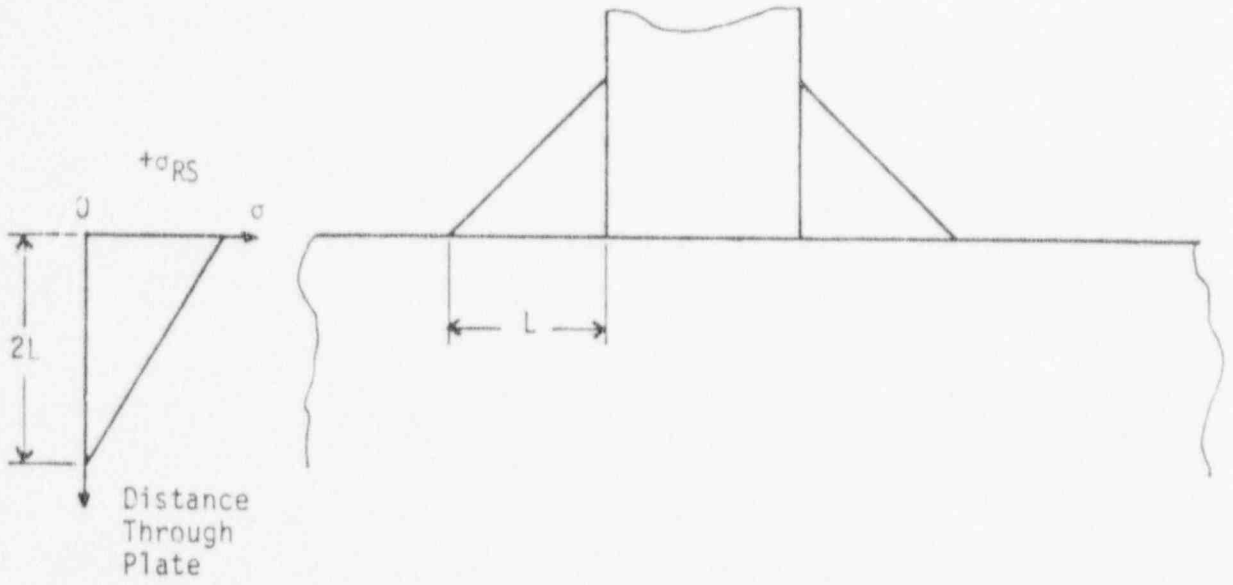

f) Through-Plate Distribution At Toe

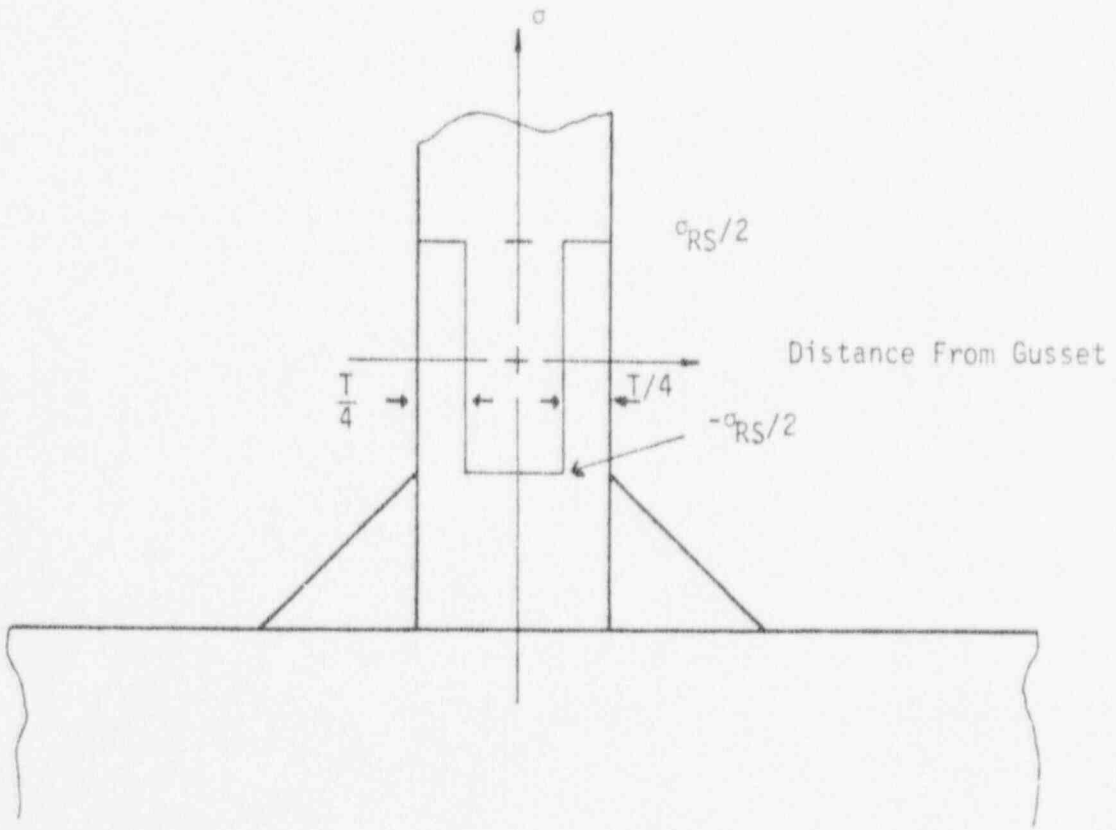

g) Through-Gusset Distribution At Toe

Figure B-5 Estimated Residual Stress For Fillet Weld (cont'd)

1. The location and orientation of flaw must first be determined. Parallel and perpendicular are references relative to the weld. The graphs which are used for surface flaws (depth less than 10%) are specified in Table B-1. A scale factor is given to incorporate the effect of transverse and parallel distributions.

2. For subsurface flaws determine the surface residual stress at the flaw location and factor that magnitude (σ_{RS}) by the appropriate through wall stress factor. The through-wall distributions to be used for this are given in Table B-2.

Example Residual Stress Determination

An example is provided here for a weld toe crack in the base plate. Assume a toe crack parallel to the weld. Use one-half (scale factor for parallel flaws) the values of Fig. B-5c (surface distribution for base plate defects) to determine the appropriate surface residual stress σ_{RS}. Here the surface residual stress, σ_{RS} is equal to 1/2 ($\sigma_R/2$) = $\sigma_R/4$. Then using Fig. B-5f determine the through-thickness factor (e.g. σ_{RS} /2 for a flaw at depth L). Thus the total residual stress would conservatively be 1/2 σ_{RS} = 1/2($\sigma_R/4$) = $\sigma_R/8$ for a flaw in that location.

SUMMARY

A methodology for handling residual stress distributions in three typical geometric details has been developed. The methodology, to be used in conjunction with a fracture mechanics evaluation, will provide stress intensity factors due to residual stress to be used in elastic superposition. The methodology developed requires only a knowledge of the material yield stress, flaw location and orientation. The values for peak stress and rate of change of stress over the length and depth have been chosen to be conservative based on experimental data from the literature.

Table B-1

Figure References for Filled Weld with Surface Flaws

Flaw Location	Orientation	Figure References	Scale Factor*
Weld	Perpendicular	Fig.B-5b	1.0
	Parallel	Fig.B-5b	½
Base Plate	Perpendicular	Fig.B-5c	1.0
	Parallel	Fig.B-5c	½
Gusset Plate	Perpendicular	Fig.B-5d	1.0
	Parallel	Fig.B-5d	½

* Scale factor on stress magnitude to be applied.

Table B-2

Figure References for Filled Welds with Subsurface Flaws

Flaw Location	Figure Reference	Scale Factor
Weld Metal	Fig. B-5f	1.0
Base Plate	Fig. B-5e	1.0
Gusset Plate	Fig. B-5g	1.0

REFERENCES

1. Egan, G.R. and R.C. Cipolla, "Stress Corrosion Crack Growth and Fracture Predictions for BWR Piping," ASME Paper No. 78-Mat-23, American Society of Mechanical Engineers, 1979.

2. McNaughton, W.P., G.R. Egan, G.S. Beaupre, and C.A. Aboim, "Analysis to Predict the Shapes of Growing Stress Corrosion Crack in BWR Piping Welds," Prepared for Electric Power Research Institute, August, 1980.

3. Egan, G.R., "Residual Stresses," BWRA Bulletin, Vol. 9, No. 3, March 1968 (Part 1), The Welding Institute Research Bulletin, Vol.9, No. 4, 7 and 9, April, July and September, 1968 (Parts 2, 3 and 4).

4. Tall, L., "The Calculation of Residual Stresses - in Perspective," Conference Proceedings, Residual Stresses In Welded Construction and Their Effects, The Welding Institute, 1978.

5. Nordell, W.J. and W.J. Hall, "Two Stage Fracturing in Welded Mild Steel Plates," Welding Research Supplement, March, 1965 p.124-5 to 134-5.

6. Cheetham, D. R. Fidler, M. Jagger and J.A. Williams, "Relationship between Laboratory Data and Service Experience in the Cracking of CrMoV Weldments", Conference Proceedings, Residual Stresses In Welded Construction and Their Effects, The Welding Institute, 1978.

7. Masubuchi, K., "Thermal Stresses and Metal Movement During Welding Structural Materials, Especially High Strength Steels," Ibid.

8. Jones, W.K.C. and P.J. Alberry, "A Model for Stress Accumulation in Steels During Welding," Ibid.

9. Ueda, P., K. Fududa and K. Nakacho, "Basic Procedures in Analysis and Measurements of Welding Residual Stresses by the Finite Element Method," Ibid.

10. Tall, L. "The Calculation of Residual Stresses - in Perspective," Ibid.

11. Dawes, M.G., "Analysis of Residual Stresses in Welded I Beam Connections," B.W.R.A. Report D7/38/64, 1965.

12. Rybicki, E.F. et al, "A Finite Element Model for Residual Stresses and Deflections in Girth-Butt Welded Pipes," Journal of Pressure Vessel Technology, Vol. 100, August, 1978 p. 256 - 262.

13. Burdekin, F.U., "Local Stress Relief of Circumferential Butt Welds in Cylinders," British Welding Journal, September, 1963 p.483 - 490.

14. Smith, G.C. and P.P. Holz, "Repair Weld Induced Residual Stresses in Thick-Walled Steel Pressure Vessels, "Oak Ridge National Laboratory NUREG (CR-0093, ORNL/NUREG/TM-153.

REFERENCES (cont.)

15. Chrenko, M., "Residual Stress Measurements on Type 304 Stainless Steel Welded Pipes," Seminar on Countermeasures for Pipe Cracking in BWR's, Vol. 2, May, 1980.

16. Shack, W.J. and W.A. Ellingson, "Measured Residual Stresses in Type 304 Stainless Steel Piping But. Weldments," Seminar on Countermeasures for Pipe Cracking in BWR's, Vol. 2, May, 1980.

17. Rybicki, E.F., et al, "Effect of Weld Parameters on in BWR Piping Systems", First and Second Semiannual Pr. Project RP1174 Electric Power Research Institute, Ma to April 7, 1979.

18. Vaidyananathan, S., A.F. Todaro, and I. Finnie, "Residual Stresses Due to Circumferential Welds." Journal of Engineering Materials and Technology, Transactions of the ASME, October, 1973, p. 223 - 237.

19. Vaidyanathan, S., H. Weiss, and I. Finnie, "A Further Study of Residual Stresses in Circumferential Welds," Journal of Engineering Materials and Technology, Transactions of the ASME, October 1973, p. 238-242.

20. Rosenthal, D. and J.T. Norton, "A Method of Measuring Triaxial Residual Stress in Plates," Welding Research Supplement, May 1945 p. 295-6 to 307-5.

21. Ueda, Y., E. Takahashi, K. Fukuda, K. Sakamoto and K. Nakacho, "Multipass Welding Stresses in Very Thick Plates and Their Reduction from Stress Relief Annealing," Transactions of JWRI, Vol. 5, No.2, 1976.

22. E. Takahashi, K. Iwai, and K. Satoh, "A Method of Measuring Triaxial Residual Stress in Heavy Section Butt Weldments," Transactions of Japan Welding Society, Vol.10, No.1, 1979.

23. Rybicki, E.F. et al, "Residual Stresses at Girth-Butt Welds in Pipes and Pressure Vessels", Battelle Columbus Laboratories, NUREG-0376 R5, 1977.

24. Wells, A.A., "Effects of Thermal Stress Relief and Stress Relieving Conditions on the Fracture of Notched and Welded Wide Plates," B.W.R.A. Report B6/23/62, 1962.

25. Egan, G.R. et al, "The Significance of the Impact Fracture of Prefabricated Leg Sections of API 52X Pipe Material for the Kavala Tower", Report No. 75-7-06-1.

APPENDIX C

DETERMINATION OF STRESS INTENSITY FACTOR

INTRODUCTION

Linear elastic fracture mechanics analyses require the calculation of crack tip stress intensity factors to quantify the conditions for unstable fracture. In analyzing component supports, some situations may be simple or straightforward whereas others may involve intricate geometries or complex loading conditions which lead to nonlinear stress gradients. Although many closed form or approximate solutions exist for K, often it is required to use numerical techniques to calculate K accurately.

This appendix provides some recommended procedures for calculating K for both simple and complicated geometries, and presents guidelines for adapting known solutions to plant-specific applications. When beginning, it is recommended that the following methods of analysis be reviewed and the simplest approach tried first:

1) Application of known solutions from the literature,

2) Applying the recommended procedures given in the ASME Code, Section XI, Appendix A,

3) Use of numerical methods.

If the calculation of K can be aided by the use of the computer, existing computer programs and methods are presented. At the conclusion of the appendix, a compilation of useful K-solutions applicable to typical support geometries is provided with the concept that this section will be updated as more solutions are developed or acquired. Before the potential sources or methods for obtaining K-solutions are discussed, some general guidelines are presented first.

PRELIMINARY CONSIDERATIONS AND GUIDELINES

Important Parameters

As introduced earlier in this report, a common way of expressing K in

terms of applied stress and flaw depth is:

$$K = F(\alpha)\sigma\sqrt{\pi a} \quad , \qquad (C\text{-}1)$$

where σ is the nominally applied stress,
α is the nondimensional flaw size, a/t,
a is the characteristic dimention of the flaw,
t is the thickness of the body, and
$F(\alpha)$ is a function that accounts for the geometry and type of loading.

The key element in calculating K from Eq. C-1 is the determination of the function $F(\alpha)$ since the information on geometry and loading form is contained in this function. When applying a known solution to a problem where either geometry and/or loading are not exact for the case at hand, it is important to recognize the limitations of adapting an existing solution. Although it is difficult to generalize, it can be stated that geometry effects can be neglected when the crack can be considered small relative to the dimensions of the body. Such a situation may involve the treatment of finite dimensions or body curvature. When variations in loading type are considered, such a statement may not be true especially if local stress concentration effects are present. In fact, a simplifying assumption regarding applied stress distributions may only be possible if the cracks are large relative to the local dimensions of the stress riser, so that the nominal stress conditions on the crack face prevail.

Given the case that the local varying stresses in the vicinity of the postulated crack were determined from a model were the geometry and boundary conditions were accurately represented, the K variation can usually be reasonably estimated or bound with the simple techniques described herein. The following subsections deal with situations commonly encountered in approximating K with available solutions.

Representation by a Flat Plate Geometry

There are many solutions for K (or $F(\alpha)$) where the crack has been modeled in an infinite, semi-finite, or finite planar geometry. These flat plate

solutions have been used by many analysts to approximate other geometries (see later the ASME Code procedure). One increasing characteristic of finite plate solutions is that in many instances they yield conservative values of K because the compliance is greater for the flat plate case than for the actual geometry which leads to larger crack opening displacement for the flat plate for a given loading, and hence higher applied K. This would be true whether the reduced compliance is due to constraint by adjacent structure, or by body curvature, however such conditions can usually be determined by inspection only if the flaws are partially through the thickness. If through-wall cracks are to be assumed, then curvature for example, will elevate K above the flat plate value, and therefore a nonconservative situation will result if flat geometries are assumed. Obviously, if the crack length is small $a/\sqrt{Rt} < 1/2$, then curvature effects can be neglected.

Elliptical versus Infinitely Long Cracks

A three-dimensional problem can be simplified to a two-dimensional geometry by modeling an elliptically shape crack as an infinitely long crack where the crack aspect ratio, a/ℓ, is zero. The use of this two-dimensional approach is conservative since the applied K for the long crack is greater at the maximum crack depth than the elliptical flaw. Although this assumption greatly reduces the geometric complexity of the problem, such an approach is only possible if there is sufficient lattitude to demonstrate flaw acceptability under this conservative assumption. It should be noted that it only takes a flaw aspect ratio of 1/10 at which the elliptical flaw and the infinitely long flaw yield approximately the same results for K at any given flaw depth.

Treatment of Local Stress Gradients

A common problem encountered is the treatment of a local stress gradient, $\sigma(x)$ where the function $F(\alpha)$ is only known for uniform loading, or a linear varying loading condition. As an example consider the case of a crack originating from a notch under nominally applied uniform tension as depicted in Fig. C-1. Two possible models for computing K are shown in

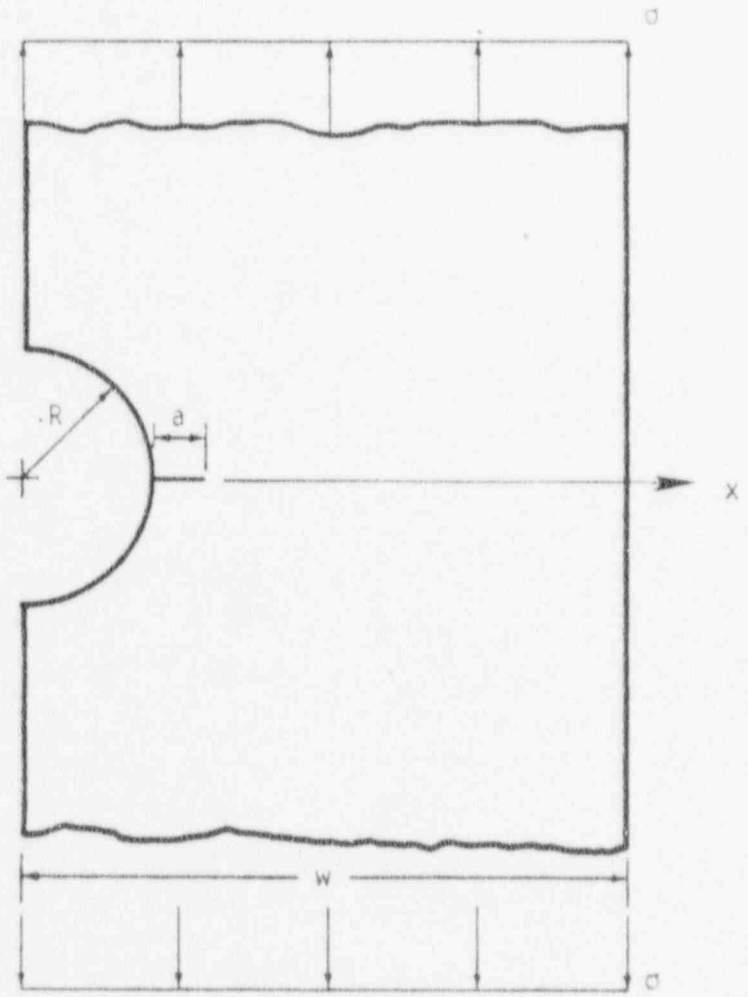

Figure C-1 - Single Edge Notched Plate Containing a Crack Under Nominal Tension.

Fig. C-2. As a first approximation, the approach shown in Fig. C-2a, where the crack is modeled as the notch depth plus flaw depth, should provide a conservative estimate for K, lacking any detailed stress distribution information regarding the magnitude of the stress concentration and distribution of stress. Any knowledge of the local stress, $\sigma(x)$, will allow analyst to improve the model to the one shown in Fig. C-2b, where the body width is taken as t-R, and $\sigma(x)$ is the local varying stress field due to the presence of the notch in the plate. The solution for K would now have to be determined numerically by techniques described later in this appendix, or the stress distribution $\sigma(x)$ can be linearized to allow the superposition of $F(a)$ from tension on bending cases. A procedure to linearize a nonlinear varying stress distribution is given in Section XI of the ASME Code (C-1) and is described later. This Code procedure will always give a conservative estimate of K as long as $\sigma(x)$ is concave upwards as depicted in Fig. C-2b.

Many times the stress variation may not be known because the stress analysis model was not refined enough to resolve accurately $\sigma(x)$. Given that the stress concentration factor K_t can be estimated from a handbook such as (C-2), the distribution of stress away from the local stress riser can be approximated by the stress drop-off from a hole in a plate under uniaxial tension. Such an expression takes the form of

$$\sigma(x) = \sigma\left\{1 + (K_t - 1)\left[1/4\left(\frac{R}{R+x}\right)^2 + 3/4\left(\frac{R}{R+x}\right)^3\right]\right\} \quad (C\text{-}2)$$

where R and x are as shown in Fig. C-1. Equation C-2 is simply away of representing the applied stress and not a technique computing K, therefore it is a simplification to the stress analysis to determine $\sigma(x)$.

LITERATURE SOLUTIONS

Some applications of fracture mechanics are straightforward, and closed-form

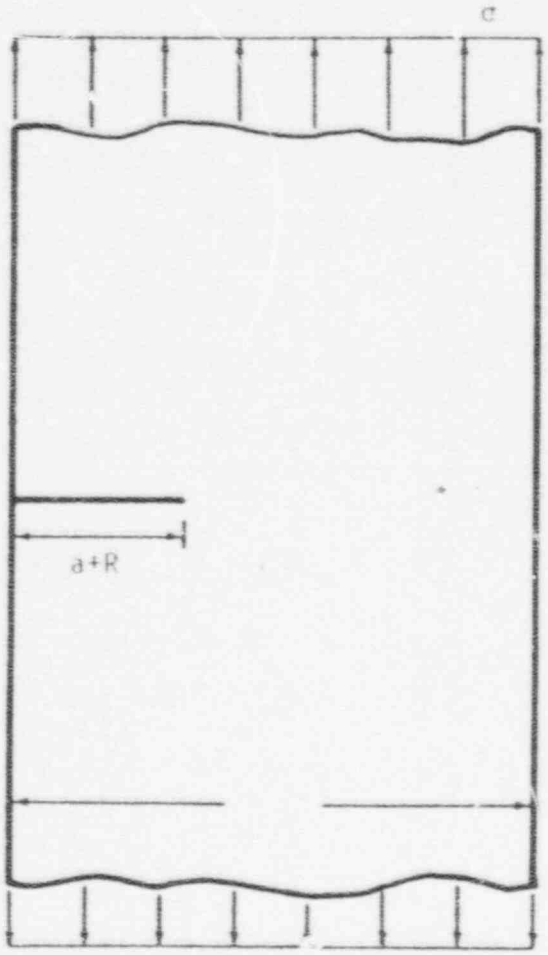

a) Flaw Model Based on Nominal (Unnotched) Stress

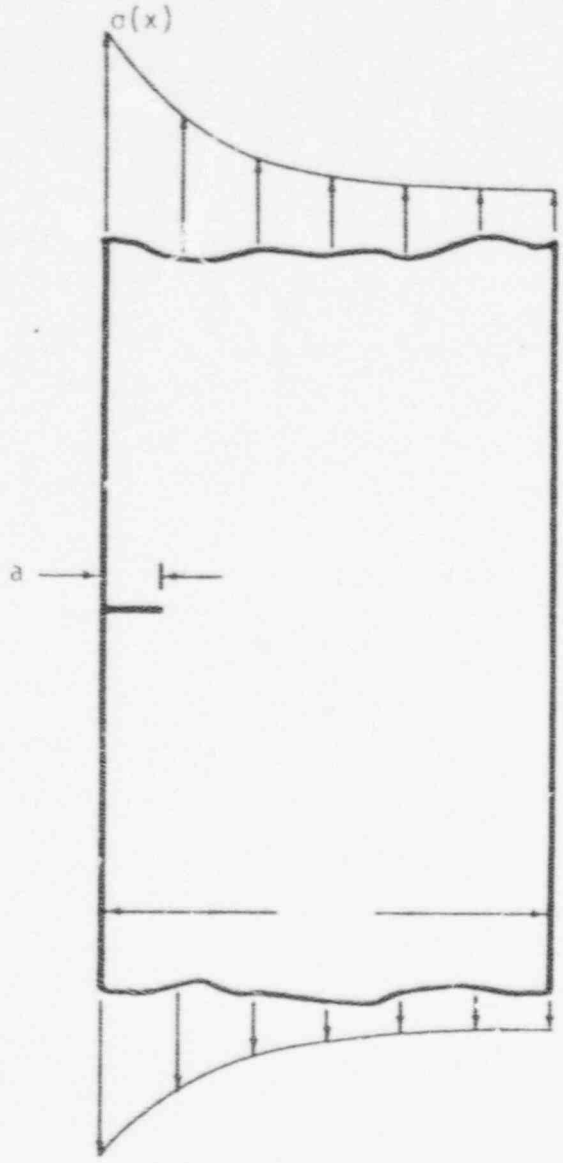

b) Flaw Model Based on Notched Stress

Figure C-2- Two Possible Flaw Model Representations of an Edge-Notched Plate Containing a Crack.

expressions can provide accurate or bounding K values for plant-specific cases. For these situations, useful stress intensity factor solutions and modeling shortcuts can be obtained by searching out articles in the literature, especially those references which are applied in nature. A list of several important sources of K-solutions including papers as well as reference texts and handbooks is provided at the end of this appendix (C-3 through C-8). These documents will provide a good starting point for obtaining established solutions. In addition to those references listed, leading fracture mechanics journals, such as International Journal of Fracture Mechanics, Engineering Fracture Mechanics, and the publications of the American Society for Testing and Materials--Special Technical Publications series (STP), and the fracture division of the American Society of Mechanical Engineers Pressure Vessels and Piping Division should also be reviewed.

ASME CODE SECTION XI, APPENDIX A PROCEDURE

Background

The flaw evaluation analysis specified by Appendix A of the ASME Code, Section XI (C-1) provides a procedure for calculating K_I for two flaw geometries: an elliptical surface crack and a buried elliptical crack. The flaw model geometries are shown in Fig. C-3 and the solution for stress intensity factor for these models comes from literature solutions for elliptical cracks in flat plates under linearly varying stress fields. The procedure for computing K_I by the Code approach as well as the complete flaw evaluation analysis has been computerized in a program called FACET (C-9). The background to the Code procedure and the source of the solutions and example analysis are presented in (C-10, C-11). The analysis requirements for computing K are described next.

Representation of the Applied Stresses

Under the present Section XI procedure, the stress intensity factor is

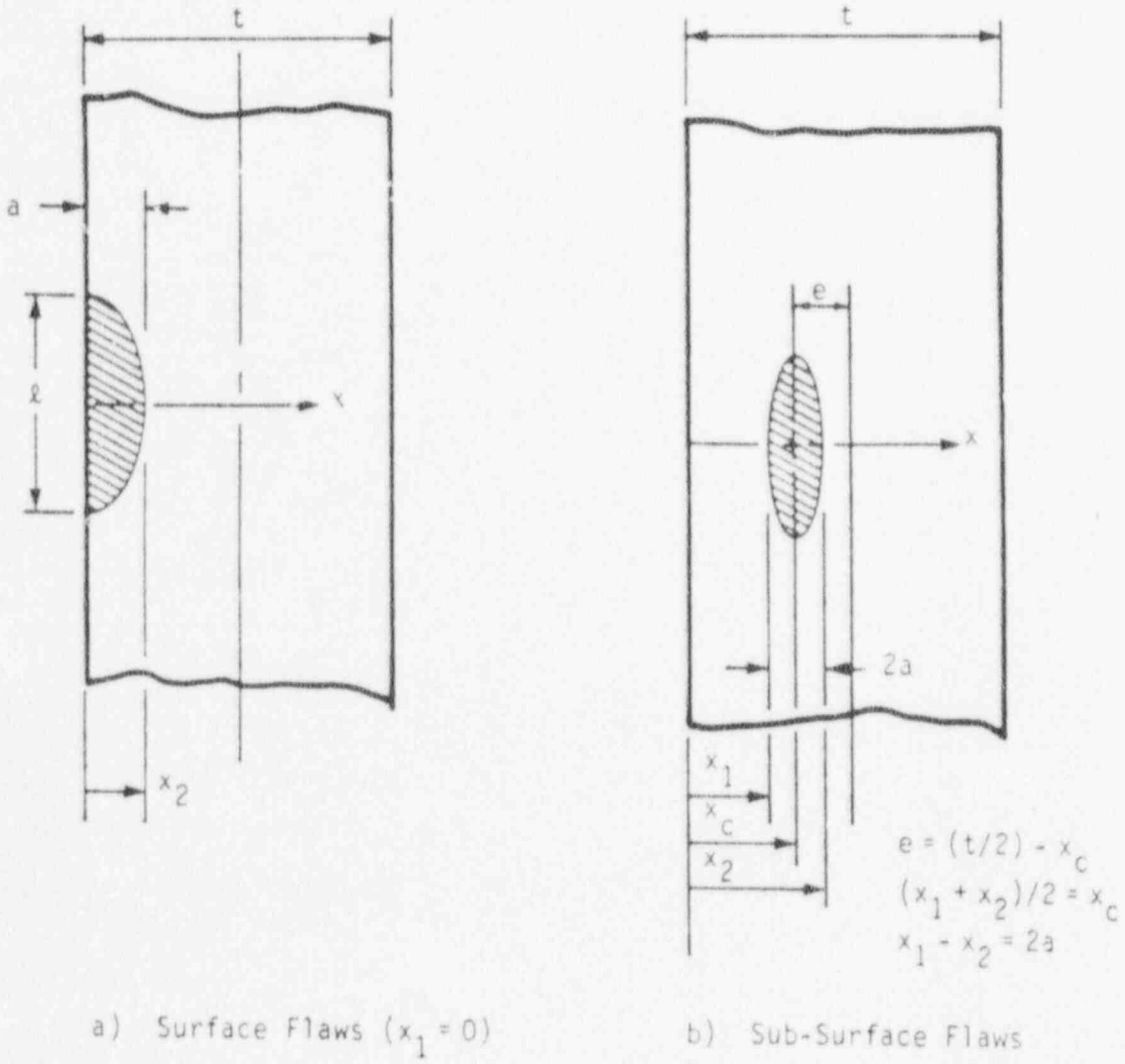

a) Surface Flaws ($x_1 = 0$)

b) Sub-Surface Flaws

Figure C-3 - Flaw Model Geometry for Surface and Sub-Surface Flaws.

evaluated from two stress states: uniform pressure or membrane stress (σ_m) and linearly varying pressure or bending stress (σ_b). For the case when the variation of stress through the component wall is nonlinear, Section XI provides a procedure to linearize (approximate) the actual stress distribution, so that effective values of σ_m and σ_b can be defined. This technique is illustrated in Fig. C-4 for both surface and subsurface flaws. For calculating K, this linearization procedure will be conservative when the actual stress distribution is concave upwards as shown in Fig. C-4. When the actual stress variation is concave downwards, this technique may be nonconservative and the analyst must exercise engineering judgment to assure that within the crack locus, the linearized stress exceeds the actual stress for all crack depths computed by this method.

For the geometry shown in Fig. C-4, one can write the equivalent linearized stress distribution $\hat{\sigma}(x)$, in terms of the actual distribution $\sigma(x)$, and crack front positions x_1 and x_2 as

$$\hat{\sigma}(x) = \frac{\sigma(x_2) - \sigma(x_1)}{(x_2 - x_1)} x + \hat{\sigma}(0) \qquad \text{(C-3)}$$

For the case of surface flaws (Fig. C-3a), $x_1 = 0$, $x_2 = a$, and $\hat{\sigma}(0) = \sigma(0)$. The membrane and bending portions are simply computed by evaluation Eq. C-3 at $x = (t/2)$ which yields:

Surface Flaws:

$$\sigma_m = \frac{\sigma(a) - \sigma(0)}{a} (t/2) + \sigma(0) \qquad \text{(C-4)}$$

$$\sigma_b = \hat{\sigma}(0) - \sigma_m = - \frac{\sigma(a) - \sigma(0)}{a} (t/2) \qquad \text{(C-5)}$$

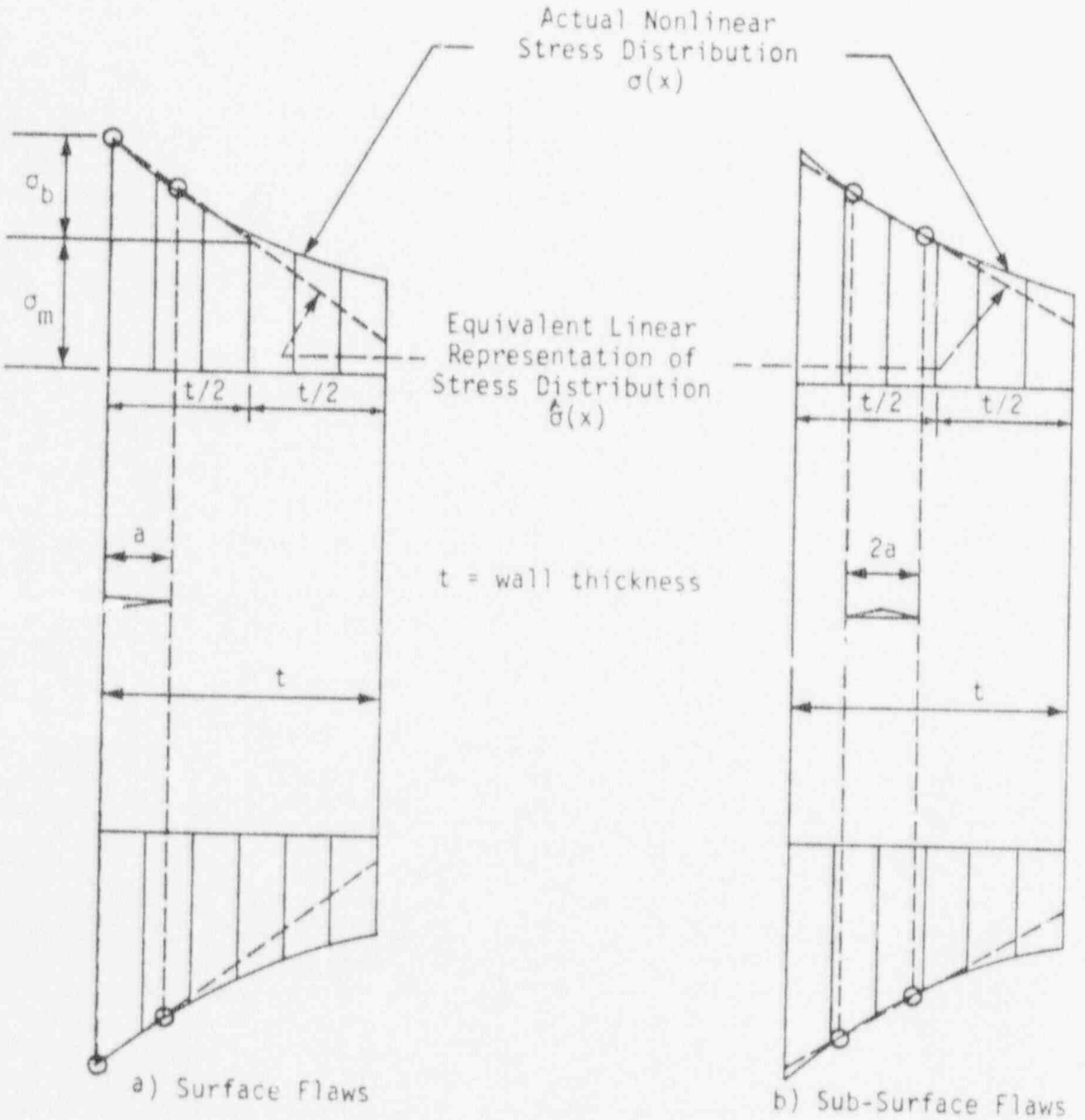

Figure C-4 - Linearized Representation of Stresses.
(Section XI, Fig. A-3200-1)

For subsurface indications, the equivalent linearized stress distribution is determined by substituting the interior flaw positions $x_1 = (x_c - a)$ and $x_2 = (x_c + a)$ into Eq. C-3. Here x_c is defined as the coordinate of the center of the elliptical flaw shown in Fig. C-3b. By similar algebraic separation, the membrane and bending components become:

Subsurface Flaws:

$$\sigma_m = \frac{\sigma(x_c + a) - \sigma(x_c - a)}{2a} (t/2 - x_c + a) + \sigma(x_c - a), \qquad (C\text{-}6)$$

$$\sigma_b = \hat{\sigma}(0) - \sigma_m = - \frac{\sigma(x_c + a) - \sigma(x_c - a)}{2a} (t/2) \qquad (C\text{-}7)$$

Calculation of the Stress Intensity Factor, K_I

Article A-3000 of Section XI presents a recommended procedure for determining the stress intensity factor (K_I). Once the applied stresses at the flaw location are resolved into membrane and bending components with respect to the wall thickness is calculated from the Mode I stress intensity factor for the flaw

$$K_I = \sqrt{\pi a/Q} \; (M_m \; \sigma_m + M_b \; \sigma_b), \qquad (C\text{-}8)$$

where

a = Flaw size

Q = Flaw shape parameter

M_m = Free surface correction factor for membrane stresses

M_b = Free surface correction factor for bending stress

σ_m = Applied membrane stress

σ_b = Applied bending stress

The parameters Q, M_m, and M_b are given in graphical form in Section XI. These curves are reproduced in this report in Figs. C-5 through C-9. Equational forms of Q, M_m, and M_b were developed in (C-9) for use in the FACET program from a combination of analytical and curve fitting techniques. These equations are given (C-9) for use instead of the graphical form. A simple but accurate expression for Q is provided below (C-10).

$$Q = 1 + 4.593\ (a/\ell)^{1.65} + 0.212\ (\sigma/\sigma_y)^2 \qquad (C\text{-}9)$$

where σ is the total applied stress $\sigma_m + \sigma_b$, and σ_y is the yield strength.

NUMERICAL METHODS

Influence Function Method

The influence function (IF) method is a numerical technique that allows for the calculation of K for nonlinear varying stress distribution to be performed very quickly and efficiently. The influence function or weight function method was developed by Bueckner (C-11) and Rice (C-12) for two-dimensional problems. The approach was expanded to three-diemensional problems by Besuner (C-13) and Cruse (C-14). The influence function (h) is a function of crack position (x), specified displacement boundary conditions (u) and geometry (k). The calculation of K for the general class of two-dimensional problems in Mode I is

$$K = \int_L h(x,u,k)\ \sigma_{zz}(x)\ dx, \qquad (C\text{-}10)$$

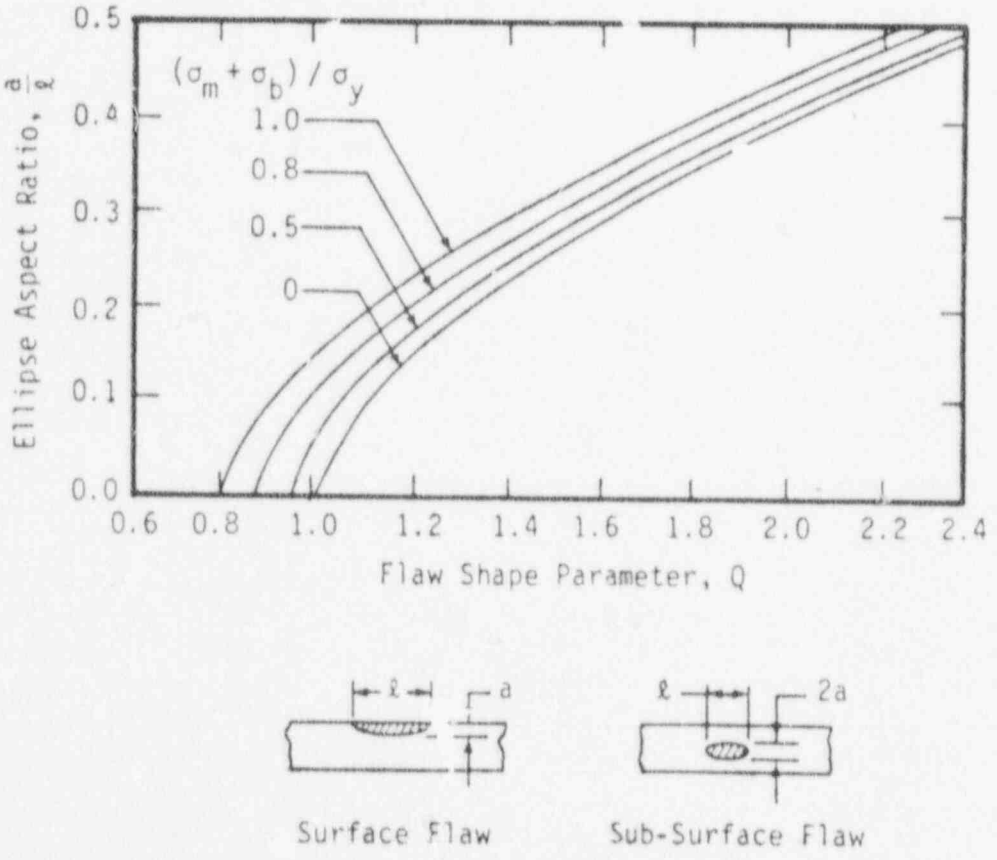

Figure C-5 - Shape Factor for Flaw Model.
(Section XI, Fig. A-2000-1)

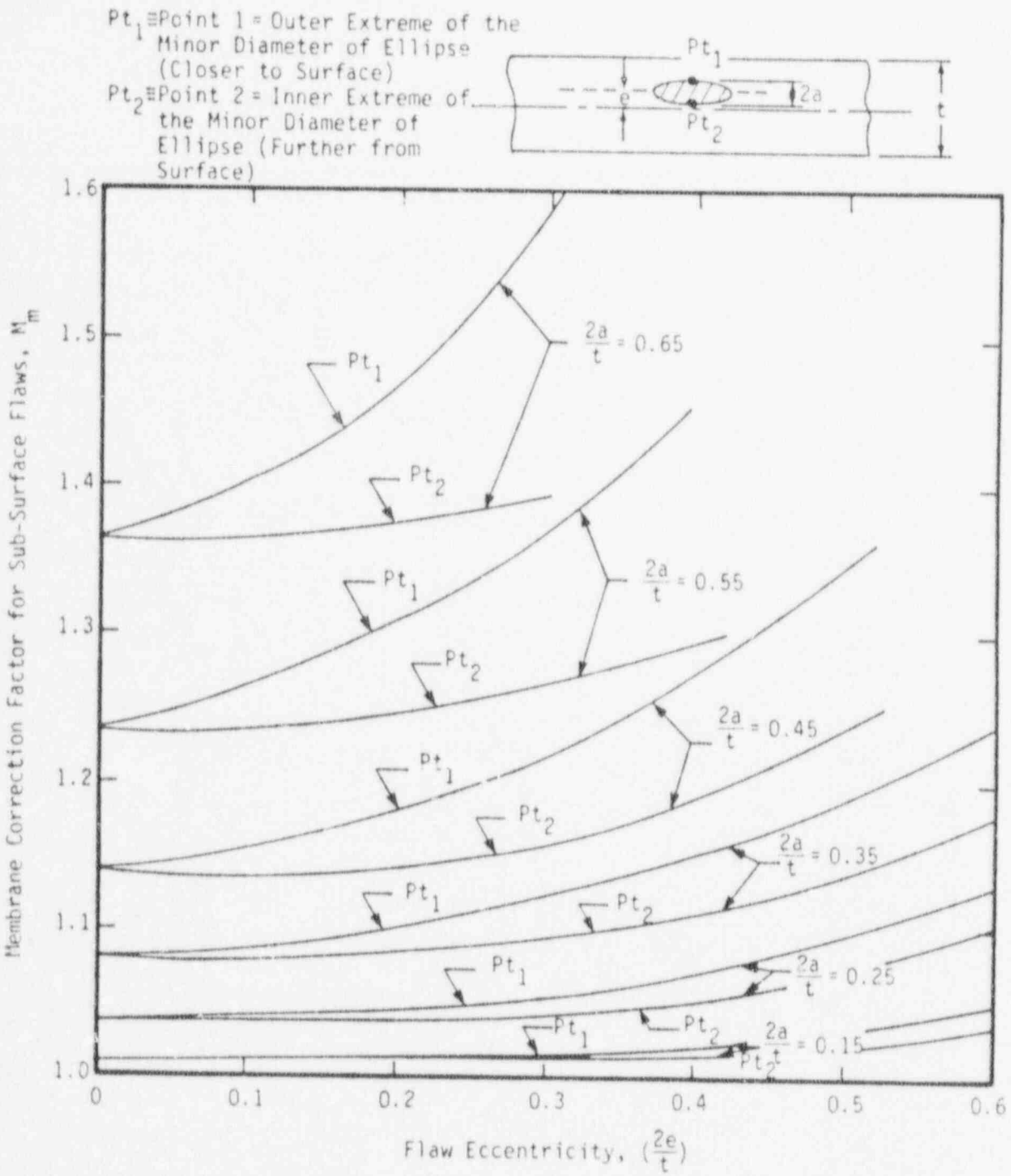

Figure C-6 - Membrane Correction Factor for Sub-Surface Flaws (From Section XI, Fig. A-3300-2).

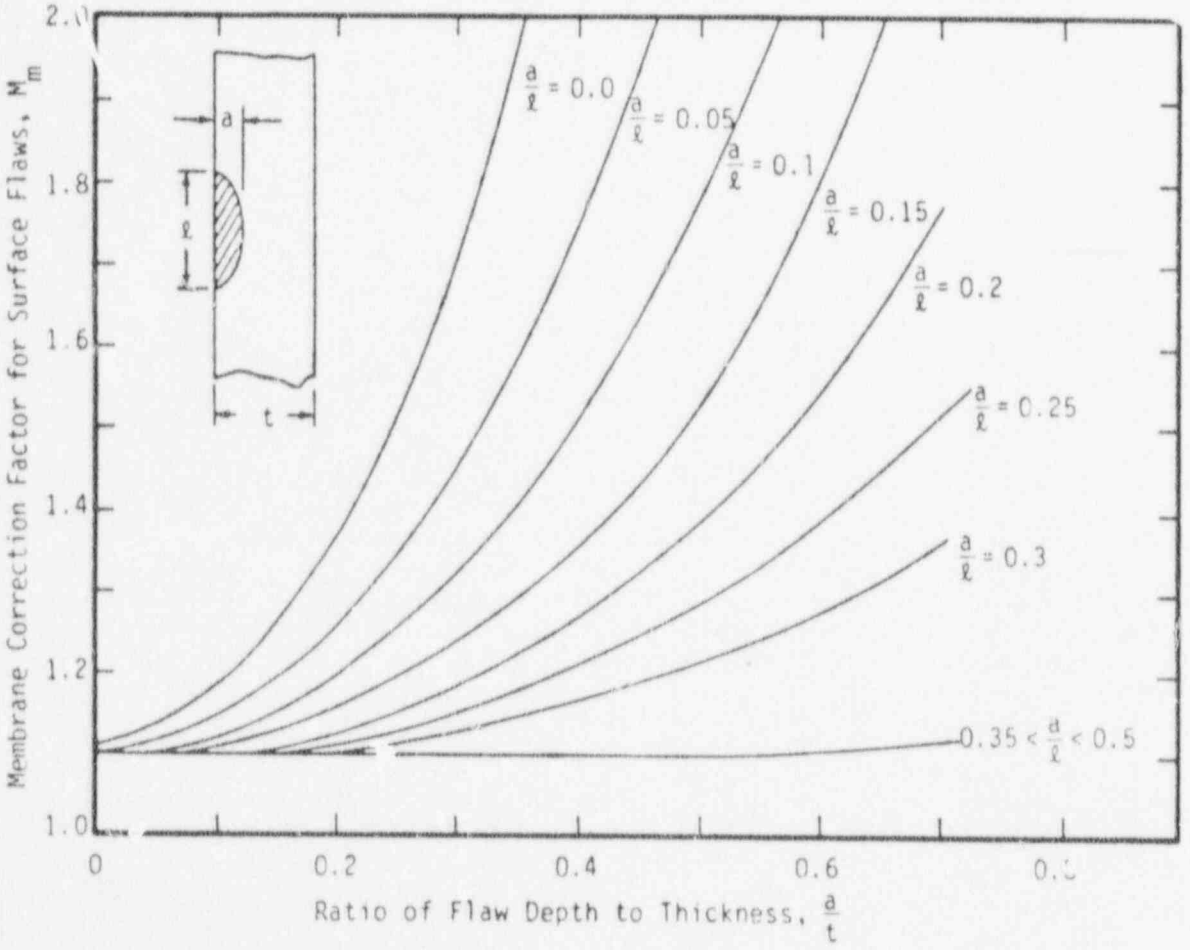

Figure C-7 - Membrane Correction Factor for Surface Flaws (From Section XI, Fig. A-3300-3).

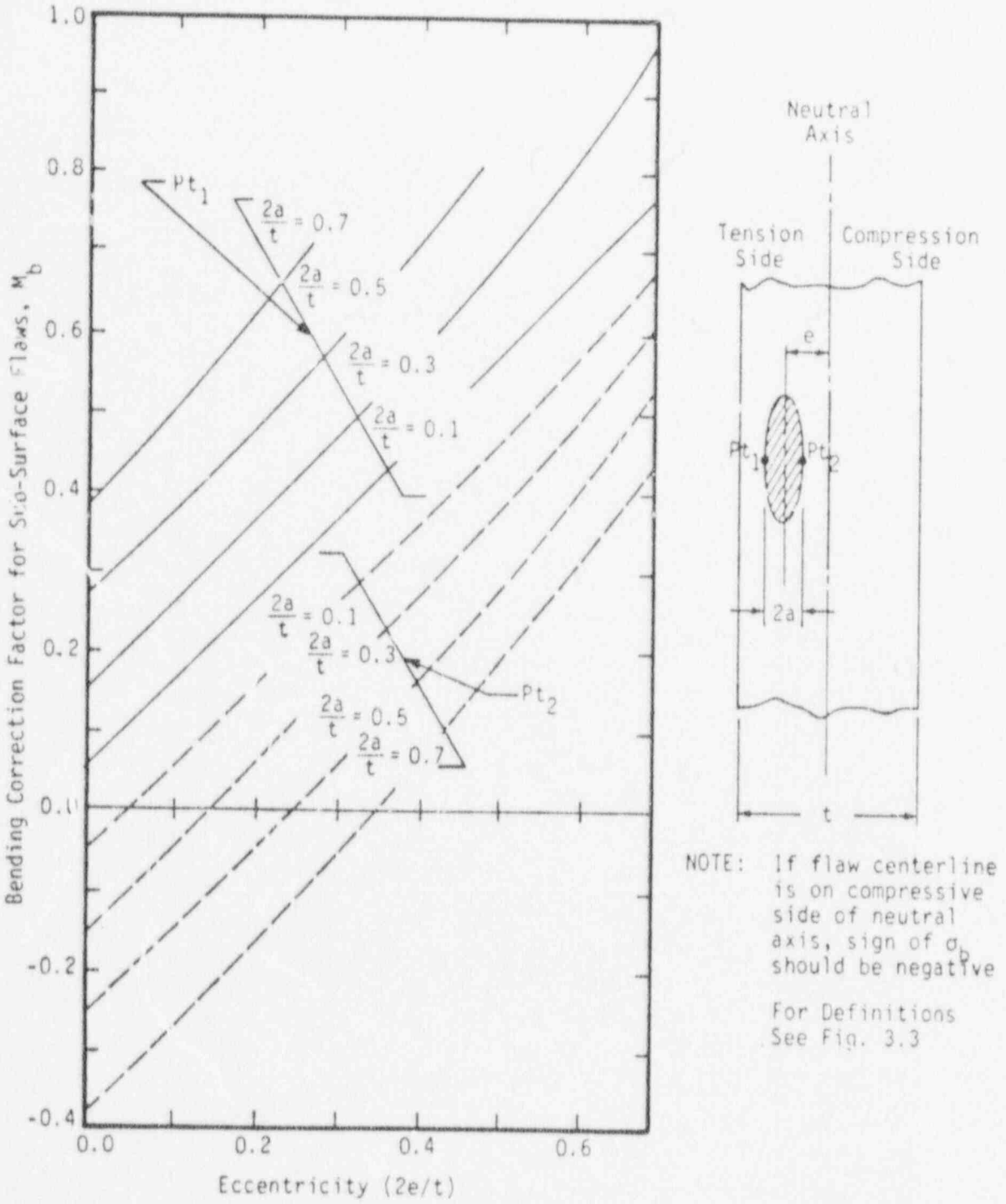

Figure C-8 - Bending Correction Factor for Surface Flaws (From Section XI, Fig. A-3300-4).

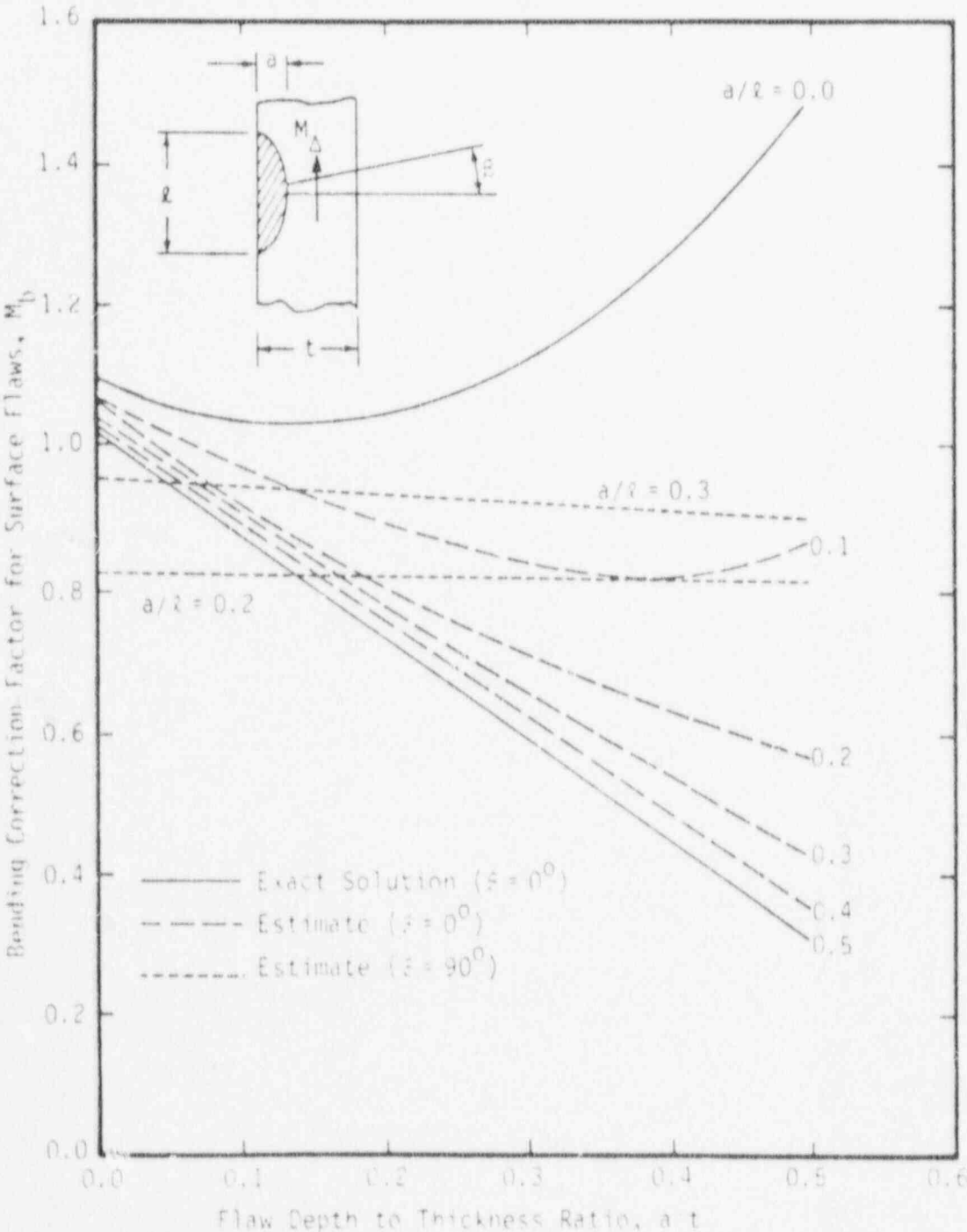

Figure C-9 Bending Correction Factor for Surface Flaws (From Section XI, Fig. A-3300-5).

where L is the crack line and $\sigma_{zz}(x)$ is the "uncracked" stress distribution normal to the crack face. Once the influence function, h, has been formulated for a given crack configuration, the stress intensity factor for any applied stress field determined for the "uncracked" geometry can be computed by simple numerical integration of Eq. C-10.

The essential features in the formulation of IF method are based on the following fundamentals:

(1) The application of elastic superposition allows the use of the "uncracked" stress distributions in the K analysis.

(2) The influence function itself is invariant with stress and provides the vehicle to calculate the effect of the crack in redistributing any stress field.

The principle of superposition reduces the K solution of an arbitrary and perhaps difficult crack problem to the solution of the stress analysis problem but without the crack and the problem of a crack body with an applied pressure that cancels the uncracked stress field to establish the fraction free boundary conditions along the crack face. This principle is illustrated in Fig. C-10. The general crack problem of (a) is considered to be the sum of two other problems (b) and (c) and, therefore,

$$K^{(a)} = K^{(b)} + K^{(c)}. \qquad \text{(C-11)}$$

Problem (b) is the same as problem (a), but without the crack. The stress field $\sigma(x)$ illustrated in (b) is simply the stress along the line of the crack locus in (a). Problem (c) is the solution to the original crack geometry of (a), but with loads on the crack face only of equal and opposite value to those illustrated in (b). Since K is the intensity of the singularity of stresses at the crack tip then $K^{(b)} = 0$ because the singularity is not present in problem (b). Hence, the principle of

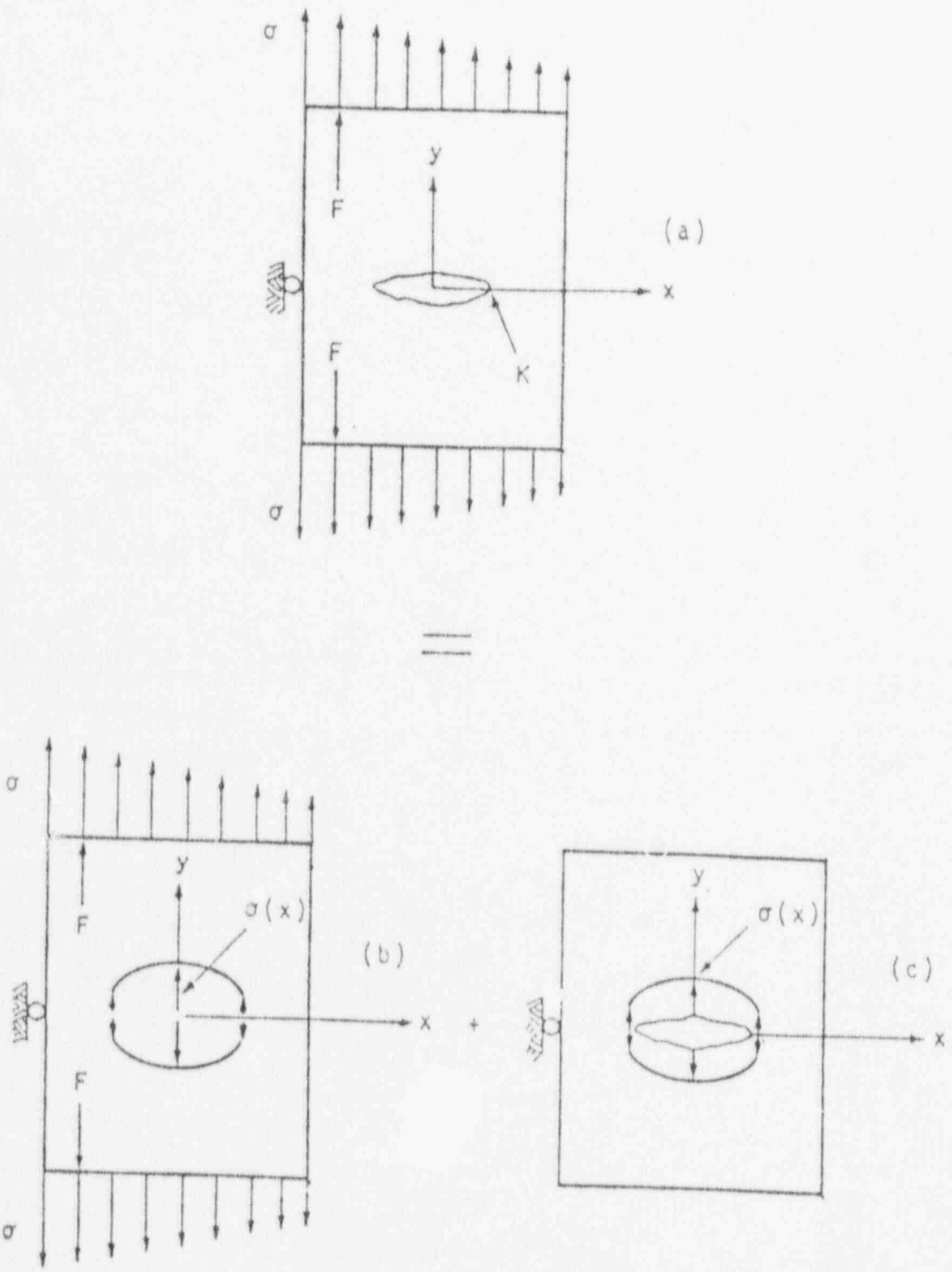

Fig. C-10 - The Reduction of a Problem, (a), Into Two Simpler Problems, (b) and (c), for Computations of Stress Intensity Factor, Illustrated for a Center-Cracked Plate

superposition reduces the K solution of a general problem to that of the determination of the uncracked stress, $\sigma(x)$, at the crack surface in Fig. C-10, and a crack problem with crack face pressures which cancel the $\sigma(x)$ distribution. The IF method is used to solve the latter problem, that of the pressurized crack. The major advantage of the IF method is the markedly reduced amount of stress analysis with cracks.

Many influence functions for specific crack geometries have been formulated, and these functions have been incorporated into a computer program called BIGIF. The BIGIF program was developed by EPRI through their sponsored research, and the program is fully supported and available through the EPRI Software Center. Complete program description and user's manual (C-15) are also available.

Other Numerical Methods

Other methods exist for determining K for specific crack geometries but applying such techniques will involve significant more effort and computer time to achieve a solution. The finite element method is a technique which is frequently used to solve complex stress analysis problems, and access to general purpose finite element codes can be obtained through computer service companies.

It should be stated that there are essentially two techniques which can be used to calculate K by the finite element method; these are either an energy-based technique (C-16, C-17), or the use of near-tip solution employing crack-tip elements (C-18, C-19). Another method which has been used is the boundary integral equations technique and some useful guidelines for using this method are presented in (C-20, C-21). The application of such methods will be very costly, probably of the order of a consequence analysis, and it is recommended that the other approaches mentioned above be tried first before an analysis is attempted where the cracked geometry is idealized in the model.

SUMMARY OF SOLUTIONS

Scope

This section provides a summary of K solutions for geometries that have direct application to component support designs. The solutions for K compiled herein were either obtained or developed from one of the methods previously discussed, and where appropriate, the source of the solution or method use to obtained a solution is sited. It is anticipated that this section will be expanded as more solutions are obtained.

Circumferential Cracks in Bolts

The solution for stress intensity factor for a circumferential crack of depth, a, in a round bar of diameter, D, is given in (C-3). For the case of uniform stress, the expression for K is

$$K_I = \sigma_m F_m \sqrt{\pi a} \qquad \text{(C-12a)}$$

where

$$F_m = (1/2)(c/b)^{-3/2}\left[1 + 0.5(c/b) + 0.374(c/b)^2 - 0.363(c/b)^3 + 0.731(c/b)^4\right] \qquad \text{(C-12b)}$$

and b is the nominal outer radius, D/2, c is the remaining uncracked ligament radius, b-a, and σ_m is the nominally applied stress based on the nominal bolt area. The accuracy of Eq. C-12 is reported to be better than 1%. For the case when the bolt is subjected to bending loads, the stress intensity factor can be computed by

$$K_I = \sigma_b F_m \sqrt{\pi a} \qquad \text{(C-13a)}$$

where

$$F_b = 0.375(c/b)^{-5/2}\left[1 + 0.5(c/b) + 0.375(c/b)^2 + 0.3125(c/b)^3 + 0.2734(c/b)^4 + 0.537(c/b)^5\right] \qquad \text{(C-13b)}$$

and σ_b is the nominally applied bending stress equal to $4M/b^3$. The accuracy of Eq. C-13 is reported to be better than 1%.

The totally applied K due to combined tension and bending loads can be obtained by summing the results from Eqs. C-12 and C-13. The application of Eq. C-12 and Eq. C-13 to bolting should be conservative when the flaw depth, a, is assumed be the sum of the thread depth plus postulated crack depth. It should also be noted that representation of an elliptical crack by a fully circumferential crack model will add to the conservation of calculating K by this model. A more accurate approach would involve the determination of the local stress distribution due to the K_t associated with the bolt thread and calculating K by the influence function method.

REFERENCES

C-1 ASME Boiler and Pressure Vessel Code, Section XI, "Rules for In-Service Inspection of Nuclear Power Plant Components", 1980 Edition.

C-2 Peterson, R.E., Stress Concentration Factors, Wiley and Sons, 1974.

C-3 Paris, P.C., and Sih, G.C., "Stress Analysis of Cracks", Fracture Toughness Testing, ASTM STP 381 (1965).

C-4 Tada, H., et.al, The Stress Analysis of Cracks Handbook, Del Research Co. (1973).

C-5 Sih, G.C., Handbook of Stress Intensity Factors for Researchers and Engineers, Vol. 1, Lehigh University (1973).

C-6 Newman, J.C., Jr., and Raju, I.S., "Analysis of Surface Cracks in Finite Plates Under Tension and Bending", NASA Technical Paper 1578, NASA Langley Research Center, December 1979.

C-7 Barsom, J.M., Rolfe, S.T., Fracture and Fatigue Control in Structures, Applications of Fracture Mechanics, Prentice Hall (1977).

C-8 Knott, J.F., Fundamentals of Fracture Mechanics, Wiley and Sons (1973).

C-9 Cipolla, R.C., "Computational Method to Perform the Flaw Evaluation Procedure as Specified in the ASME Code, Section XI, Appendix A, Part I: General Description and Background", EPRI RP 700-1, Key Phase Report NP-1181, September 1979.

C-10 Marston, T.U. (ed.), "Flaw Evaluation Procedures -- Background and Application of ASME Section XI Appendix A", ASME Task Group on Flaw Evaluation, EPRI NP-719-SR (August 1978).

C-11 Bueckner, H.F., Methods of Analysis and Solutions of Cracked Problems, Chapter V, Ed. by G.C. Sih, Noordhoff (1972).

C-12 Rice, J.R., "Some Remarks on Elastic Crack-Tip Stress Fields," International Journal of Solids and Structures, Vol. 8, pp 751-758 (1972).

C-13 Besuner, P.M., "Fracture Mechanics and Residual Fatigue Life Analysis of Complex Stress Fields," EPRI 217-1, Technical Report 2 (July 1975).

C-14 Cruse, T.A. and Besuner, P.M., "Residual Life Prediction for Surface Cracks in Complex Structural Details, " AIAA Journal of Aircraft, Vol. 12, No. 4, pp. 369-375 (April 1975).

C-15 Cipolla, R.C., Besuner, P.M., and Peters, D.C., "BIGIF: Fracture Mechanics Code for Structures - User's Guide (Manual 2)" EPRI RP 700-1, NP-838, August 1978.

REFERENCES cont'd

C-16 Hayes, D.J. "A Practical Application of Bueckner's Formulation for Determining Stress Intensity Factors for Cracked Bodies" Int. J. Fracture Mechanics, Vol. 8 (1972)

C-17 Parks, D.M. "A Stiffness Derivative Finite Element Technique for Determination of Crack Stress Intensity Factors" Int. J. Fracture Vol. 10 (1974)

C-18 Henshell, R.D. and Shaw, K.G. "Crack Tip Finite Elements are Unnecessary" Int. J. Numerical Methods Engineering Vol. 9 (1975)

C-19 Barsoum, R.S. "Application of Quadratic Isoparametric Finite Elements in Linear Fracture Mechanics" Int. J. Fracture Vol. 10 (1974)

C-20 Heliot, J., Labbens, R. and Pellissier-Tanon, A. "Application of the Boundary Integral Equation Method to Three Dimensional Crack Problems" Century 2 Pressure Vessels and Piping Conference, San Francisco ASME (1980)

C-21 Besuner, P.M. "The Application of the Boundary Integral Equation Method to the Solution of Engineering Stress Analysis and Fracture Mechanics Problems" EPRI RP 217-1, Technical Report No. 3, May 1975.

APPENDIX D

POSTULATED FLAW SIZE AND ACCEPTANCE CRITERIA

INTRODUCTION

The purpose of Appendix D is to establish the postulated or "reference" flaw size, a_r, to be assumed in the analysis, and to give the background and basis for the definition of the "reference flaw". There will be two ways a reference flaw size can be established 1) by selecting a bounding flaw size based on a statistical analysis of initial flaw size data of similar fabrication procedures, and 2) by defining a flaw size based inspection. If a_r is to be established by inspections, then a demonstration of the reliability of the inspection system to detect that flaw size will be required.

This appendix presents guidelines and recommendations on selecting a value a_r from a bounding review of flaw size data. The guidelines given herein are preliminary, since this project task has not been completed. Also presented in this appendix of an appropriate safety factors specified in the ASME Code and the selecting of an appropriate safety factor to be applied to the final results for acceptance which is consistant with the current Code.

POSTULATED FLAW SIZE

Welded Structures

The ASME Code Appendix G (D-1) provides the rules for establishing the size and shape of the flaw to be postulated in the beltline region of a welded pressure vessel. The defect to be used in an Appendix G analysis is to be a sharp surface connected flaw, normal to the direction of maximum stress. For section thicknesses 4 to 12 inches (10.2 to 30.5 cm), the reference flaw is to have a depth of 25% of the section thickness, and a surface length of 1 1/2 times the section thickness. For the case when the section thickness is greater than 12 inches (30.5 cm), the reference flaw size determined for the 12-inch (30.5 cm) section will be assumed.

A problem arises if sections smaller than 4 inches (10.2 cm) are encountered with the Appendix G procedure since the flaw size to be assumed is held at 1-inch (2.54 cm). To adopt Appendix G procedures for support designs will become to prohibitive for thin sections common of structural shapes. Flaw size data are currently being reviewed to establish a rational way to determine a bounding value for a/t. Unpublished flaw data on T-1 steel weldments contain flaw depths associated with common weld imperfections including slag, porosity, weld metal cracks and heat affected zone cracks. At this time, the information on slag defects has been completed and these data suggest 90%-90% nondimensional flaw size of a/t = 0.16. This histogram of slag defects is shown in Fig. D-1. The mean slag defect size is a/t = 0.03. A log-normal distribution seems to fit the data reasonably well.

Forged/Machined Surfaces

For as-forged surfaces or surfaces which have been machined (not welded), the flaw size that would result from such practice will be much less than that for a welded structure. Little data have been collected on this type of fabrication so that the recommendations provided in this appendix are based on the following engineering considerations:

1) Forged and/or machined parts are inspected after fabrication.

2) Cold work hardened layers caused by machining abuses should be very small.

3) The depth of surface defects due to forging and machining practices is independent of section thickness.

The recommendations given herein are preliminary and it is anticipated that further research will provide more data so that a_r for forged members will have a rational basis.

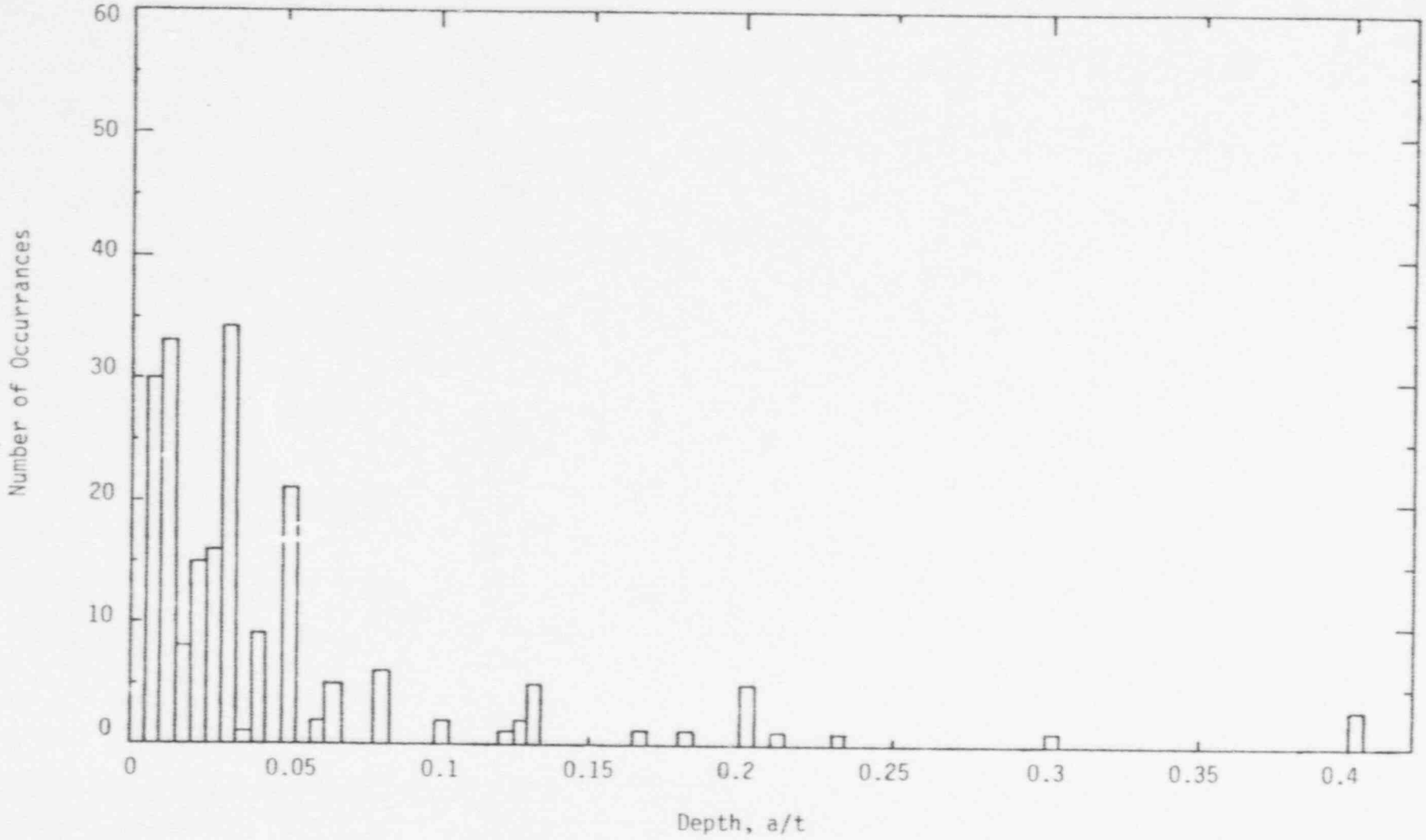

Figure D-1 Histogram of Slag Defects from Weldments of T-1 Steel

Reference Flaw Size Procedures

The following are preliminary procedures for determining the reference flaw size a_r.

1) The flaw to be assumed will be elliptical in shape and treated as a sharp crack. The flaw will be surface connected and located on the maximum stress plane.

2) The flaw depth will be established per Table D-1 for the appropriate fabrication practice used.

3) The length of the flaw, ℓ, will be 1 1/2 times the section thickness or a length which produces a crack aspect ratio, a/ℓ, to 1/6, whichever is less.

4) A subsurface flaw should be assumed, if it is believed that the subsurface defect would be worse than a surface flaw.

ACCEPTANCE CRITERIA

Although a flaw acceptance criterion for defects in supports does not exist, a set of conditions can be established which reflect the intent of the ASME Code, specifically the criteria used in Appendix G of Section III (D-1) and Appendix A of Section XI (D-2) specified in IWB-3600. In the approach advocated in this report, a reference flaw size is used to establish an acceptable level of toughness. The final factor to be applied at the end of the evaluation should reflect the uncertainty in the analysis as well as the type of event and the probability of occurrence of such events. All these factors are reflected in the judgements used to establish the existing margins in Code.

The Code requires a check on either flaw size, or applied K (or load) to establish whether a flaw can remain in a component. Depending on the desired safety factor, (f), the two conditions can be written as:

TABLE D-1

PRELIMINARY RECOMMENDATIONS ON POSTULATED FLAW SIZE

FABRICATION	SECTION THICKNESS RANGE	FLAW DEPTH
Welded	1" to 4"	t/8
	4" to 12"	t/5
	>12"	2.4"
Forged/Machined	N/A	0.030"

$$\frac{a_c}{a_f} \geq f_a, \qquad \text{(D-1)}$$

or $$\frac{K_{Ic}}{K_I} \geq f_p, \qquad \text{(D-2)}$$

where a_c is the critical flaw size, a_f is the final flaw size, and f_a and f_p are the safety factors to be satisfied. It should be noted that f_a and f_p in general are not the same and may have different values and still provide the same assurance against failure.

A summary of the margins provided by Code analyses is given in Table D-2. In Appendix G of Section III the safety margin is contained in the calculation of K_I where f_p is between 1 to 2. In the analysis a postulated flaw size which is 25% of the wall thickness is assumed. These requirements are for normal operating conditions for pressure retaining components, and no definitive rules are recommended for emergency of faulted conditions that the principles of Appendix G may be applied where applicable with any postulated loadings, defect sizes, and fracture toughness which can be justified for the situation involved. In Appendix A of Section XI, actual defects sizes as measured by the inspection system, and under normal conditions the acceptance criteria are focused on assuring at least a factor of safety of three against vessel rupture (i.e., $f_p \geq 3$), and for accident conditions, this factor is reduced to $\sqrt{2}$.

In the evaluation procedure outlined herein, elements of both Appendix G and Appendix A are present. For the situation for using a reference flaw approach assuring adequate toughness under accident loading conditions, the Appendix A criteria for emergency and faulted conditions. Applying this to our case:

$$a_r < a_c/2 \qquad \text{(D-3)}$$

$$K_I < K_{Ic}/\sqrt{2} \qquad \text{(D-4)}$$

where K_I is the maximum applied K_I for the flaw size a_r.

TABLE D-2

SUMMARY OF CODE SAFETY FACTORS

	Normal Operation		Emergency/Faulted	
	f_a	f_p	f_a	f_p
Appendix G Section III	*	1 to 2	--	--
Appendix A Section XI	10	$\sqrt{10}$	2	$\sqrt{2}$

*Reference Flaw Equal to 25% of Wall Thickness is Postulated

REFERENCES

D-1 ASME Boiler and Pressure Vessel Code, Section III, Division 1 Appendices - Appendix G, "Protection Against Nonductile Failure," 1980 Edition.

D-2 ASME Boiler and Pressure Vessel Code, Section XI, Appendix A, "Analysis of Flaw Indications", 1980 Edition.

APPENDIX E

EXAMPLE PROBLEMS

INTRODUCTION

As illustrated examples, three sample evaluations are performed to demonstrate the procedural steps, the nature of the assumptions, and calculations which will be required in a fracture mechanics assessment. These problems are provided only as examples, however they do accurately reflect the geometries and possible loadings commonly encountered in component supports. The three examples presented in this appendix are:

1) Welded I-beam connection

2) Pin-column support for steam generator

3) Reactor coolant pump anchor stud.

It is anticipated that these examples will be expanded and others possibly added during the course of the project.

WELDED I-BEAM CONNECTION

Description

This example deals with the analysis of a welded I-beam connection. A typical weld detail for the intersection of two I-beams to form a T-connection is shown in Fig. E-1. This geometry is typical of a beam lattice to support pipe whip restraint members. At the location illustrated in Fig. E-1, the connection is between a W14x342 beam and a built-up beam, with another W14 beam acting as a brace. Although this geometry and the analysis which follows is not for a component support but for a pipe support structure, the analysis and loadings should still be representative of a frame support composed of moment-resisting members. The beams were supplied to an ASTM A36 specification and the connection was fabricated with E7018 electrodes with no post-weld heat treatment.

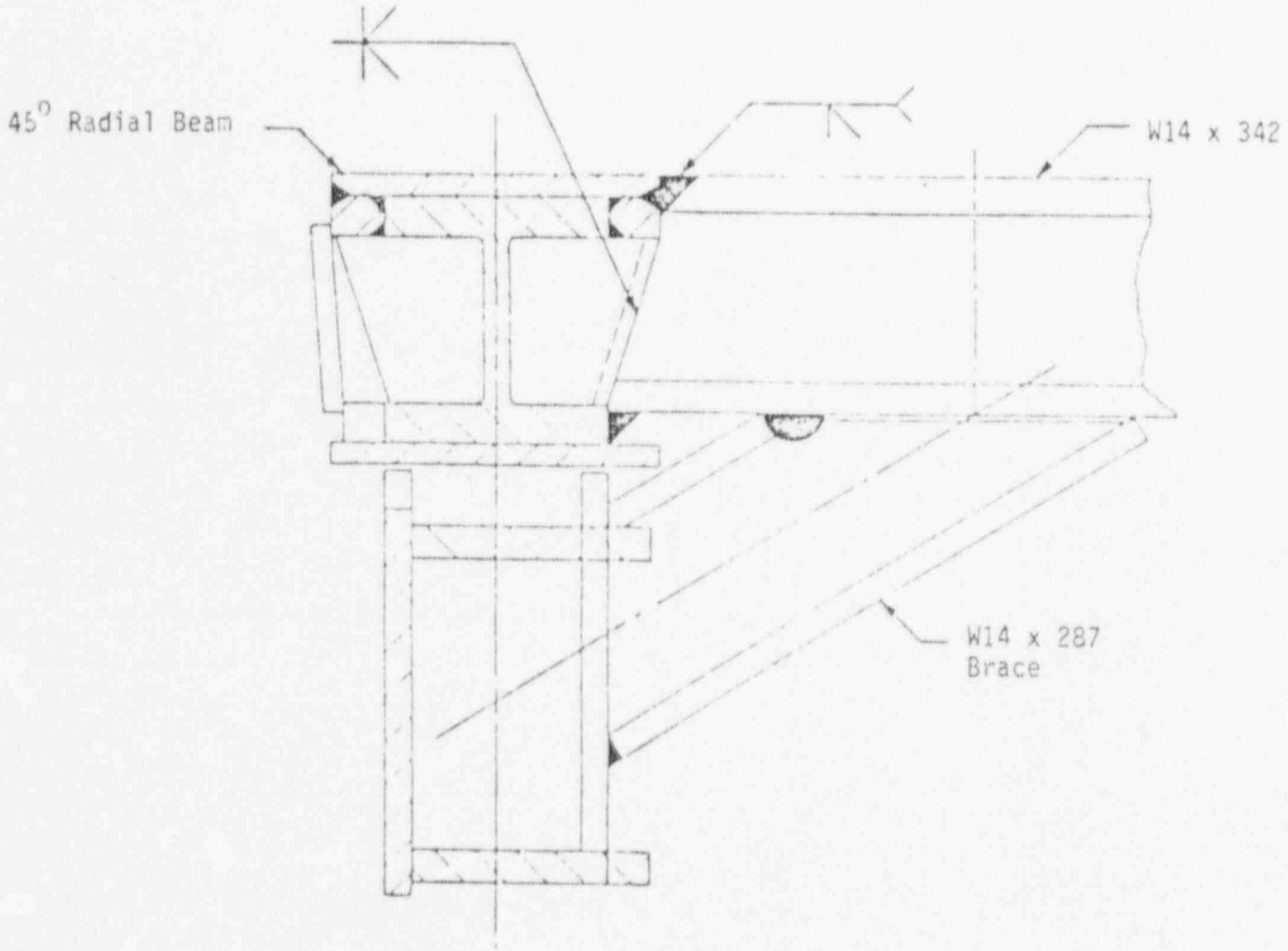

Figure E-1 Schematic Diagram Showing the Weld Detail for a T-Connection.

A stress analysis was performed to determine the local axial and bending moments at this connection, and these loads were used to determine the local axial and bending stresses. These bending moment distributions for two postulated loading cases are shown in Figs. E-2 and E-3. These applied loads give rise to a maximum stress of 10 ksi (68.9 MPa m^{-2}) at this location. Residual stresses due to welding were also included. Rather than use the generic procedures outlined in Appendix B, the references given in Appendix B were reviewed and a residual stress profile was estimated from the expected distribution for two butt-welded plates. This distribution is shown in Fig. E-4. The peak weld residual, σ_w, is taken to be the yield strength of the material, 36 ksi (248 $MPam^{-2}$), and the distribution was assumed to be cosine in shape.

Calculation of Stress Intensity Factors

Three crack models were postulated: (1) an edge crack in the top flange, (2) a semicircular crack in the top flange centered on the web, and (3) an edge crack at the end of the top flange. A schematic diagram representation of these postulated cracks is given in Fig. E-5. The influence function method was used to calculate K (see Appendix C). An edge crack in the top surface of the flange as shown in Fig. E-5a represents a worst case flaw with respect to the applied loads. The effect of residual stresses is small since the distribution along the weld would be in equilibrium. The semicircular crack is used to assess the total K situation when residual weld stresses as shown in Fig. E-4 are present. For the edge crack originating on the top flange, the bending stress about the weak plane is conservatively added to define the univariate stress along the crack plane. The applied stress intensity factor is shown in Fig. E-6. To assess the effect of residual stress due to welding, the calculated K for a semi-circular crack was determined. This K distribution is shown in Fig. E-7. Due to local residual stress, the K value increases then decreases and a peak K level of 46 ksi $\sqrt{in}$ (51 $MPam^{1/2}$) was calculated.

Determination of Critical Flaw Size

The fracture toughness of the A-36 material was estimated from the curves

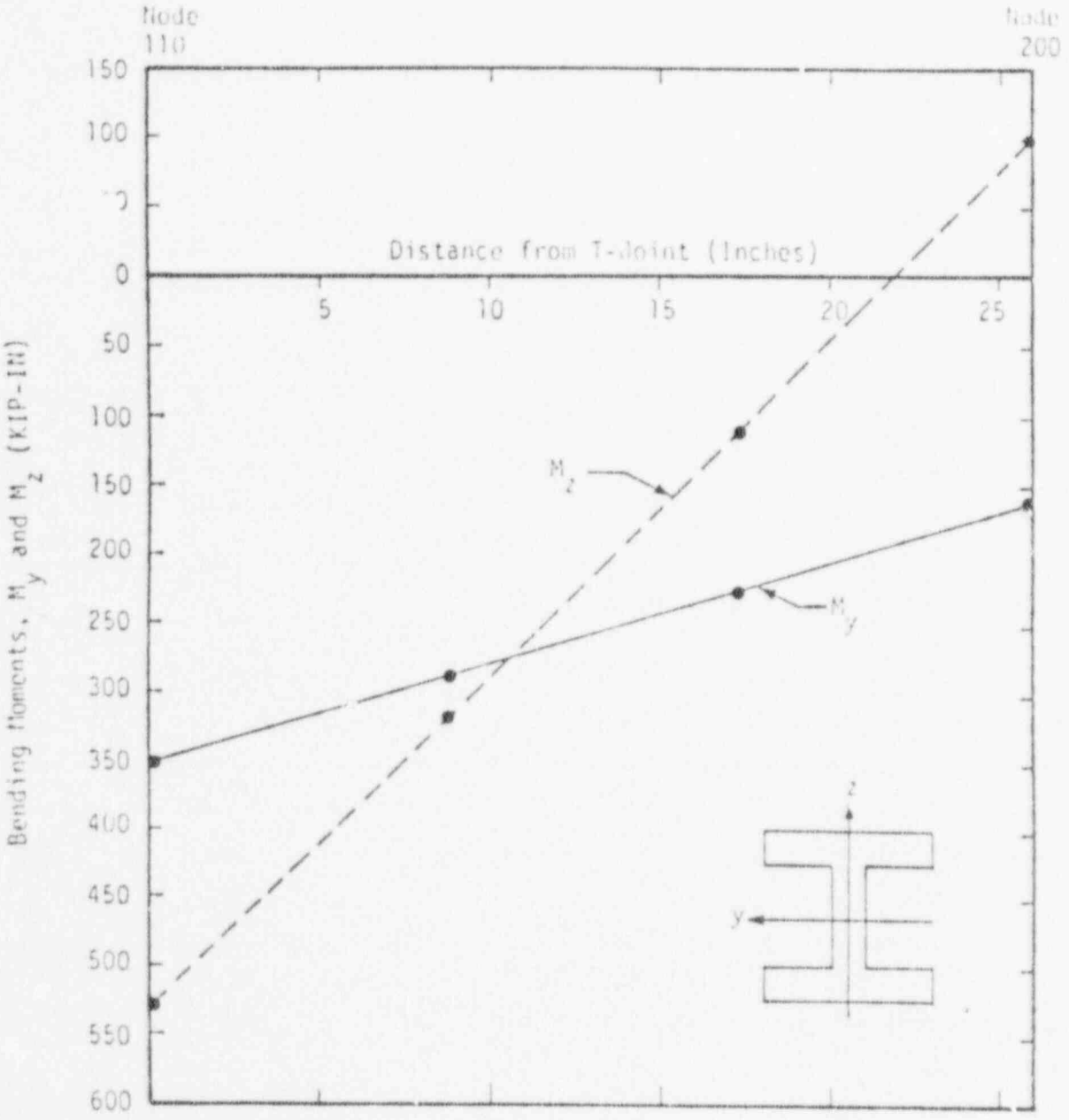

Figure E-2 - Bending Moment Distribution in T-Beam 110 to 200 (Case 1)

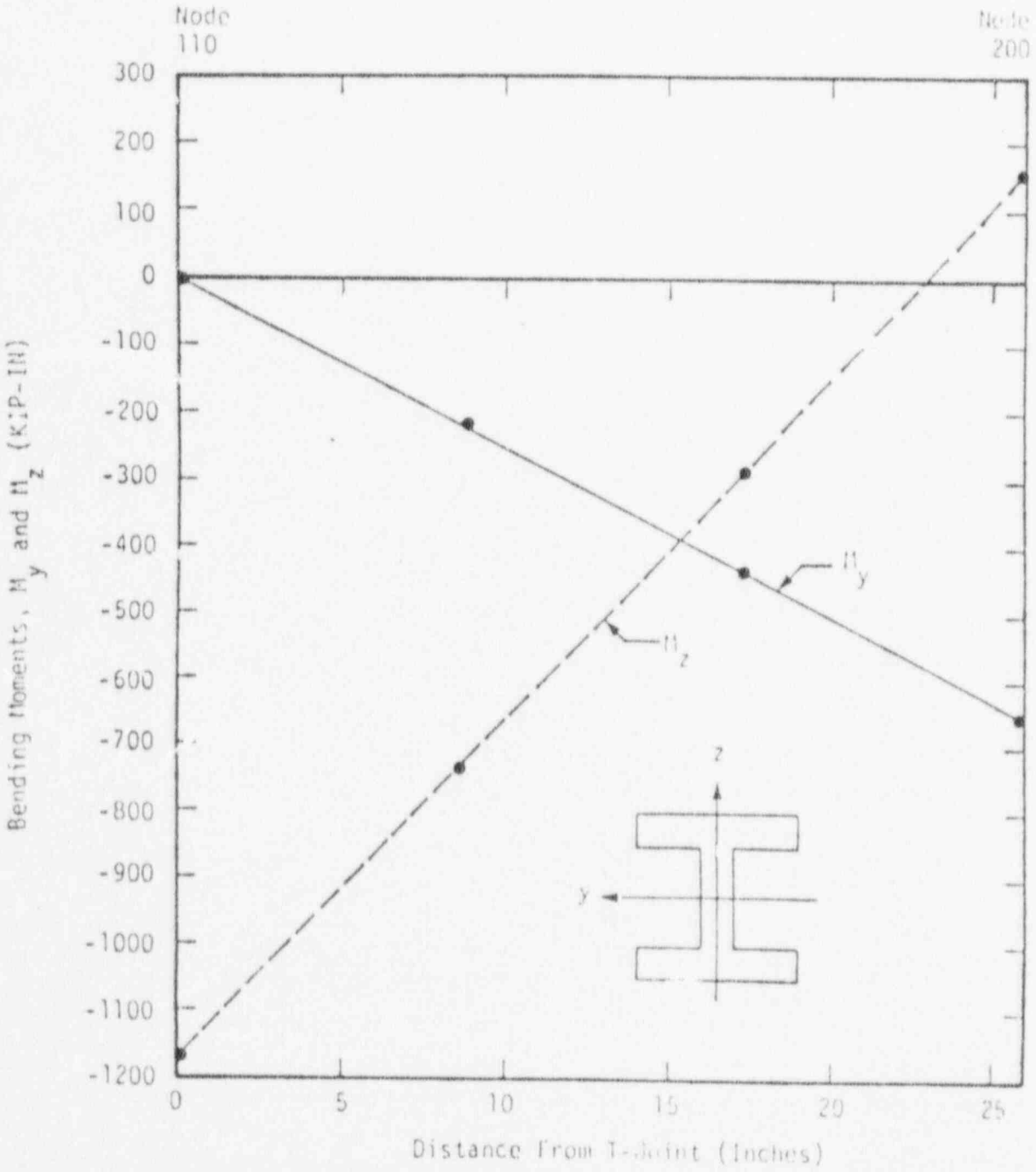

Figure E-2 - Bending Moment Distribution in T-Beam 110 to 200 (Case 2)

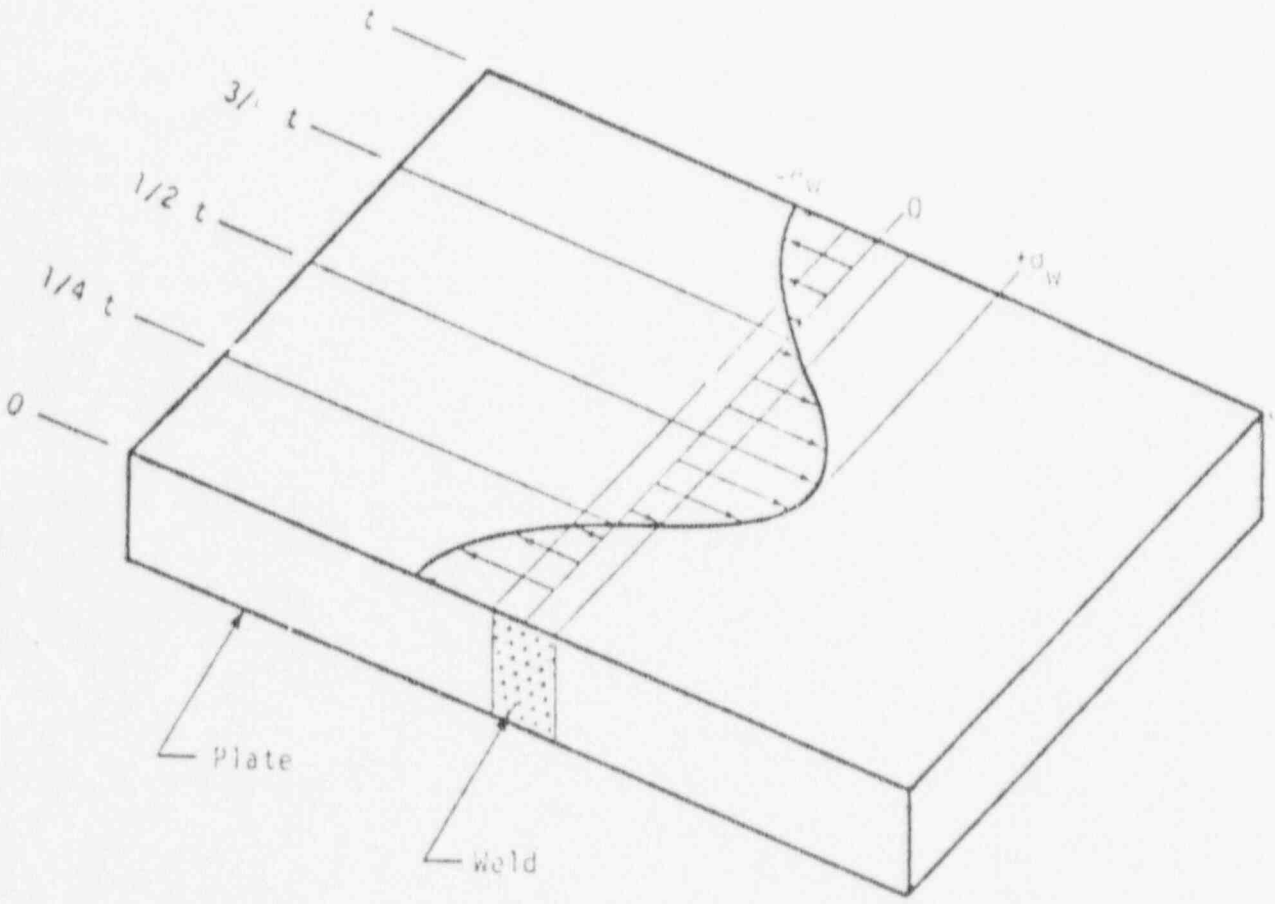

Figure E-4 - Transverse Variation in Residual Surface Stress Along the Weld Line.

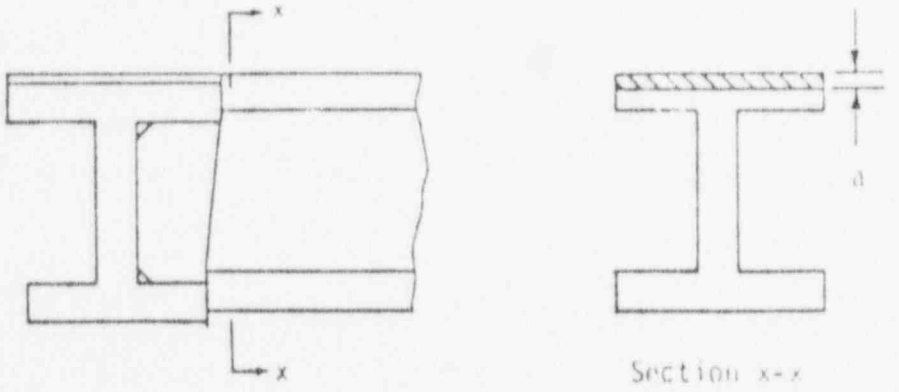

a) Edge Crack in Top Surface of Flange.

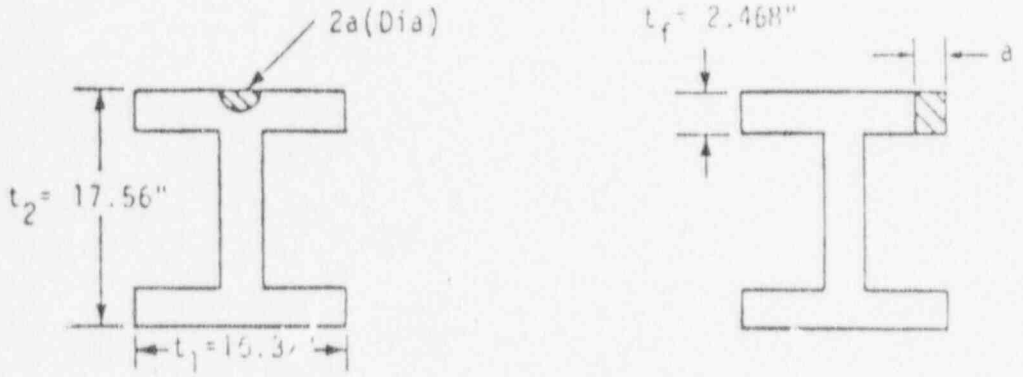

b) Semicircular Crack in Top Flange.

c) Edge Crack in the End-of-Flange.

Figure E-5 - Schematic Showing Flaw Model Locations in T-Connection.

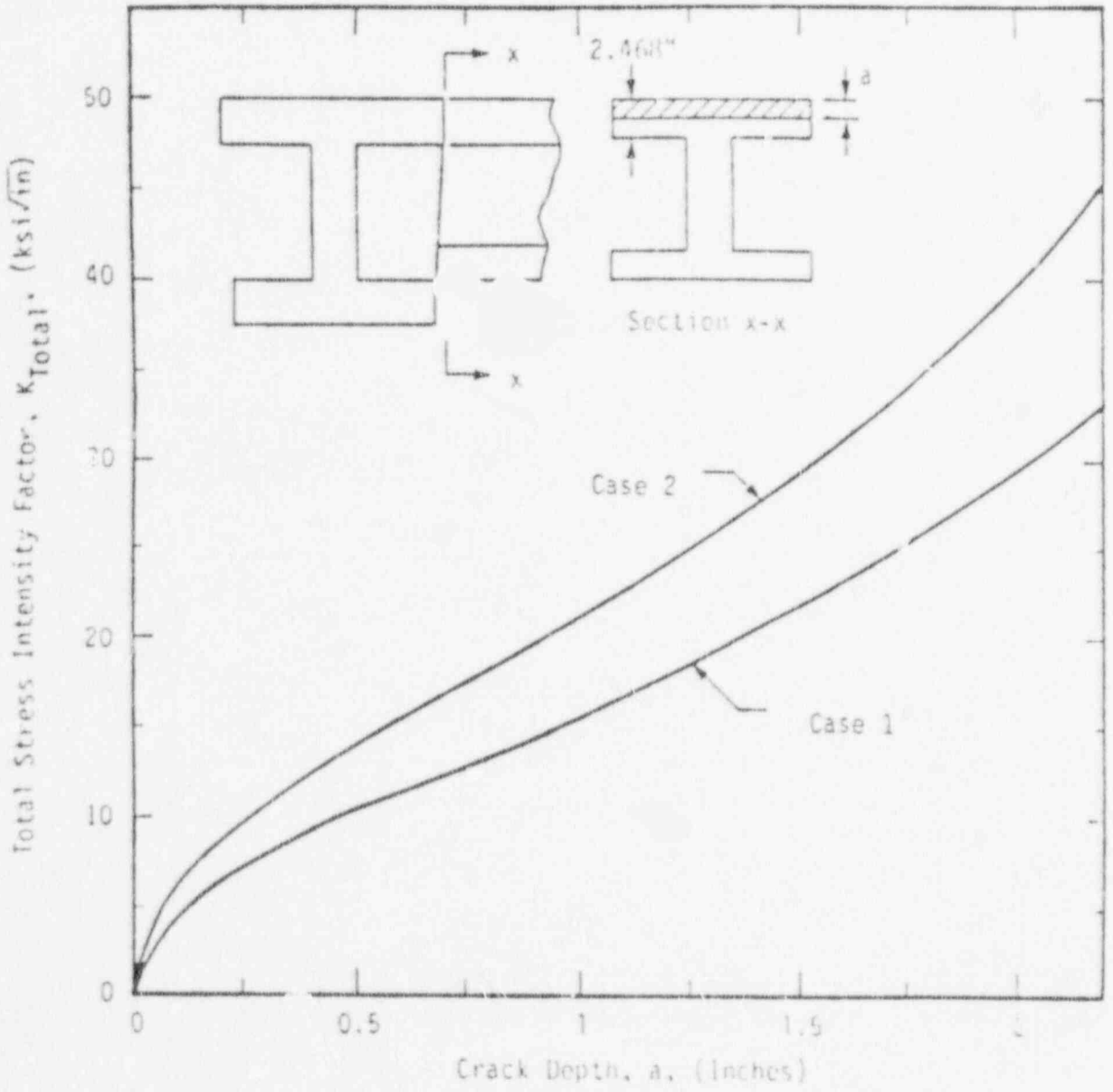

Figure E-6 - Total Stress Intensity Factor for an Edge Crack in the Flange of the T-Connection Weld

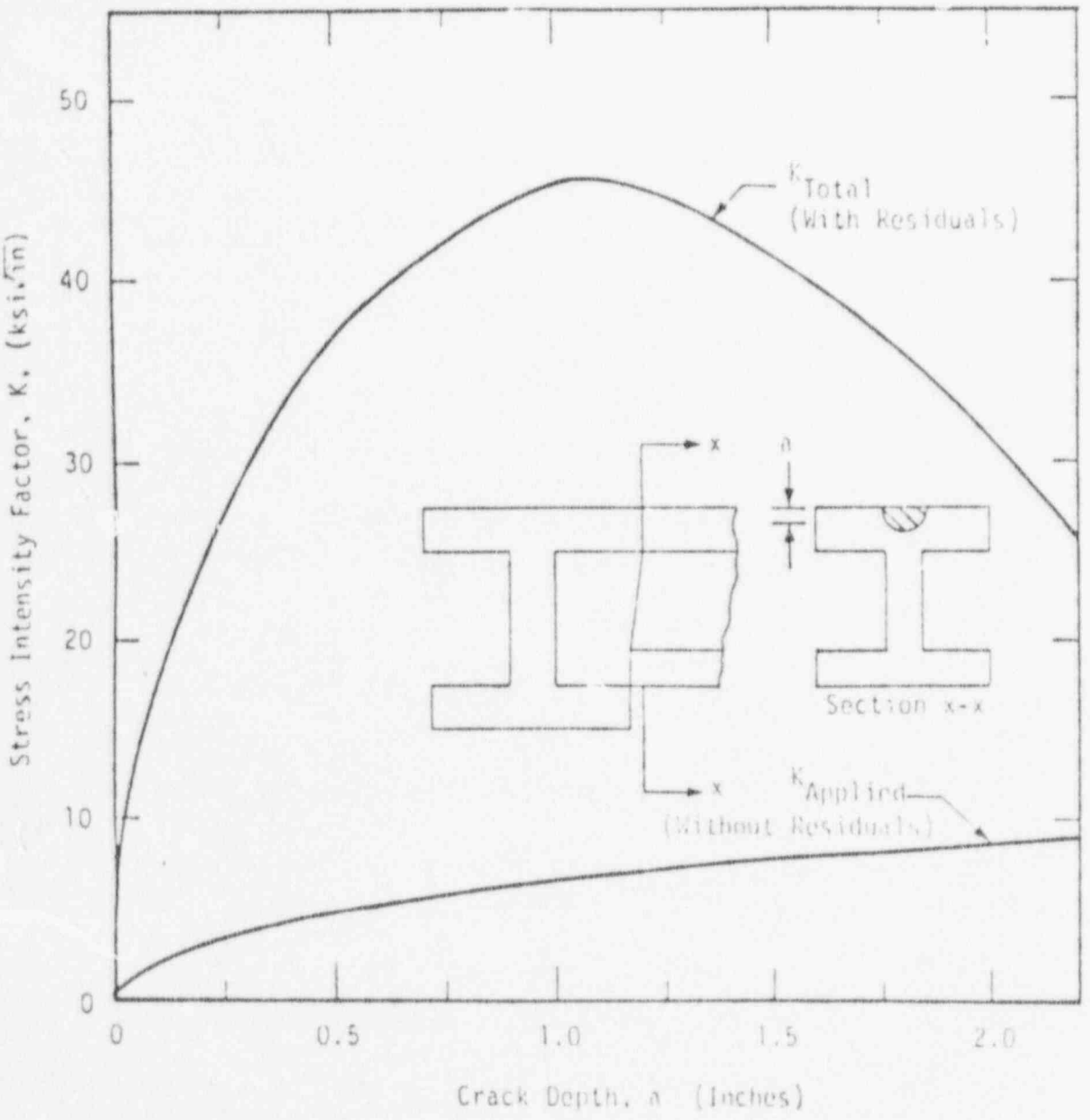

Figure E-7 - Stress Intensity Factor for a Semicircular Flange Surface Crack in the T-Connection Weld (Case 2)

provided in Appendix A. In this example, the plate properties are assumed to be limiting and the toughness at 75°F (24°C) is taken to be 75 ksi $\sqrt{in}$ (80MPam$^{1/2}$). This K_{Ic} value is the 90%-90% bound value given in the graph for A-36 in Appendix A.

For the long crack at the top of the flange (Fig. E-6), the critical crack depth is approximately equal to the flange thickness or 2.4 inches (6.1 cm). For the semicircular crack, the applied K never exceeds K_{Ic} within the flange thickness. Clearly for these cases, the value of a_c is large relative to the thickness of concern.

PIN-COLUMN SUPPORT

Descripiton

The geometry of a pin-column steam generator support is shown in Fig. E-8. This geometry is also typical of coolant pump support. The support design includes a pipe-column which has a clevis at each end, and the pipe-clevis arrangement is attached to trunnions with pins. An evaluation is performed on the clevis where a crack is postulated at the maximum stress plane on the inside surface of the hole.

The clevis was supplied to an ASTM A 540 B23 specification, and has a yield strength of 125 ksi (862 MPa m^{-2}) and an ultimate tensile strength of 140 ksi (965 MPa m^{-2}). A chemical analysis of the material indicated the alloy supplied was 4340 steel.

Stesss Analysis

Under normal plant operating conditions, the columns are under compressive loading due to the dead weight. For a postulated faulted condition, the design is to resist an over turning moment which can generate a peak axial load of 2100 kips (9341 MPa). To determine the stress distribution at the postulated flaw location, a finite element model of the clevis was developed as shown in Fig. E-9 and the resulting stress distribution is given in Fig. E-10.

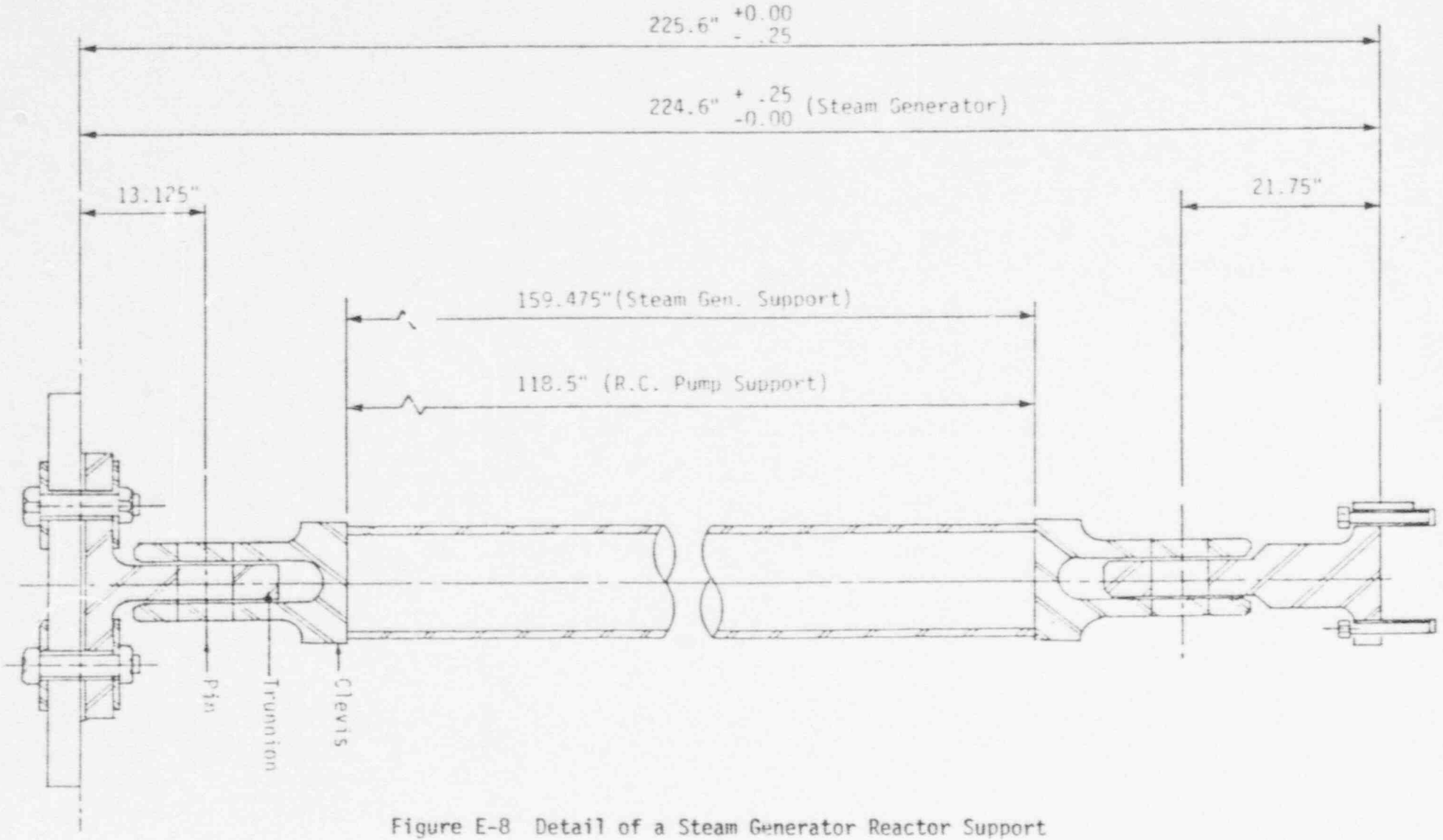

Figure E-8 Detail of a Steam Generator Reactor Support

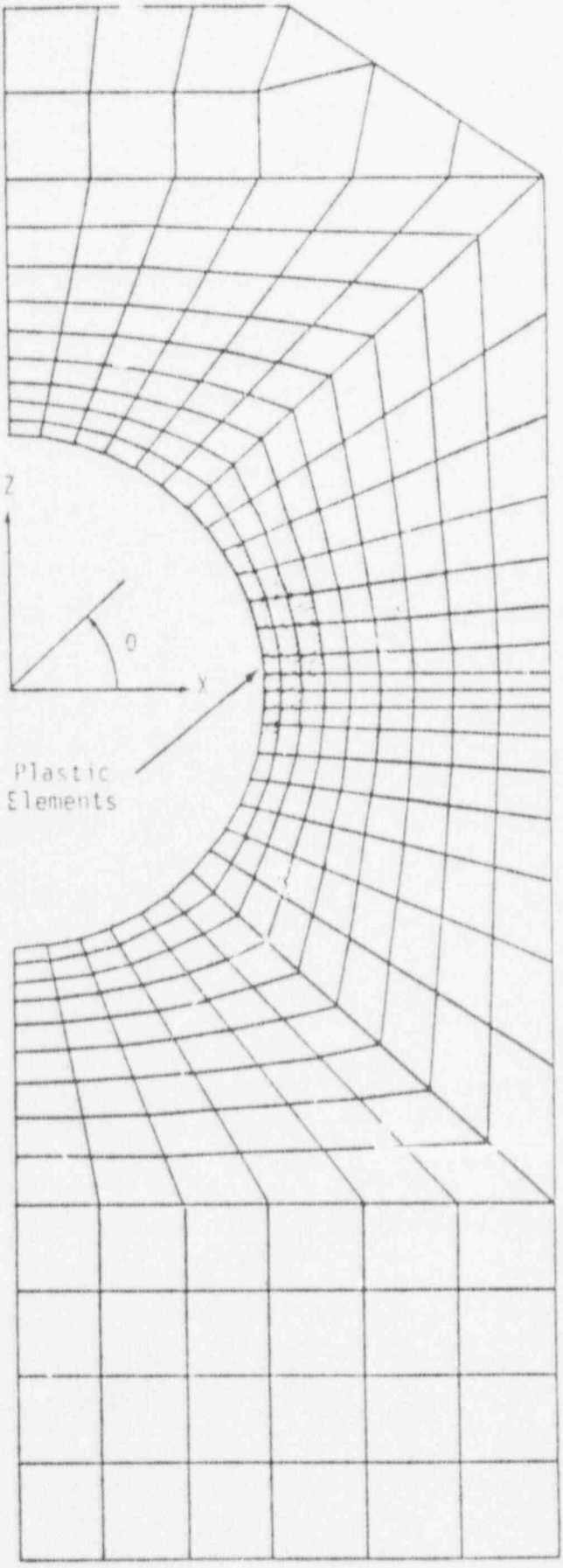

Figure E-9 Finite Element Model of Clevis

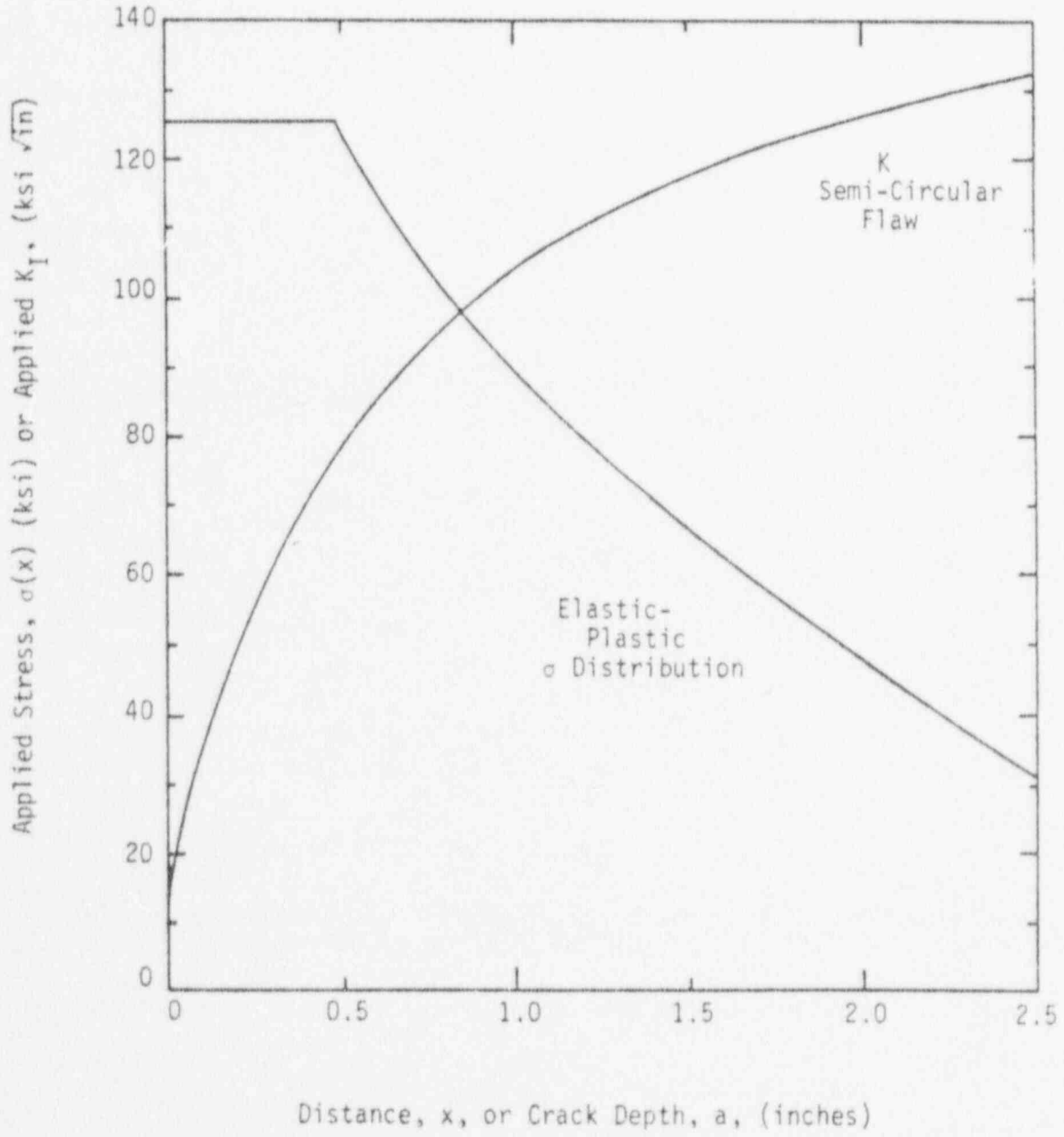

Figure E-10 Applied σ and K Distribution for Clevis Under Maximum Faulted Condition

Under these loading conditions the inner surface of the hole becomes plastic, and the finite element model allowed the material to yield according to the stress-strain typical of 4340. The yielding was contained to a region which was about 1/2 inches (1.27 cm.) in depth from the hole surface.

Determination of Critical Flaw Size

Rather than using the elastic situation, the elastic-plastic stress distribution was used to calculate the stress intensity factor. This approach will allow for a more realistic estimate consistant with a K-calculation based on strain. The influence function method (see Appendix C) was used to calculate K_I for a semicircular crack as shown in Fig. E-11. The resulting K distribution is shown in Fig. E-10.

The fracture toughness for the material was assumed to be the 90%-90% bound taken from the curves provided in Appendix A for the case when no data for the actual material are available. The value of K_{Ic} at an assumed temperature of 75°F (24°C) is 82 ksi$\sqrt{in}$ (90 MPam$^{1/2}$). From Fig. E-10 the flaw size at which $K_I = K_{Ic}$ is 0.56 inches (1.42 cm). A reference flaw size, a_r, of 0.28 inches (0.71 cm) would demonstrate an acceptable condition given that a factor of two on flaw size is adopted. The same value for a_r will result from the criterion based on load since K_I at a=0.28 inches (0.71 cm) is equal to $K_{Ic}/\sqrt{2}$.

PUMP ANCHOR STUDS

Description

In this example the anchor studs for a reactor coolant pump are evaluated to demonstrate the important steps required for applying the procedures to bolting. The studs are assumed to be nominally 2 1/4 inches (5.72 cm) in diameter with 8UN2A threads. The studs were purchased to an ASTM A 540 B23 Class 3 specification and the material supplied was 4340 alloy. The yield strength of the material is 150 ksi (1034 MPam^{-2}) and the tensile strength is 175 ksi (1207 MPam^{-2}). A summary of the bolt dimensions is given in Table E-1.

Under accident loads, the bolted design is such that the over-turning moment will produce a maximum stress in the studs of 100 ksi (690 MPam^{-2}) based on the nominal area. The loading will produce primarily a uniform axial stress and any bending effects are neglected.

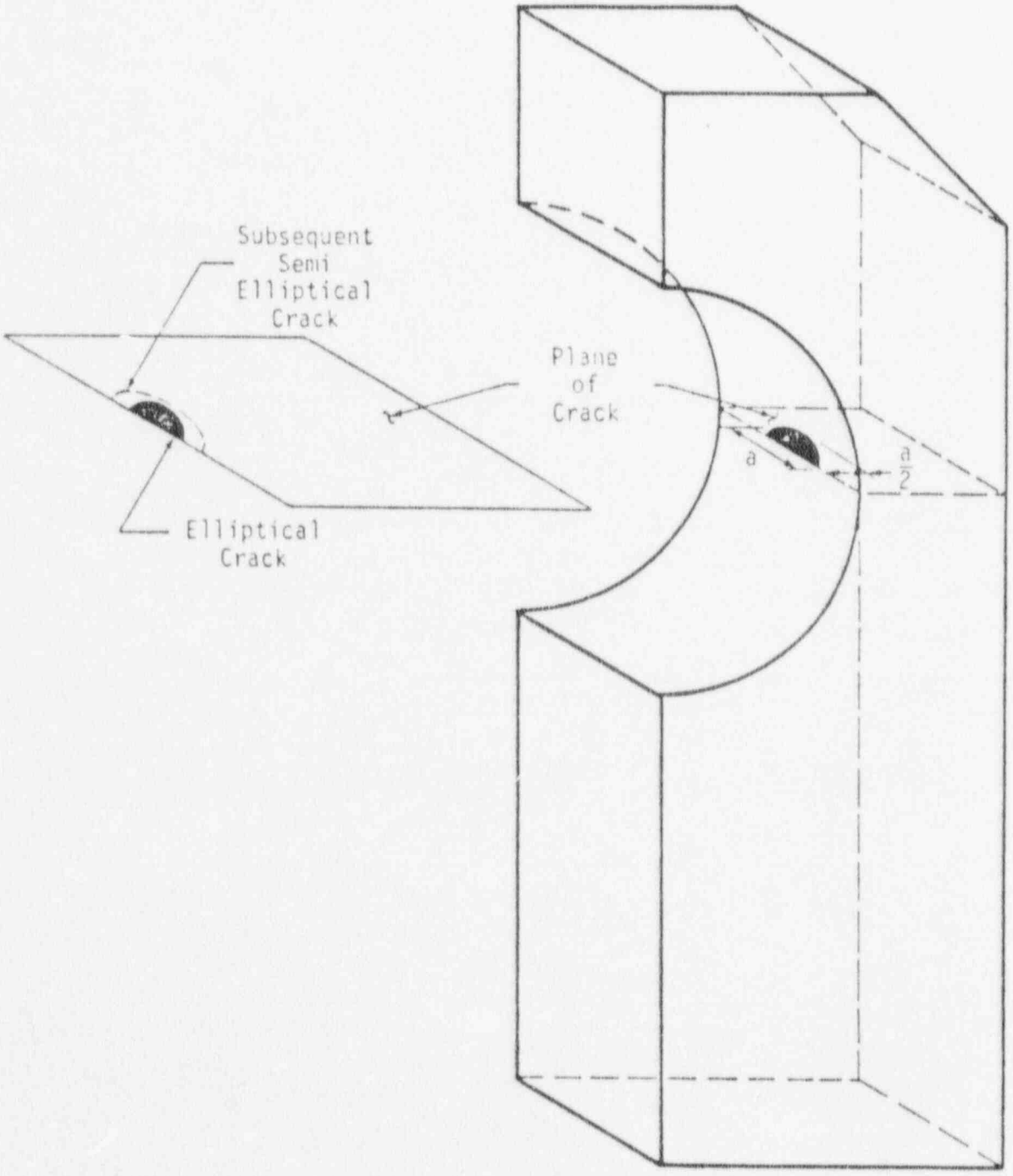

Figure E-11 Schematic Diagram Showing Flaw Location

TABLE E-1

Summary of Stud Geometry

Bolt/Thread Description:	2 1/4" - 8UN2A
Major Diameter	2.2401" ± 0.0075"
Minor Diameter	2.0942"
Area Ratio (Major/Minor)	1.154
Thread Depth	0.077"

Determination of Fracture Toughness

The static fracture toughness of the material was determined when no toughness data are available for the actual material. From the statistically based lower bound curves provided at the end of Appendix A, the 90%-90% tolerance bound value for K_{Ic} for A540 is given as 82 ksi $\sqrt{in}$ (90 MPa $m^{1/2}$). This toughness level was determined for an assumed lowest service temperature of 75°F (24°C).

Calculation of Critical Flaw Size

The critical flaw size is calculated for the situation when

$$K_I = K_{Ic} = 82 \text{ ksi } \sqrt{in} \ (90 \text{MPa } m^{1/2}) .$$

The applied stress intensity factor as a function of crack depth was computed for the case of a complete circumferential crack. The K-solution provided in Appendix C (Eq. C-12) was used to calculate K_I for an applied stress of 100 ksi (690 $MPam^{-2}$), and these results are plotted in Fig. E-12. The critcal crack depth (thread depth plus flaw depth) is calculated to be 0.155 inches (0.394 cm) for a toughness of 82 ksi$\sqrt{in}$ (90MPa $m^{1/2}$). This calculation indicates that a flaw approximately equal to the thread depth or 0.078 inches (0.198 cm) would be critical under the assumed loads. The reference flaw which would indicate acceptance would be half that value according to Eq. D-3 or 0.039 inches (0.099 cm). The acceptance criterion based on load can be investigated by entering the curve in Fig. E-12 at a K_I level equal to $K_{Ic}/\sqrt{2}$ or 58 ksi $\sqrt{in}$ (64 MPa $m^{1/2}$). The reference flaw size to give acceptability would be 0.010 inches (0.025 cm), so clearly under the conditions assumed in this analysis, the criterion based on flaw size is less restrictive.

However these computed crack depths are indicative of the conservative model for calculating K_I where the thread depth is considered to be part of the crack, and the crack is assumed to be completely circumferential. When the analysis for K was repeated for the case of an elliptical crack with $a/\ell = 1/3$ and including the stress concentration effect of the thread modeled, a more realistic estimate for K is achieved. These results are shown in Fig. E-13 and were generated by using the influence method (see Appendix C).

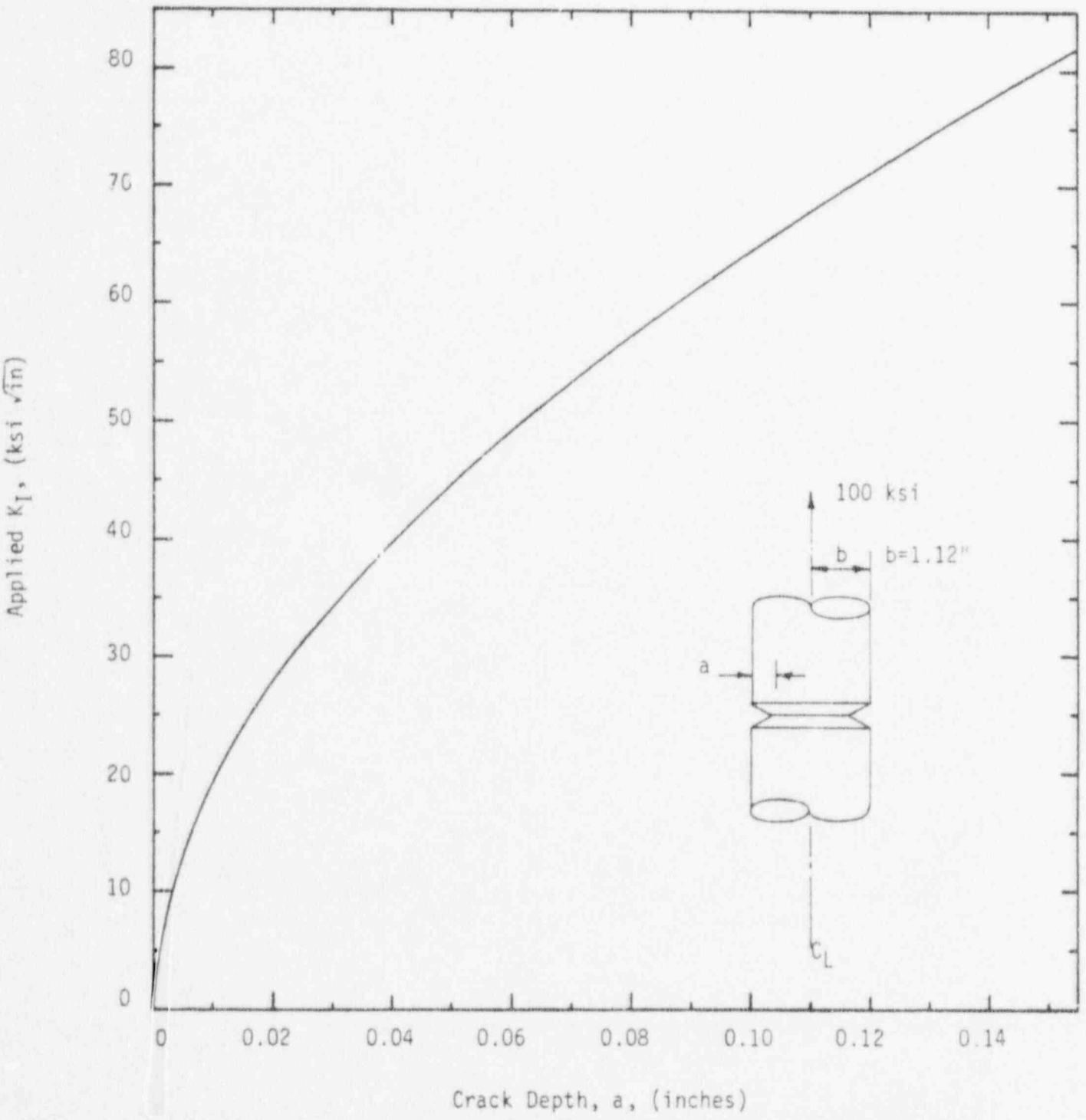

Figure E-12 Applied Stress Intensity Factor For a Circumferential Crack

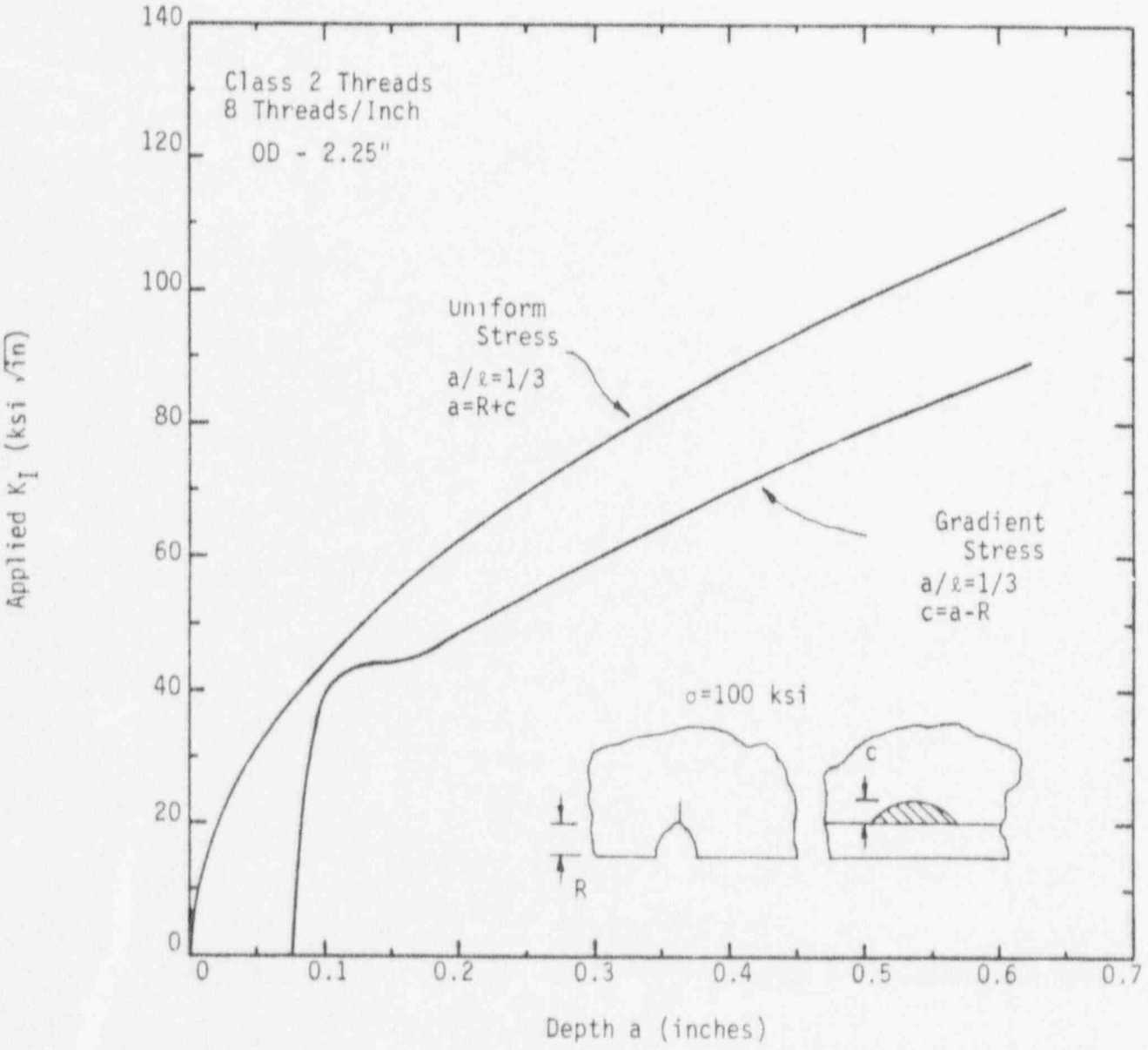

Figure E-13 Applied Stress Intensity Factors for an Elliptical Crack

In the analysis where the local thread conditions were modeled, a stress concentration factor of 3.5 for the thread was assumed. The critical crack depth becomes 0.35" - 0.077" or 0.273 inches (0.693 cm) if the uniform stress model is assumed, and a larger critical flaw size can be demonstrated if the analysis is refined to include the stress gradient.